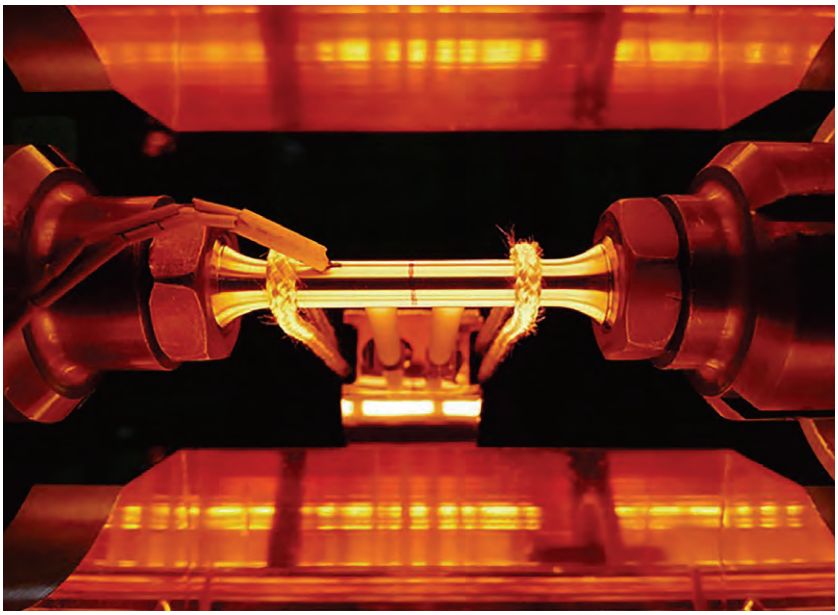

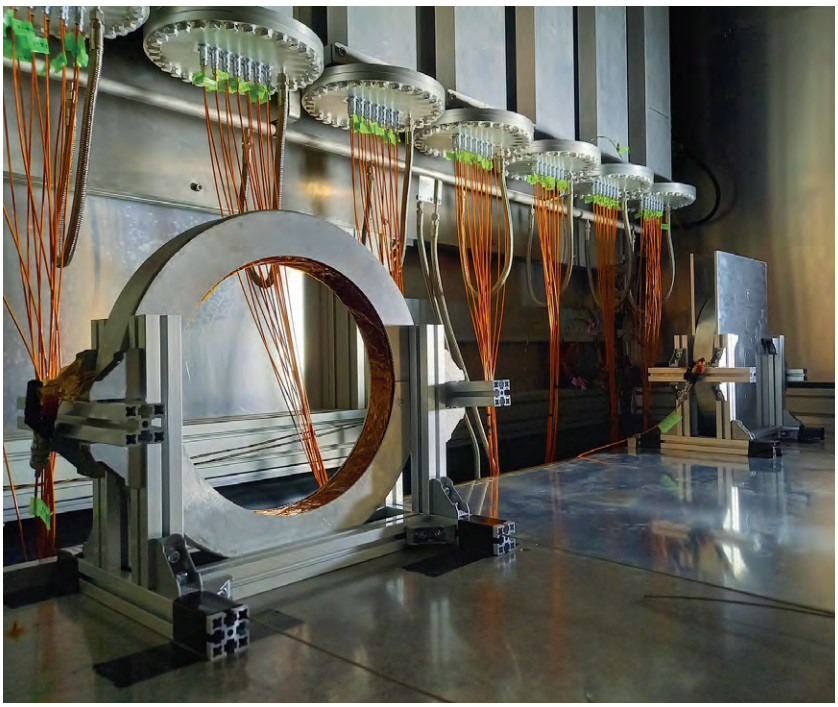

J-PARC

ANNUAL REPORT 2021

Vol.1: Highlight

Editorial Board (April 2022 – March 2023)

Cover photographs


Photograph ① : Concentrated Line
Image credit: Junko KITAGISHI

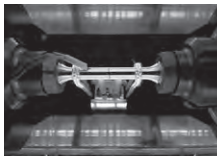
Photograph ② : Can You Stand the Heat?
Image credit: Stefanus HARJO


Photograph ③ : First Operation with MUMON-CT
Image credit: Hina NAKAMURA

J-PARC Annual Report 2021

Contents

Preface

In Japanese fiscal year (JFY) 2021, from April 2021 through March 2022, we made great progres at J-PARC in many fronts as a few of them are picked up below.

Still the COVID-19 pandemic continued throughout JFY2021 and made it difficult for foreign collabolators to visit J-PARC. However by taking various preventive measures against COVID for J-PARC staffs and domestic users, we successfully continued operation of J-PARC accelerators and user facilities.

We achieved 740kW stable beam operation of RCS for MLF. In total about 3480 hrs (145 days) of net user beam time corresponding to very high availability of ~96.4 % was provided.

One of the major news from MLF is the completion and start commissioning of H-line in the muon facility after ~10 years of construction!

The Main Ring operated and provided beam of 40 and 14 days for HD and NU, respectively, during April to June. The stable beam at 64kW for HD and 515kW for NU was achieved. After the operation, MR entered long shutdown for major upgrade for higher beam power. The construction and installation of all the upgraded components have completed by the end of March, 2022. The commissioning will be started from April 2022.

During long shutdown, the neutrino group has continued to upgrade the beam facility to accept higher beam power toward 1.3MW for T2K/HyperK projects. The hadron experimental facility (HEF) has also continued to upgrade the facility including the construction of beamline for COMET experiment. One of the scientific highlights from HEF is the measurements of scattering between Σ (a baryon containing s-quark with very short lifetime of 0.15ns) and proton with the highest precision ever achieved.

In this volume, we report the progress made at J-PARC in JFY2021.

On behalf of the J-PARC staff members,
Director of J-PARC Center
Takashi Kobayashi

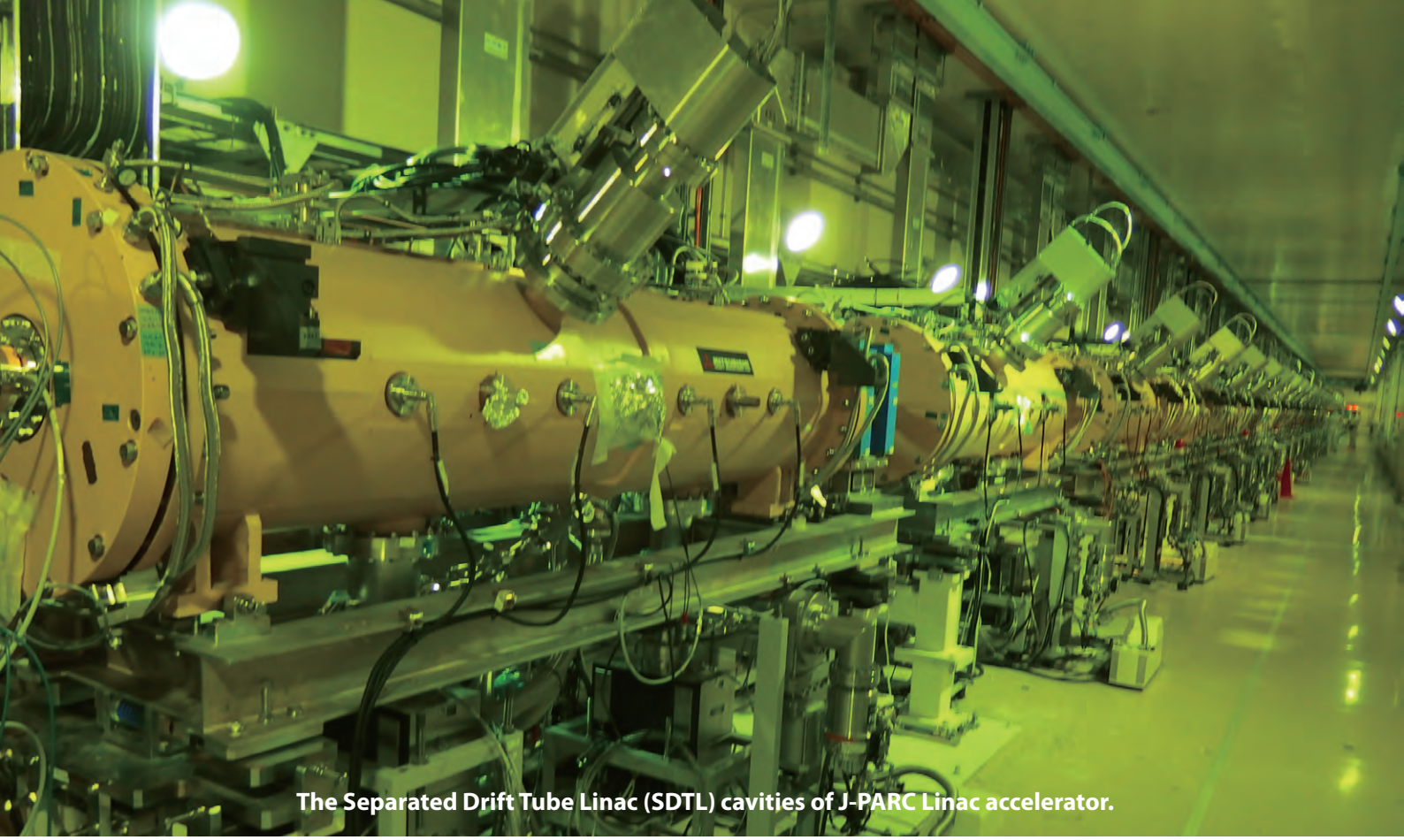

The Separated Drift Tube Linac (SDTL) cavities of J-PARC Linac accelerator.

Accelerators

Overview of the Accelerator

The J-PARC accelerator complex consists of a 400 MeV linac, a 3 GeV Rapid Cycling Synchrotron (RCS) and a Main Ring Synchrotron (MR, 30 GeV). The proton beam from the RCS is delivered to the Materials and Life Science Experimental Facility (MLF) for neutron and muon experiments as well as injected to the MR. The MR has two beam extraction modes: fast extraction (FX) mode for the Neutrino experimental facility (NU) and slow extraction (SX) mode for the Hadron experimental facility (HD).

The operation in Japanese fiscal year (JFY) 2021 is illustrated in Fig. 1. The topics related to the beam operation are as follows:

(1) Operation for the MLF

The beam operation as an operation run of Run#86, which started late in November 2020, and continued on schedule until the end of April 2021. Soon after the

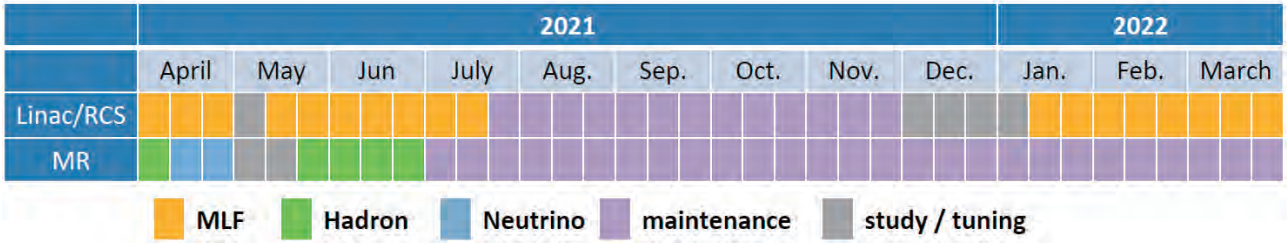

Fig. 1. Accelerator operation in JFY2021..

beginning of JFY2021, on April 5, 2021, the beam power for the Materials and Life Science experimental facility (MLF) user program increased from 630 kW to 740 kW. After almost a week-long shutdown at the beginning of May, the user program resumed for the MLF at 740 kW beam power on May 10 as an operation run of Run#87. However, the beam power for the MLF user program had to be reduced from 740 kW to 630 kW from June 24 due to insufficient cooling capacity of the cooling water system of the RCS in summer. The MLF user program has been performed on schedule until July 20 ,before the summer shutdown.

The neutron production target of the MLF was replaced during the summer shutdown. Due to the delay of the target related work, the beam user operation was postponed to January 15, from the original schedule of the end of November. The beam power for the user operation is scheduled at 740 kW as before the summer shutdown.

We had carried out an accelerator study for about 1 month in December because the MLF user operation was canceled (as an operation run of Run#88). After the year end's scheduled shutdown, the linac tuning was started on January 7 followed by the RCS. The MLF user program started on January 15 as an operation run of Run#89 and continued until the end of March as scheduled.

(2) Operation of the MR for the Neutrino Experiment (FX mode) and Hadron Experiment (SX mode)

The neutrino user operation was carried out from April 8 to the end of Run#86 at a beam power of 510 kW after HD user operation, which was continued from March 27.

The user program resumed for the hadron on May 11. The maximum beam power of 64 kW was achieved through repeated adjustments, and the utilization operation was carried out at this power. The hadron user program was continued until the end of June.

From May 19 to 25, the Main Ring synchrotron (MR) suspended the normal hadron user operation and carried out a test run for the COMET experiment. In this test operation, a bunched slow beam of 1.8 kW was extracted at an energy of 8 GeV instead of the usual slow beam extraction done at an energy level of 30 GeV. This test operation for the COMET phase 1 experiment succeeded by significantly improving several parameters, such as extraction efficiency and spill duty, which are very important to realize the goal of the COMET experiment.

From July, the MR entered a long maintenance period for an upgrade until the fall of 2022.

The operation statistics for JFY2021 (from April 2021 to March 2022) are shown in Table 1. The net user operation hours and the beam availability rate for each experimental facility were as follows: 3,480 hours (96.4%) for MLF; 347 hours (93.6%) for NU; and 954 hours (93.7%) for HD. These statistics show that the linac, the RCS, and the MR operated with high availabilities.

Figure 2 shows the number of stop events and stop time by components in JFY2021. The stop time includes not only the stop events during scheduled operation but also during beam studies and tuning. There were several causes of the stop.

For the linac, HVDC and SDTL were still dominant. However, the cause of the stoppages in SDTL was not the SDTL cavity, most of them were due to malfunction of LLRF. LLRF troubles were also counted as troubles in each cavity. The RCS outage was mainly due to RF. The RF outage was not due to the cavity, but to the failure of the capacitor and the life of the vacuum tube in the amplifier. The MR had only one downtime event, which was the trouble of the power supply of the QM, but it was restored within a short period.

Table 1. Operation statistics in hours for JFY2021.

Facility	User time (hours)	Net time (hours)	Availability, total (%)
MLF	3,608	3,480	96.4
Neutrino (FX)	371	347	93.6
Hadron (SX)	1,016	952	93.7

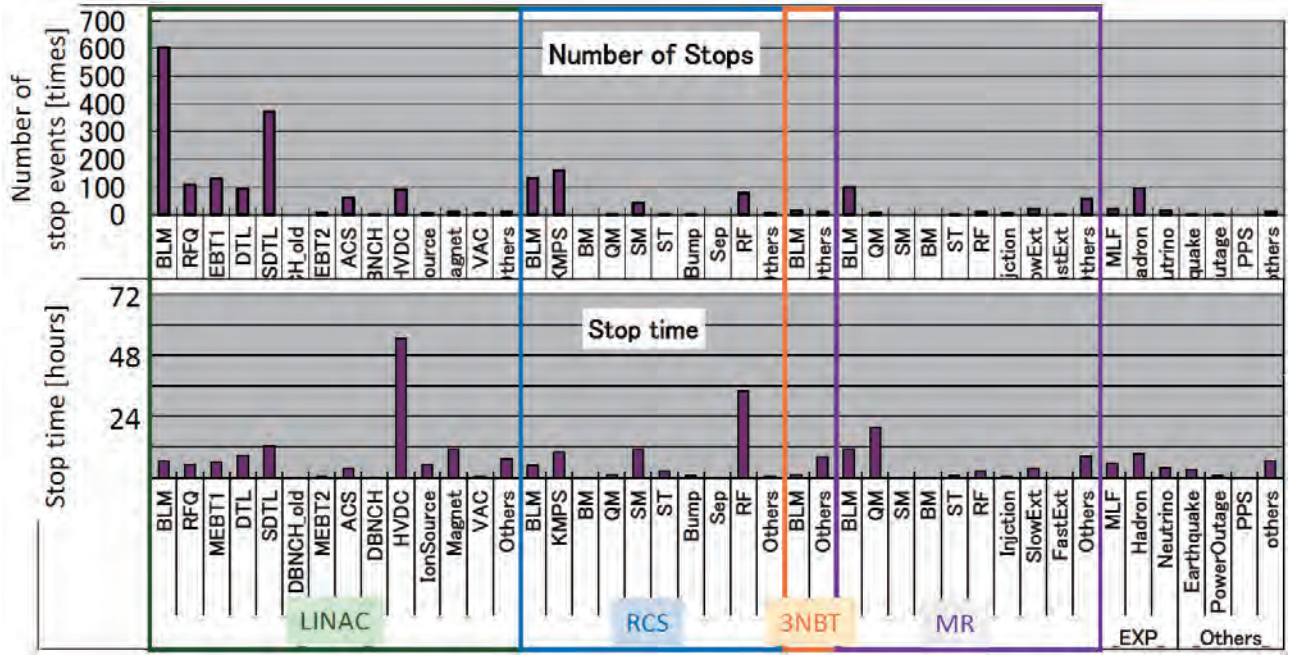

Fig. 2. Number of stop events and stop time by components in JFY2021.

Linac

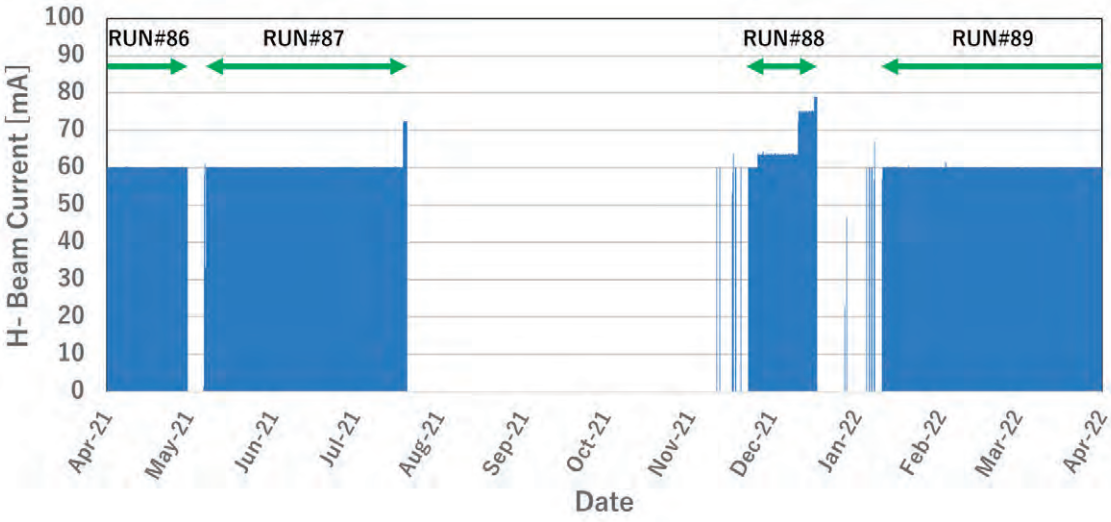

Fig. X-1. Operation history of the ion source in JFY2021.

Overview

The J-PARC linac has been operated with a nominal peak beam current of 50 mA. High availability of more than 95% (to the MLF), the same as in JFY2020, was also kept during JFY2021 at the linac. Beam studies have been conducted to resolve some issues, such as the beam loss mitigation and confirmation of the feasibility for further high intensity operation due to the demand of the downstream facilities.

Accelerator components status

The operation history of the ion source in JFY 2021 is shown in Fig. X-1. Presently, the ion source is being operated with a beam current of 60 mA for the user operation. At the end of RUN#88, the ion source extracted more than 75 mA beams for high-intensity beam (1.44 MW equivalent at the RCS) studies at the linac and the RCS. Figure X-2 presents the history of the continuous operation time and the beam current increase of the RF ion source (from 2014). The replacement cycle has

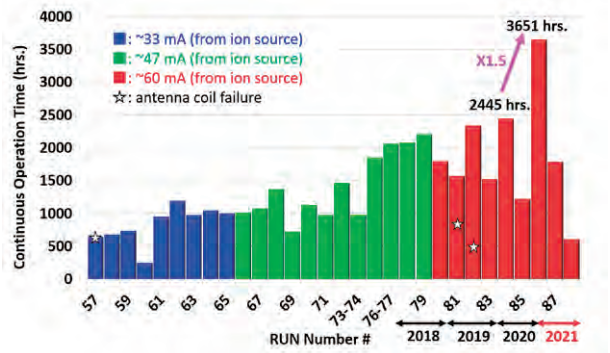

Fig. X-2. History of the continuous operation time of the RF ion source.

gradually extended with the increased operational experience. In RUN#86 (November 20, 2020 – April 30, 2021), the continuous operation time of the ion source has been extended to 3,651 hrs. (5 months), which was 1.5 times longer than the previous record (2,445 hours in RUN#84). After the operation, it was confirmed at the test bench that the beam emittance was kept stable even after the 5-month continuous operation. No cracks, pinholes or any thickness variation of the enamel coating were observed from a direct investigation of the antenna coil. From these results, the ability of the J-PARC RF ion source to operate continuously for 5 months at a peak current of up to 60 mA, with a duty factor of 2 % and injection power up to 30 kW, has been confirmed. The next goal is to achieve a 7-month-long run, which corresponds to the full duration of the J-PARC user operation in one year.

The RFQ trip rate was approximately 10 times per day at 25-Hz beam operation to the MLF in FY2021. This situation is almost the same as before. To reduce the down time of the linac due to the RFQ trip, an auto-restart system for the RFQ trip has been running for two years. The system prevents about 10 minutes no-beam time in a day. After about two years of operation, the system was found to have no negative impact on RFQ.

After the Great East Japan Earthquake in 2011, we could not operate with the designed rf power in some SDTL cavities due to the multipactor effect. After wiping the inner surface of the cavity with acetone, the multipactor region disappeared completely, except in the SDTL05A. Therefore, we tried wiping by using dilute sulfuric acid in the summer of 2020, however, the multipactor region did not disappear completely and even spread again, almost to its former state. In the 2021 summer shutdown, we checked the cavity and found some unwiped areas on its inner surface. Then, we tried to wipe the inner surface again with dilute hydrochloric acid. As a result, the multipactor region has almost disappeared, and no trend of increase has been observed so far. We think that the reason why this result was different from the previous cleaning is not only due to the type of acid, but also because the second time we treated the remaining unwiped areas.

The operation of the ACS cavities was more stable than the other accelerator sections. The number of trips of all the ACS cavities was less than once per day.

RF system status

We have been handling two types of klystrons, a 324-MHz klystron and a 972-MHz one. Two failed 324-MHz klystrons, whose operation time had lasted more than 80,000 hours, were replaced in JFY2021. The operation times of the klystrons as of the end of March 2022 are shown in Fig. X-3. Among a total of twenty 324-MHz klystrons, six of them reached more than 82,000 hours of operation, which corresponds to the entire period since the start of the linac operation. Most of the 972-MHz klystrons reached more than 50,000 hours of operation.

Due to the discontinuation of digital devices, including the CPU and DSP&FPGA boards, we upgraded

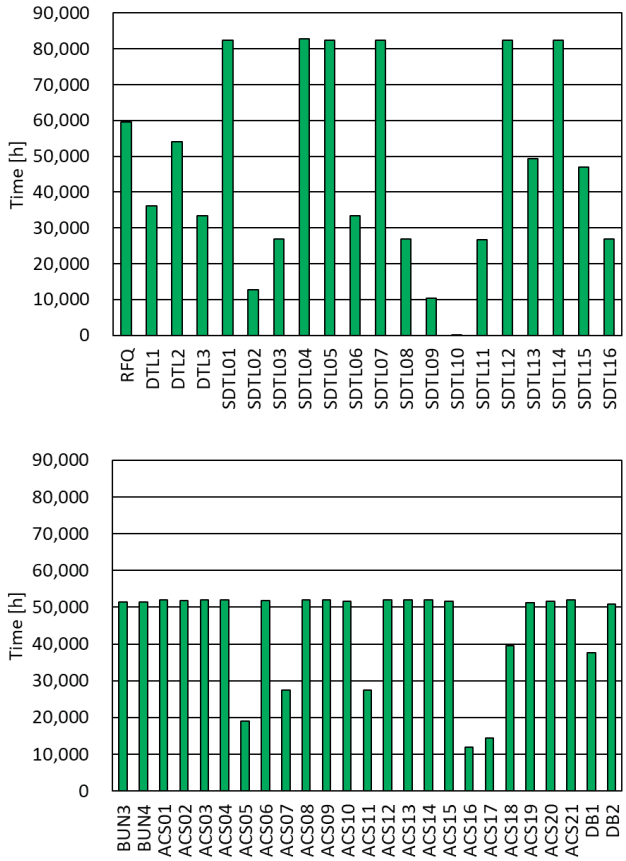

Fig. X-3. The operation time of the 324-MHz klystron (top) and 972-MHz klystron (bottom) as of the end of March 2022.

the digital part by newly developed digitizers for 324-MHz acceleration RF stations (RFQ, DTL 1-3, SDTL 01-16) in 2020 and 2021. The present LLRF feedback system has been completely replaced by a newly developed LLRF system based on μTCA.4 for MEBT1 (BUN1, BUN2, CHOP1, CHOP2) in the summer of 2021. This new system works very well now and is expected to improve the beam quality with newly implemented functions.

Beam monitor development

It is important to measure and adjust the beam profile in the transverse and longitudinal directions because we need to stabilize the beam and mitigate the beam loss. We have been able to utilize beam monitors that measure a transverse profile in all sections of the J-PARC Linac, but not yet the longitudinal one. Therefore, we have been developing a bunch shape monitor (BSM) which can measure a longitudinal beam profile in the Linac. The longitudinal profile measurement was successfully conducted at the MEBT1 with peak currents of 50 mA and 60 mA in the beam commissioning. Detailed analysis is ongoing combined with the beam simulation to evaluate the beam emittance.

Previously, BSMs were installed at MEBT1 and MEBT2, respectively. The new BSM was installed in the L3BT in the summer of 2021, and this allows measurement of the longitudinal profile of beams accelerated up to 400 MeV in the Linac. We are currently tuning it to be used for the beam tuning.

Beam study

We continued beam studies at the interval of the user operation and before and after long-term shutdown for beam loss mitigation and long-term stability.

Presently the IBSt (intra-beam stripping) in the H- beam at the ACS section is identified as the dominant source of the beam loss. The IBSt-mitigation lattice with ACS "temperature ratio" between transverse and longitudinal planes (T≡Tx,y/Tz) set to be 0.7, i.e. with systematically reduced quadrupole magnets strength, was successfully applied in the user operation since May 2019, and achieved a reduction of residual radiation dose by 40% as compared to that with using an original equipartition design (T=1). Beam studies were continued towards the next goals with T=0.5 and 0.3. Unlike present operation with T=0.7, T=0.5 and 0.3 lattices are in the resonance region. Therefore, the longitudinal focus should be also modified to stabilize the beam. On the other hand, we need better control of the beam emittance for a precise lattice setting.

Based on the efforts in the previous years, much-improved results were achieved for T=0.5 and 0.3 in May 2021, as shown in Fig. X-4, after fine-tuning with iterative matching in the MEBT2. Compared with T=1.0, an integrated beam loss in the ACS section were mitigated by 50% and 55% with T=0.5 and T=0.3, respectively.

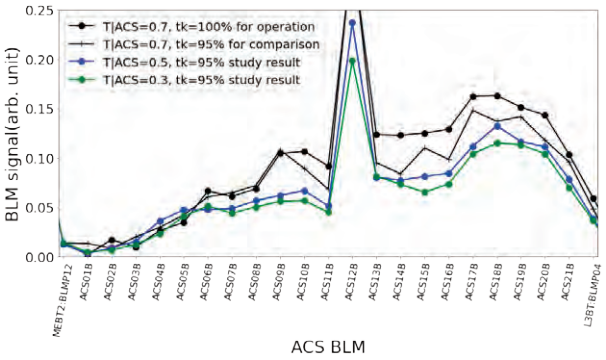

Fig. X-4. Optimized beam loss pattern measured by beam loss monitors (BLMs) at the ACS section for IBSt mitigation lattices with T=0.3, 0.5 for the first time in May 2021.

On the other hand, we found sensitive dependence of the loss mitigation effects on the upstream emittance fluctuation in the later beam study in December 2021. We plan further studies to investigate and achieve higher stability and reproducibility of beam parameters from the J-PARC linac frontend, together with lattice study for the reliable application of beam loss mitigation lattices in the future.

RCS

Operational status

The output beam power delivered to the MLF was 630 kW at the beginning of JFY2021, and a week later, it was immediately increased to 740 kW. Meanwhile, the number of the protons for NU was 6.7e13 particles per pulse, which corresponds to a 510 kW-beam of MR, and 1.8e13 particles per pulse, which corresponds to a 64.5 kW-beam of MR for HD users. Figure 1 shows the change in RCS output power with respect to time.

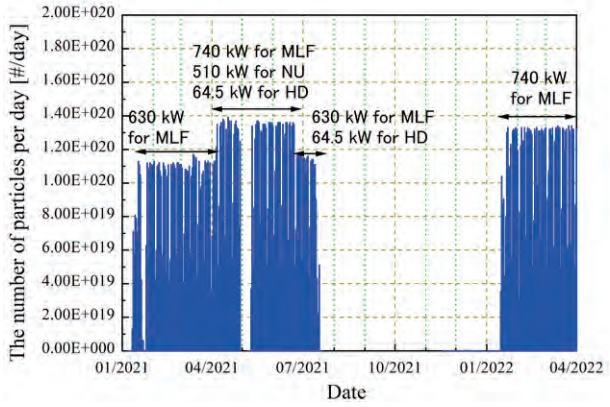

Fig. 1. Changes in the RCS output particles over time.

This year, the operational status of the RCS was quite stable and no major incidents occurred. The availability of the RCS is summarized in Table 1. The operation time for the MLF over the year was approximately 3609 h, excluding the commissioning time, and downtime due to RCS was approximately 25 h. The availability for the MLF was evaluated according to these values and it was 99.3%. For the Neutrino and Hadron users, the availabilities of RCS were also kept more than 99%.

Table 1. Summary of availability

Facility	User time (h : m)	Trouble in RCS (h)	Availability of RCS (%)
MLF	3608 : 48	24 : 52	99.3
Neutrino	371 : 28	1 : 36	99.6
Hadron	1016 : 53	4 : 20	99.6

Maintenance and improvements

- New RF cavity

In recent years, we tried to confirm the potential of RCS that can output more than 1 MW beam. Our study results had revealed that RCS had enough performance capability to accumulate a 1.5- MW beam. However, the RF system did not have the capability to accelerate a beam of more than 1 MW. Therefore, when we tried to accelerate a 1.5- MW beam, it was lost in the midst of the acceleration period. This was because the power consumption of the RF exceeded the capacity of the power supply, but the required current for 1.5 MW acceleration was quite high and it was not likely to be feasible only by increasing the capacity of the power supply.

We investigated the reason for the increase in power consumption and found that a combination of the push-pull operation of the vacuum tube in the amplifier and the multi-harmonic driving in one cavity causes the unbalance on each tube. In the original design, upstream and downstream of the acceleration gap were excited by two tubes independently. Although each tube should generate half of the acceleration voltage (12 kV) in the ideal push-pull operation, actually the anode voltage of VT1 is much larger than VT2 in multi-harmonic operation. The anode voltage exceeds the limitation by the un-balance and the requirement of the anode current is increased.

To solve this issue, we developed a new cavity that ensures that only the downstream of the gap is excited. This configuration enabled us to reduce the input current of the cavity. We completed construction of one this new cavity and was installed in the RCS tunnel during the summer shutdown period of 2021. Figure 2 shows the new cavity in the RCS tunnel.

Finally, we tried to accelerate a 1-MW beam with the new cavity and confirmed its performance. It can accelerate a 1-MW beam with less power consumption. The power consumption for this new cavity was reduced from 820 kW to 487 kW at the 1-MW beam acceleration. Figure 3 shows a comparison of the anode current for the original (red) and the new cavity (blue).

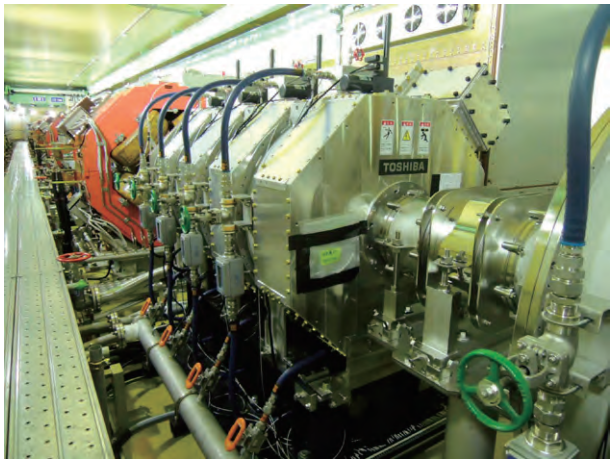

Fig. 2. New cavity in the RCS tunnel.

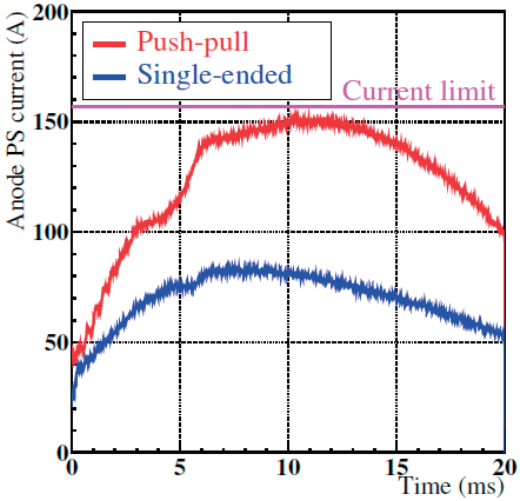

Fig. 3. Anode current of the original cavity and the new cavity with a 1-MW beam acceleration.

• Recovery of the cooling water performance

In June 2020, we tried to implement a two-day continuous user operation. However, this 1-MW demonstration showed a serious issue with regards to achieving stability. We found that when the outside temperature increases, the supply temperature of the cooling water becomes uncontrollable and increases. This induces the temperature interlock of the vacuum tube in the RF final stage amplifier. We need to improve the cooling water system to establish a stable 1-MW operation in all seasons.

In the summer shutdown period of 2021, we carried out the recovery work of the cooling water system performance. Our investigation indicated that this low performance would be due to the contamination of the heat exchange unit. Therefore, we disassembled and washed the heat exchange unit in the same period. Fig. 4 shows the plates of the heat exchanger. In this unit, primary and secondary cooling water flows alternately between the layered plates. We found out that the plate surface of the secondary loop was contaminated with sludge. All of the plates were washed by chemical cleaning process in the factory. Figure 5 shows

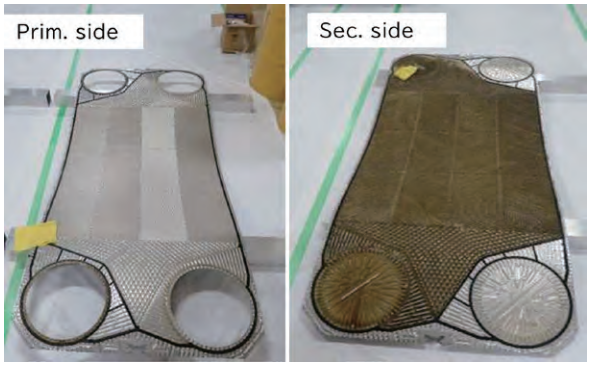

Fig. 4. Plates of the heat exchanger.

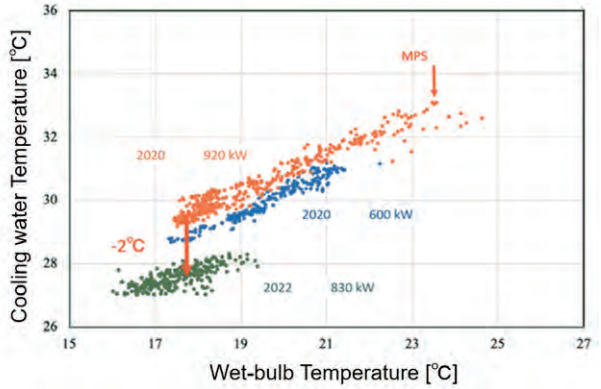

Fig. 5. Cooling water temperature as a function of the wet-bulb temperature and beam power.

the cooling water temperature as a function of the wet-bulb temperature and beam power. After the recovery work, the cooling water temperature was reduced in spite of the higher beam power.

Beam study results

• Implementation of a smaller vertical injection beta

In the RCS, one of the high radio-activated point is the chamber of the injection foil. Previous study results indicated that the source of this activation is the large-angle scattering particles caused by the interaction between the foil and the circulating beam. The foil interaction with the beam also induces the emittance growth. In order to reduce the foil scattering effect, we implemented a smaller vertical beta function (β_y) of the injection beam and used a smaller foil. From the numerical simulation, the original β_y of 7 m was minimized to 2 m. This smaller beam enables us to reduce the vertical foil size from 20 mm to 14 mm. The beam test by using this new injection parameter and smaller foil showed that the beam loss in the collimator area was significantly reduced. The foil hitting rate of the circulating beam was also measured to be reduced 30%. We adopted this new operation parameters in 2021 for a month at 700 kW beam power to the MLF users. The residual radiation was significantly reduced at the injection, collimator and the 1st arc section. As a result, a smaller injection beam and a smaller size foil were implemented for the user operation in March 2022.

• Progress on the kicker magnet (KM) impedance reduction.

In the 1-MW beam operation, beam instability occurred with some operation parameters. The beam instability restricted the allowable operation parameter for the 1-MW operation. This instability was due to the reflection of the wake voltage from the power supplies

of the extraction kicker magnets. To solve this issue, we developed a damping system of the wake voltage in the power supply. The damping system consists of diodes and resistors. We have 8 kicker magnets, and we installed one damping system in one kicker power supply. We tried 1 MW beam acceleration with this condition, and the test result indicated that the impedance and the beam instability were well reduced as expected.

Summary

RCS has established a continuous, stable user operation. In JFY 20021, RCS delivered 6.4e13 ppp proton beam for 740 kW beam power to the MLF and 6.7e13 ppp, which corresponds to 510 kW beam power at the MR. These values will be increased steadily with careful monitoring of the neutron target status and beam loss.

We carried out two major improvement works. A New RF cavity was tested. It works well and reduces the power consumption. The thermal exchanger in the cooling water system was washed. The performance of the system seemed to improve and the temperature of the cooling water was reduced.

We also continued the beam test to reduce the beam loss. A smaller injection beam with a smaller size foil and new damping system in the kicker magnet power supply were successfully implemented, and this resulted in significant improvements not only for beam loss mitigation but also for a better beam quality.

MR

Operation overview

The MR beam operation was scheduled from April to June in JFY2021. The beam was delivered either to the neutrino facility with fast extraction (FX) mode or to the hadron experimental hall with slow extraction (SX) mode. For the FX operation the beam was extracted in one turn with the cycle of 2.48 s. The beam was delivered to the neutrino facility for the T2K long baseline neutrino experiment. For the SX operation the beam was extracted in about 2 s of debunched beam spill with the cycle of 5.2 s. The beam spill was delivered to the hadron experimental hall to produce various secondary particles for the experimental users.

The operation was mostly stable for both the FX and SX modes and the availability was 93% as the ratio of the net operation duration to the assigned operation duration. For FX mode, the beam power was 510 kW with 2.6×10^{14} protons per pulse. Minimizing the beam losses and the localization were our concerns. The beam loss power was maintained at an acceptable amount of about 850 W.

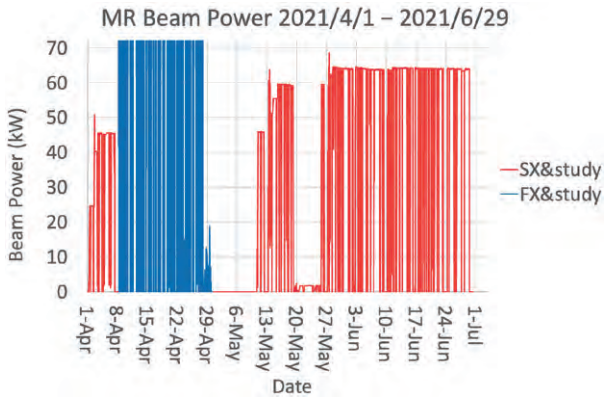

Fig. 1. MR beam power in JFY2021. The beam power of SX and study is shown in red and that of FX and study is shown in blue (out of scale).

Efforts have been made to increase the higher beam power for the SX mode. The most important concern has been the beam instability, that results in beam losses, at the debunching process before the extraction. The beam power has been upgraded to 64.5 kW with suppression of the instability (Fig. 1). Beam study was performed for a diffuser for the beam loss reduction during the extraction. A diffuser is a material installed in front of electrostatic septum (ESS) ribbons. It is intended to cause multiple Coulomb scatterings to the beam and to reduce the beam to hit the ESS ribbons. The beam loss was successfully reduced to about 40% with one diffuser with the beam power of 10 kW. Further improvement is anticipated with two diffusers.

Operation at the extraction energy of 8 GeV was performed for the COMET experiment. The beam power was 1.8 kW for phase I of the experiment. The extraction efficiency was improved to 99.1% from the 97.3% achieved in the previous operation in 2018. The spill duty was improved to 55% from the 16% in the previous operation.

Circuit breaker incidents

The circuit breaker for the magnet power supplies was accidentally opened on June 29 during the SX operation. The same incident has occurred several times. It resulted in the fatal damage of the ESS ribbons

in February 2021. The damaged ESS was replaced with a spare. We have continued the operation with countermeasures for protection of the ESS and installed devices to search for the cause, such as transformer failure. The switch of the pressure release valve of the transformer which was used for the oil pressure sensor turned out to be broken. We plan to change the switch. Meanwhile, damages of the devices, such as transformers, by the sea water vapor are of serious concern. Besides, we are preparing an ESS spare for the sustainable SX operation.

Upgrade works toward the 1.3-MW operation

Beam power upgrade is planned with the fast-cycling scheme. Long shutdown was scheduled for the hardware upgrade from July 2021 to May 2022.

Beam power of 500 kW was achieved with a cycle time of 2.48 s and accelerated protons of 2.6×10^{14} per pulse. The next target is to realize a beam power of 750 kW with a cycle time of 1.32 s and 2.1×10^{14} protons per pulse (ppp). Even further beam power has been demanded from the neutrino user community for the discovery of CP violation and precise measurement of the mixing parameters in the lepton sector. A new target of 1.3 MW is planned with the cycle time of 1.16 s and 3.3×10^{14} ppp (Table 1).

Table 1. Beam Power Upgrade Concept.

	Beam Power	Cycle Time	Number of accelerated protons
Present	500 kW	2.48 s	2.6×10^{14} ppp
Original Design	750 kW	1.32 s	2.1×10^{14} ppp
New Plan	1.3 MW	1.16 s	3.3×10^{14} ppp

The new magnet power supplies have been constructed. All six power supplies for the bending magnets were completed by the end of JFY2020. The production and installation of new magnet power supplies of quadrupole families of QDN, QFN and QDR were completed in JFY2021 (Fig. 2). Present power supplies are reused for other quadrupole families. Many quadrupole families require new cablings because of the family configuration change (one family to two families) and the higher voltage requirement for faster cycling. The cablings were completed in JFY2021.

Two second harmonic cavities were installed at insertion A in the summer of 2020. The power amplifier and anode power supply for one of the cavities were installed in JFY2021. Those for the other cavity will be installed in JFY2022. The present two second harmonic cavities will be converted to fundamental cavities. The total number of the fundamental cavities will then become nine, and the accelerating voltage should be sufficient for the 1.3 s operation.

The injection and FX devices have been prepared for the faster cycling. For injection kickers, the matching resistor box was upgraded for countermeasure against heat of the beam loading. For the FX kickers, the high voltage charger was upgraded and ready for the 1-Hz operation. For faster cycling, we plan to replace all septum magnets, two low-field magnets and four high-field magnets. The new low-field septum magnets are eddy current type magnets (Fig. 3). All these devices will be installed before the beam test in 2022 except for SM32. It is one of the four high-field septum magnets. Water leak in the coil was observed during the test operation. We decided to make a new coil and the magnet should be ready for the user operation in JFY2022.

Fig. 2. New magnet power supply for a quadrupole family of QDN.

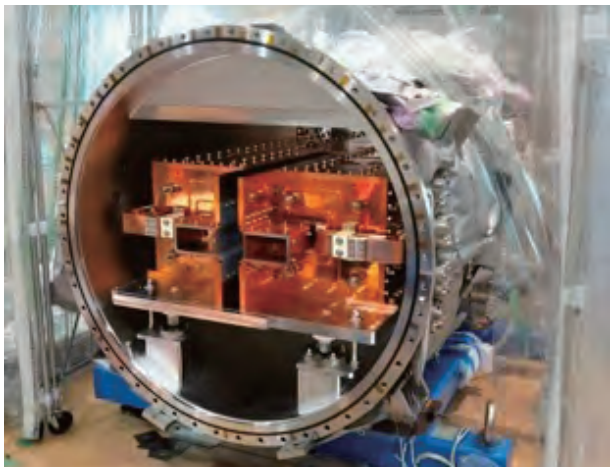

Fig. 3. Eddy current type septum magnet for the fast extraction.

Two additional collimators were installed in JFY2021. Another collimator is planned for installation in JFY2022. The collimation system in the MR injection region will be upgraded for a capacity of 3.5 kW beam loss as compared to the present 2 kW.

Further upgrade is planned for the operation of 1.16 s. The number of RF cavities should be increased for faster acceleration. RF anode power supplies should be upgraded for the beam loading compensation of high-intensity beams. These upgrades are planned for JFY2025. Circuits of beam position monitors will be upgraded for high-intensity beams and more precise measurements by JFY2024. With the parameter tuning of main magnet power supplies for the 1.16 s operation and the beam tuning for higher intensity, we plan to achieve the beam power of 1.3 MW in JFY2028

Materials and Life Science Experimental Facility

Overview

The proton power ramp up and instrument upgrades at the MLF were still progressing under COVID-19. Although we had to comply with the COVID-19 restrictions, the neutron and muon beams were supplied as normal. The beam power of the MLF was ramped up to 700 kW from 600 kW from April 2021 and the availability at 700 kW was more than 90%. The MLF received 740 kW during the MR operation period with slow extraction mode, which is the highest power ever attained for long-term user operation at the MLF. According to the power ramp up, it became more important to perform radiation works of targets maintenance safely and on schedule. From this point of view, a long enough summer maintenance period was secured to check the progress carefully by not only the MLF but also the J-PARC management, which led to the late start of the user operation in January 2022. The summer maintenance of 2021 was finished safely on schedule.

Progress was made in the development of neutron instruments, such as low-temperature Digital image correlation technique for hybrid neutron diffraction (BL19), completion of the polarization system of the Polarized Neutron Spectrometer (BL23), noise reduction method based on deep learning which can shorten measurement time to one tenth of the conventional neutron reflectometry measurement on BL17, H_2O / D_2O vapors supply system, New 2D scintillator detectors for a single crystal diffractometer (BL18) and Fe/Ge polarizing supermirror with m = 6.2 (the highest achieved in the world).

In the muon H line, the on-beam commissioning performed since the first beam delivery in January 2022 was completed successfully, and the S-type experiment (DeeMe; an approved proposal for conducting a muon-electron conversion experiment at J-PARC MLF. http://

deeme.phys.sci.osaka-u.ac.jp). The initial analysis of the samples returned by Hayabusa-2 was performed using a non-destructive elemental analysis method with negative muon capture characteristic X-rays at the D-line.

We initiated a series of internal group discussions to establish MLF's future plan, "MLF2030", based on the existing instruments and devices. This plan is expected to be connected with or to improve the plan of target station 2 of the MLF.

The users visits from abroad were seriously limited by COVID-19. Many proposals were canceled and some of them were conducted by beamline scientists without user's visit. On the other hand, several workshops were held online, such as the target system workshop with SNS of Oak Ridge National Laboratory, the18th Korea-Japan meeting on neutron science hosted by JSNS (The Japanese Society for Neutron Science), J-PARC MLF and KNBUA (The Korean Neutron Beam Users Association), the Annual meeting of industrial application at J-PARC MLF with 352 participants, including 150 attendees from companies, collaborative scientific and technical series of workshops with the Australia's Nuclear Science and Technology Organisation (ANSTO), the 5th Neutron and Muon School (NM-school) was held as KEK-IINAS (Inter-Institution Network for Accelerator Science) School for both lectures and remote hands-on (https://mlfinfo.jp/sp/school/5th-nms/index.html).

In conjunction with the reopening of the neutron user program at Japan Research Reactor - 3 (JRR-3), J-JOIN was formed by JAEA, KEK, CROSS, Tokyo University and Ibaraki Prefecture. A portal site of J-JOIN has been opened which provides one-stop consultation for neutron and muon use to support users, who are not familiar with that field, to allow access to neutron and muon experiments.

Neutron Source Section

At the beginning of fiscal year 2021, the beam power was raised to over 700 kW from 600 kW on April 5, which was the highest level of beam power on record for the long-term user program at the MLF. The stable operation continued, but due to the humid and hot weather in the summer, the beam power had to be decreased to 600 kW again from June 24 in order to increase the cooling capacity margin of the accelerator devices. The beam operation ended on July 17, before the start of the long outage.

The maintenance works during the long outage were carried out carefully and successfully. As the beam power increases gradually to the final goal of 1 MW, promotion of the radiation work safety, especially in the maintenance period, becomes more and more important. In order to check and review the criteria for radiation work safety and procedures of maintenance works, sufficient maintenance period was secured and parallel works that could increase the risk of radiation release or contamination were avoided to concentrate on each maintenance task one by one. The results of check and review were used to improve the planning of maintenance works from the next year on. These procedures led to the late start of the user operation from January 2022. On October 18, specimens were cut out from the forefront wall and the beam window of the used target vessel which was operated with 740 kW

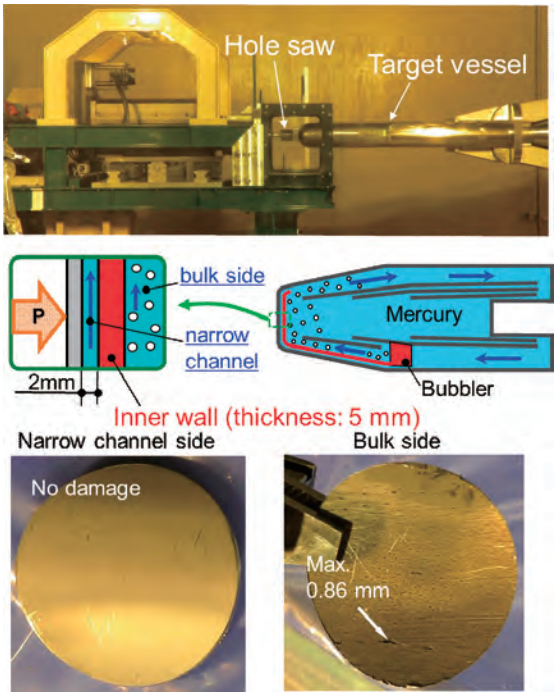

Fig. 1. Cutting machine (top) and structure of the target vessel (middle) and the surfaces of an inner wall specimen (bottom).

at maximum to investigate the efficiency of technologies for pitting damage mitigation, which involve the double walled structure with a narrow channel and the microbubble injection into the mercury flow as shown in Fig. 1. The maximum damage depth on the bulk side

of the inner wall specimen was less than 1 mm and the surface of the narrow channel side was almost intact, which was a promising result for the stable beam operation with greater beam power. On November 1, the used mercury target vessel was replaced with a new one with an improved structure of the mercury flow channel. That is, the bubble generator was installed at a position 92 mm closer to the beam window than the former one to increase the bubble number density near the beam window for promoting the pressure wave mitigation effect. The maintenance work to replace a vacuum pump of the gas process system, which is a crucial device for the target replacement, was a significant task. It needed special care to suppress the release of radioactive materials and the requirement was fulfilled through a well-prepared procedure plan. The remote handling test of the moderator/reflector assembly was carried out for the first time since the beam operation of MLF started in 2008.

The cooling tower of the coolant water loop for the devices of the 3GeV proton beam transport line was replaced as a countermeasure against aging deterioration. The increased cooling capacity will contribute to a stable beam operation in summer.

The beam operation for the user program started on January 15. The neutron source continued its stable operation at 730 kW after the long outage period and the average operational efficiency in fiscal year 2021 reached 95.9 %.

Neutron Science Section

1. User program

For most users from abroad, it is still difficult to visit Japan because of the COVID-19 restrictions, so, many proposals have been canceled or some of them have been conducted as a deputized experiment by beamline scientists. It was previously reported in Annual Report 2020 that the 2021A proposal call for short-term and one-year proposals was merged with that for the 2020B period, and no long-term proposals were called for 2021 due to the delay in conducting the approved ones of 2018L, 2019L and 2020L. In the period of the 2021B-call, we received 338 neutron proposals, including short-term-, one-year-, NUP (new user promotion) and post deadline proposals. 137 of them have been approved. Although the number of submitted proposals showed an abrupt drop in 2020A, fortunately it is recovering and now there are even more proposals than in 2020.

2. Instruments up to date

BL17 is the neutron reflectometer (NR), which enables us to study mechanisms or functions of thin film material by revealing surface structures and buried interfaces. To prove dynamical phenomena varying in time, it was necessary to shorten the measurement time which is longer in the conventional NR, from several tens of minutes to few hours for one measurement. The BL17 team developed a new data processing method based on deep learning, which can successfully eliminate statistical noise from the raw data obtained in a rather short time, like one tenth of the conventional NR [1]. It means that we can effectively extract the signals out of short measurement data and explore dynamic behavior of surface or interface.

3. Other activities

It has been over 14 years since the operation of the MLF started. We always need to look at the future vision of the MLF to improve continuously the facility and neutron science. In order to establish a clear vision of the MLF potential, we initiated a series of group discussions about the MLF's future plans, named "MLF2030", branched into three scientific (or instrumental) groups of fundamental instruments, elastic instruments, and inelastic instruments. In addition to the scientific groups, specific device groups of neutron polarization, detector, vacuum (chamber), and chopper had independently summarized their future direction. We will soon open our discussions to the public in order to build our future plan together with the external community.

Australia's Nuclear Science and Technology Organisation (ANSTO) is one of the most significant national infrastructures for research in Australia, operating the research reactor OPAL. The MLF has arranged cooperation on research and development in neutron science with ANSTO since 2016. In 2021, the arrangement has entered the second five years and was expanded to include the registered institute CROSS. At the beginning of the renewal, collaborative scientific and technical series of workshops were held online,

and the following topics were discussed: 1) dynamics, 2) sample environment, 3) reflectometry, 4) small angle diffraction, 5) structural analysis, 6) neutron polarization, 7) deuteration, 8) imagining technique, 9) computation, 10) industrial.

4. Award

Prof. Hideki Seto received the JSNS (Japanese Society for Neutron Science) Science Prize for the application and development of neutron scattering to soft matter research.

Dr. Takashi Ohhara won the Research Award from Crystallographic Society of Japan for the structural chemical study with hydrogen atoms as a key by high precision single-crystal neutron diffraction method.

Reference

[1] H. Aoki *et al.*, Sci. Rep., 11, 22711 (2021) .

Neutron Instrumentation Section

The neutron instrumentation section has been developing neutron detectors and neutron supermirror devices.

As for neutron detector development, a ^{3}He-gas based multi-wire two-dimensional neutron detector system has been intensively developed for neutron reflectometers [1]. A new electro-optical circuit board was produced to increase the count rate capability and replace the present board (Fig. 1(a)). The board functions to calculate an incident position of a neutron and send digital data to a DAQ system through optical fibers. The new single board is implemented with new FPGAs, which accept 128 channels for x and y wires. This improves the signal processing speed and power consumption, thus ensuring the reliability of the detector system. The developed board can process the x and y signals far less than the system coincidence time of 0.5 μs, enabling a count rate capability of up to 1.27 MHz (Fig. 1(b)). This board fulfills the requirements for the high-count-rate MWPC detector system.

As for the supermirror device, a new neutron polarizing supermirror has been developed based on the modified multilayer scheme. A polarizing supermirror is an optical device that produces highly polarized neutrons with a wide bandwidth by magnetic reflection. The new polarizing supermirror is based on thousands of Fe/Ge bilayers deposited by using ion beam sputtering. The thicknesses of the iron layers should be decreased bellow 3 nm for higher critical angle more than $m = 5$, where m represents a factor compared to

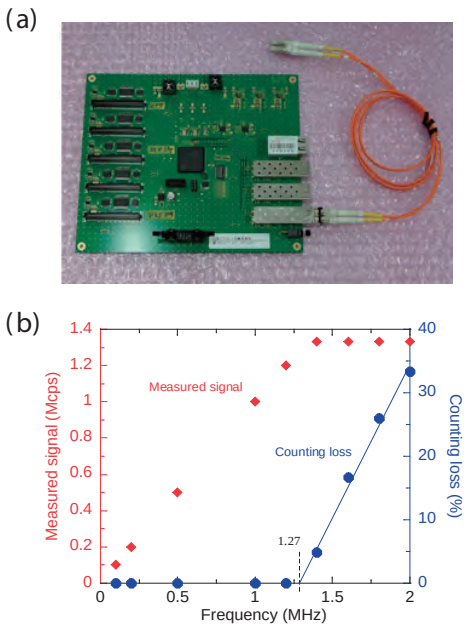

Fig. 1. (a) A photograph of the developed electro-optical circuit board for ^{3}He based MWPC detector system, and (b) measured count rate characteristics of the electronics board.

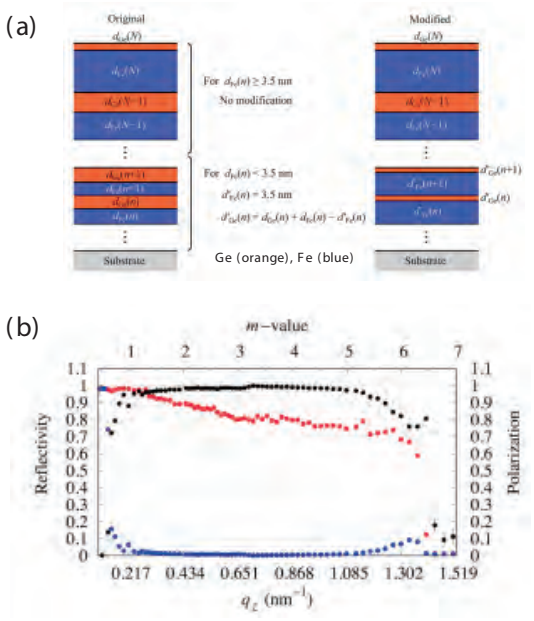

Fig. 2. (a) A schematic of the original (left) and modified (right) layer sequence for the polarizing supermirror, and (b) polarized neutron reflectivity profile with the new Fe/Ge polarizing supermirror. R+ and R- are shown in red and blue [2].

that of nickel. However, such thin iron layers lose spontaneous magnetization, where the magnetic reflectivity decreases significantly. To overcome this problem, a modified multilayer scheme is proposed, where the minimum thickness for the iron layers is kept at 3.5 nm while those of Germanium decrease to less than 2 nm (Fig 2(a)). The magnetization of the thin iron layers is maintained at a high level thanks to the ferromagnetic interlayer exchange coupling (IEC) between the iron layers. The new Fe/Ge polarizing supermirror that positively incorporates this ferromagnetic IEC has extended the magnetic reflection to the higher m-value of 6.2 (Fig. 2(b)). This is the highest m-value achieved to date in the world [2].

References

[1] K. Toh, *et al*., Nucl. Instr.& Meth. A **726** 169 (2013).

[2] R. Maruyama *et al*., J. Appl. Phys. **130** 083904 (2021).

Muon Section

1. Commenced production of the third muon production target

In response to the remarks by the Muon Advisory Committee (MAC) and the International Advisory Committee (IAC) of J-PARC, the Muon Science Section received a budget for the production of a new muon target in FY2021. This is to reduce the current risk of operating without a spare target as a result of the unexpected failure of target Unit #1 in FY2019, which was replaced with a spare (Unit #2). The project will be carried out over two years, with the target storage container fabricated in the first year and the rotating target body in the second year. This is because it is necessary to reexamine the applicability of the Hot Isostatic Pressing (HIP) technique in advance, which is the key to target fabrication.

In the meantime, the rotating feeder unit was replaced as part of the maintenance in the summer shutdown period. It is recommended to replace it every two years, considering the wear and tear on the bearings. This was the first time since the rotating target itself has been replaced, and the work was carried out following careful preparation (see Fig. 1). However, turbulence in the motor torque was confirmed during the test operation after the work, presumably caused by misalignment of the joint connecting the motor shaft and the rotating shaft on the vacuum side.

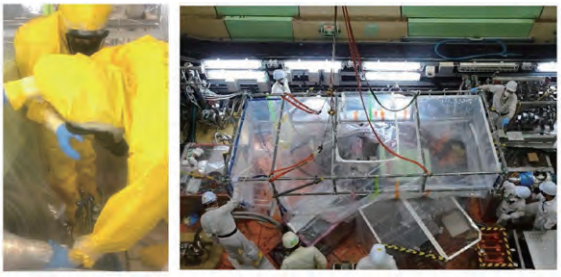

Fig. 1. A snapshot of the target maintenance work (left) which was conducted within a greenhouse set-up in the M2 tunnel (right).

To resolve this problem, another adjustment was attempted near the end of the maintenance period. However, subsequent beam operations revealed that the situation had not improved, suggesting that the connection accuracy between the motor shaft and the rotating shaft was inadequate due to manual work. Therefore, it was decided to replace during the next maintenance period the flexible joint for the connection with one that has a higher tolerance for shaft misalignment, and the model selection and testing proceeded.

2. Commissioning of the H-Line

The H-line, a new beamline, has been under construction since FY2012 in Experimental Hall No.1 of the MLF building. It is a general purpose beamline that can deliver both positive and negative muons and has branches to two experimental areas named H1 and H2. The designed surface muon flux reaches 10^8 muons/s with a proton beam power of 1 MW owing to a large acceptance (108 mSr) capture solenoid and other beamline magnets with large apertures.

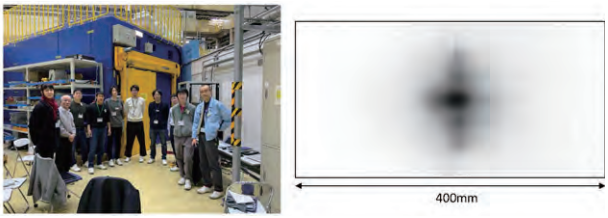

Fig. 2. The H1-commissioning team headed by T. Yamazaki (left), and the muon beam profile measured by an imaging plate at the exit to the H1 area.

As for the beamline to H1, the installation of cooling water piping and power cables progressed during the summer shutdown period and was almost completed by the end of November. In addition, the review of the facility modifications, including those for MUSE by the Nuclear

Regulation Authority, which had been delayed due to COVID-19 during this period, was finally completed and operation permit was granted. The beam commissioning started in January 2022. During the beam commissioning, a large positron/electron background appeared because the DC separator had not yet been installed. Although this made beam commissioning difficult, the commissioning team was able to measure the beam intensity, profile, and momentum of the surface muons (see Fig. 2). The beam intensity of negative muons at several momenta was also measured.

3. Renovation of the beam kicker system on the S-Line

The S line is designed and built mainly for surface muon beams, and the beam kicker system allows muon experiments to be performed simultaneously in two areas, S1 and S2, by splitting a double pulse into two single pulses. The stable operation of the kicker device is very important as S2 begins operation in 2021.

The kicker device has encountered several problems since the start of the S-Line operation in 2017. One of these is the failure of the MARX board, which continues to occur several times a year. Since the failure was found to be caused by a certain component, the replacement of all 384 components on the MARX board was carried out during the summer shutdown period before the full-scale simultaneous operation of the S1 and S2 areas began.

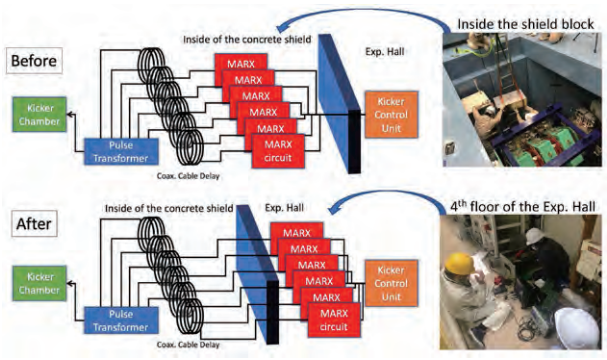

Fig. 3. A schematic illustration of the beam kicker sys-tem before and after the relocation of the power supply.

Drastic measures were also taken during the summer shutdown period to address another issue: the location of the kicker power supply. The kicker power supply was installed inside the concrete shielding of the S-Line to reduce the potential impact of noise generated by the electric field kicker on the experimental equipment. Therefore, the concrete shield had to be opened and replaced every time a MARX board failed, making the work extensive and difficult. To resolve this issue, the kicker power supply unit was relocated to the power supply yard to facilitate access during repairs (see Fig. 3). Upon the completion of the relocation work, the entire system was confirmed to be operational within the required specifications. Since then, although the MARX board failed due to a cause other than the replaced component, the operation could be resumed within a maximum of half a day after the failure detection, a significant improvement over the previous situation in which it took up to seven days to resume operation.

4. Laser system for Ultra-slow muon

Ultra-low velocity muons can be produced by resonant photoionization of thermal muonium from hot W-foil targets. In particular, a high-energy pulsed coherent Lyman-α light source is one of the most critical elements for the efficient generation of ultra-low-velocity muons. The high photon energy of vacuum ultraviolet light causes degradation of optical materials over time. In addition, photochemical reactions that occur between vacuum ultraviolet light and residual gases cause degradation of the performance of the Lyman-α steering mirror. Degradation of the optics leads to a loss of ultra-slow muon yield and beam downtime for optics replacement. The surface of the mirror becomes noticeably cloudy when the same area is continuously irradiated with Lyman-α light for an extended period of time.

This year, we introduced a drive mechanism that changes the laser reflection position of the mirrors for vacuum ultraviolet light and restores the reflectivity of the two mirrors. This device adds a mirror displacement function to the mirror mounts that can adjust the horizontal angle and vertical tilt of the mirrors. The mirror mount located upstream has a rotation stage to rotate a ϕ50 mm circular mirror and a linear-motion stage (30 mm stroke). The mirror mount on the down-stream side uses a 50 mm square cylindrical mirror, which introduces horizontal and vertical motions. These stages have built-in encoders that record the movement history of the mirror positions, allowing the laser reflective surface to be set to the unirradiated area when the reflectivity of the mirror decreases. The new mirror steering and displacement device enable the mirror irradiation position to be adjusted by remote control without opening the vacuum chamber to the atmosphere.

Technology Development Section

We developed a current-biased kinetic inductance detector (CB-KID) to perform high spatial resolution imaging with a high energy resolution and a large sensitive area. High speed readout circuit, named Kalliope-DC, was used to read signals from four output channels of CB-KID under pulsed neutrons by a delay-line technique. Neutrons are converted into charged particles in a ^{10}B conversion layer to create quasi-particle hot spots in CB-KID. The CB-KID detects a neutron based on local changes in kinetic inductances in X and Y meanderlines under modest DC bias currents (Fig. 1). We demonstrated the spatial resolution of 16 μm [1] and a homogeneity of neutron image in a sensitive area of 15 mm×15 mm [2].

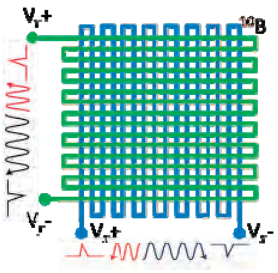

Fig. 1. Schematic illustration of the CB-KID detector.

As a practical test of the CB-KID imaging, we compared the SEM image with the neutron transmission image with a test sample containing many Gd islands of different sizes (Fig. 2) [3]. The gray-colored stripes in Fig. 2(a) were produced by re-deposition of the stainless-steel mask during ion milling of the sample, but they are not visible by neutrons as in Fig. 2(b). Hence, two Gd islands in yellow dotted ovals around two Gd islands are not shown clearly with a SEM probe while those in violet ovals can be discerned in the transmission image of Fig. 2(b). We demonstrated a good linearity between the Gd-islands sizes of neutron images and SEM images over the wide range from 20 μm to 130 μm (Fig. 3). Fig. 4 shows the CB-KID neutron transmission image (0.1 to 1.13 nm) of a Wood's metal sample. We found that the bright dendritic lines manifested from a Cd-rich phase are visible among four-different phases of the Wood's metal. This can be utilized as a tool to study the pattern formation in solidification of alloy.

In summary, we demonstrated an example of the practical implementations of the CB-KID neutron transmission imaging as SEM observations can do using the test sample with various different-sized Gd islands. We also demonstrated that the CB-KID imaging clearly observed a needle-like fine Cd-rich phase while it is not so easy to observe it with SEM. We consider that the CB-KID system can widely be used as a useful tool to investigate various samples in the fields of material sciences.

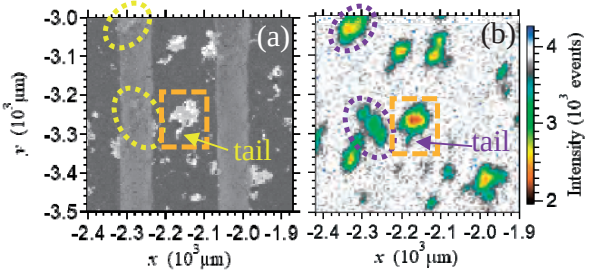

Fig. 2. (a) the SEM image and (b) neutron transmission image observed by CB-KID with a Gd test sample deposited on a Si substrate. A Gd island in a dotted square appears clearly in both images including a fine tail.

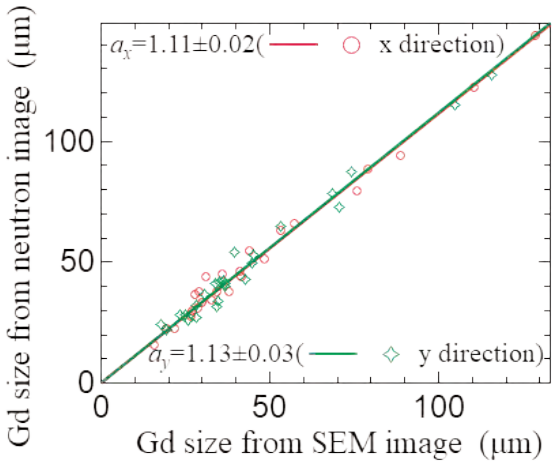

Fig. 3. Good correlation of the sizes of the various Gd islands estimated by the neutron transmission (vertical axis) and SEM imaging (horizontal axis) over the wide range.

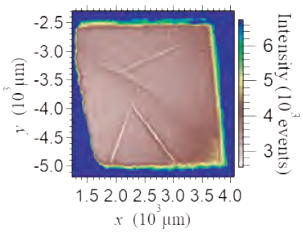

Fig. 4. Neutron transmission image of a Wood's meal taken with neutron wavelengths from 0.1 to 1.13 nm. Needle-like Cd-rich phases can be seen clearly as one of the four different phases of the alloy.

This work was partially supported by a Grant-in-Aid for Scientific Research (Grant Nos. JP16H02450, JP21H04666, JP21K13566) from JSPS and the MLF project program (No. 2020P0201).

References

[1] H. Shishido *et al.*, Phys. Rev. Applied **10** (2018) 044044.

[2] T.D. Vu *et al.*, Supercond. Sci. Technol. **34** (2021) 015010.

[3] T.D. Vu *et al.*, Nucl. Inst. Meth. Phys. Res. A **1006** (2021) 165411.

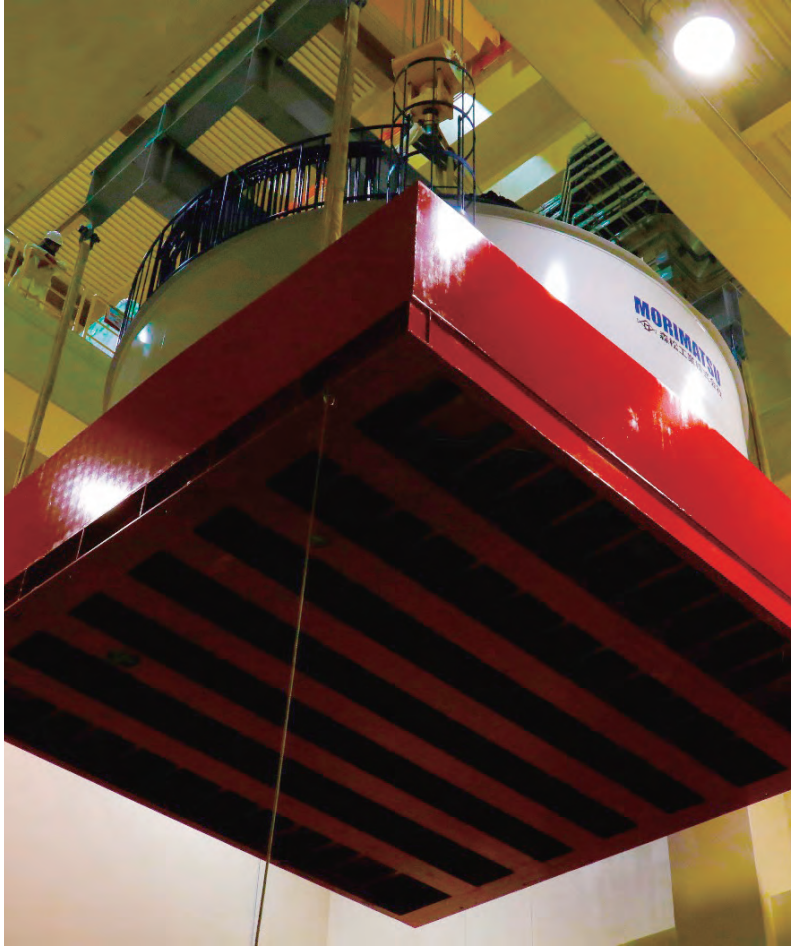

Particle and Nuclear Physics

Neutrino Experiments

As continuation of JFY2020 beam run, Neutrino Experimental Facility restarted beam operation on April 8th, and ended the JFY2021 run on April 27th. With stable operation of 510kW beam power, total integrated POT (proton-on-target) since 2009 of 2.17×10^{21} (so-called neutrino mode) and 1.65×10^{21} (so-called anti-neutrino mode) were accumulated. The next beam run is scheduled to start from fall 2022, after one-and-half-years-long maintenance and improvement work period.

The T2K Experiment was carried out without ND280 due to COVID travel restriction. On-axis INGRID, new detectors Wagasci and BabyMIND were successfully operated. The far-detector SuperKamiokande (SK) doped with 0.01% gadrinuim was successfully operated, and showed neutron capture rate as expected. SK will increase the concentration to 0.3% for the coming beam run. Re-analysis of data with a new nuclear model, new cross section data, and improved flux tuning is in progress.

NINJA experiment, aiming at precision study of neutrino-nucleus interaction with hybrid emulsion detectors, successfully carried out a pilot run with heavy-water target and a novel time stamp mechanism.

Many improvement works toward 1.3MW beam power was carried out in JFY2021, as well as various maintenance work. One of the biggest works is to replace magnetic horns with high-power-withstanding new horns. Construction of the new horns were in progress in Japan and in Colorado. Another big work is to

replace the heat exchanger of the target with new high-capability one, and design, test, and fabrication was in progress. Also carried out were fabrication of a new magnet for the primary beamline and its power supply, high-speed DAQ, strengthening of interlock, and a new facility for radio-active water processing. Detail of the work is reported as the Highlight article.

T2K conducted ND280 upgrade to improve detector performance and systematic errors to best utilize the high-statistics achieved by high beam power. Construction of new detectors SuperFGD, High-angle TPC, and ToF detectors were carried out under heavy disruption by COVID. They are not yet recovered from the delay caused by COVID, and investigating the way to minimize the impact.

HyperK project is proceeding soundly. Excavation of access tunnel was started. New 50-inch PMT fabrication and their test is in progress. Off-site IWCD, intermediate water Cherenkov detector, is under investigation of site candidate, civil construction methods, and cost estimation.

At MLF, JSNS2 experiment to search for sterile neutrinos continued data taking until June 22nd with 700kW beam power. New trigger dedicated for detecting sterile neutrino has been installed, and 1.45×10^{22} POT was accumulated. Blind analysis is in progress for the data. From January 15, 2022, data taking was resumed and continue until June. A new step, JSNS-II has started. The TDR was submitted and stage-II was requested at the PAC meeting. A new detector at 48m from the target, outside of the MLF experimental hall, is under construction. The stainless steel tank construction was completed, and fabrication of inside equipments such as acrylic vessel will be started from 2022.

Dr. Chris J. Densham at Rutherford Appleton Laboratory, a collaborator of T2K experiment, was awarded the 2021 Institute of Physics Prize for Outstanding Professional Contributions to accelerator science and technology for his novel contribution to the high-power target.

Hadron Experimental Facility (HEF)

J-PARC Hadron Experimental Facility (HEF) was developed for the fixed-target particle and nuclear physics experiments using secondary particle's beams produced by slowly extracted (SX) high-intensity proton beam from Main Ring (MR) synchrotron as well as the 30-GeV primary proton beam. In 2021, the beam operation to HEF was performed at the maximum beam power of 64.5kW during March 27th to April 7th and May 10th to June 29th, including the 8-GeV beam tuning and extinction measurement for COMET experiment during May 20th to 25th. In total 6 experiments were conducted at K1.8, K1.8BR, KL, and high-p beam lines.

In 2021, about 1 year shutdown of MR operation has been scheduled for the power supply upgrade. In this period, construction of new beam line (C-line) for COMET experiment and change-over of the spectrometer have been processing, in addition to the ordinary maintenance works. The C-line is branched from the high-p beam line (B-line) in Hadron Hall and delivers 8-GeV beam to Hadron South Hall. The construction of C-line in Hadron Hall including the air-tight and

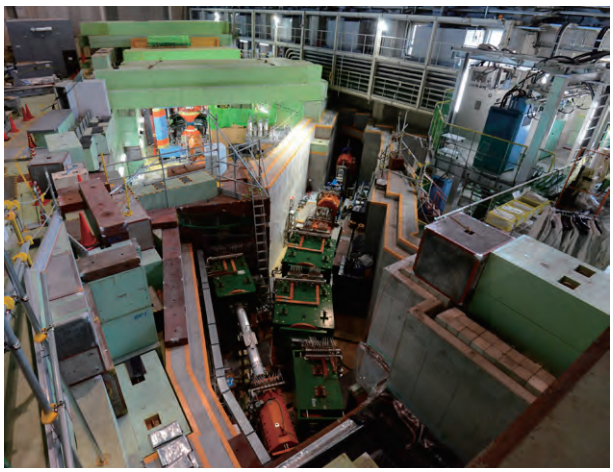

Fig. 1. Photograph of the branch point of B (to up direction in the figure) and C (to right up direction) lines in Hadron Hall taken before closing the shielding structure.

radiation shielding structure was completed (Fig.1). At K1.8 area, KURAMA spectrometer with a single dipole magnet was dismantled. Then three magnets for high-resolution S-2S spectrometer with Q-Q-D configuration were installed.

Strangeness/Hadron Experiments

Data-taking of two experiments on X-ray spectroscopy of Ξ^--Fe atom (E03) and search for *H*-dibaryon (E42) was completed at K1.8 beam line. These experiments used KURAMA spectrometer to measure outgoing K^+ in the (K^-, K^+) reaction. Pilot data were obtained to estimate the production rate of $^3_\Lambda$H and tagging rate of its mesonic decay for $^3_\Lambda$H lifetime measurement (E73) at K1.8BR beam line. Beam and detector commissioning and Run-0 data-taking were performed at high-p beam line by the E16 which aims to study in-medium mass modification of vector mesons and the generation mechanism of hadron mass.

Several results from the experiments were published in FY2021, E40 conducted at K1,8 in 2018 to 2022 reported differential cross sections for $\Sigma^- p$, $\Sigma^+ p$ elastic scattering, and $\Sigma^- p \rightarrow \Lambda n$ inelastic scattering (see highlight article). E62 conducted at K1.8BR in 2018 reported measurements of the 3d→2p transition X rays of kaonic ^{3}He and ^{4}He atoms using superconducting transition-edge-sensor microcalorimeters with an energy resolution better than 6 eV [1]. The energies of 6224.5 ± 0.4 (stat) ± 0.2 (syst) eV and 6463.7 ± 0.3 (stat) ± 0.1 (syst.) eV and widths of 2.5 ± 1.0 (stat.) ± 0.14 (syst.) eV and 1.0 ± 0.6 (stat.) ± 0.3 (syst.) eV were determined, for kaonic ^{3}He and ^{4}He, respectively. These values are nearly 10-times more precise than in the previous measurements. These results exclude the large strong-interaction shift and widths as shown in Fig.2. These results confirmed that the standard antikaon-nucleus interaction models work well in these atomic systems.

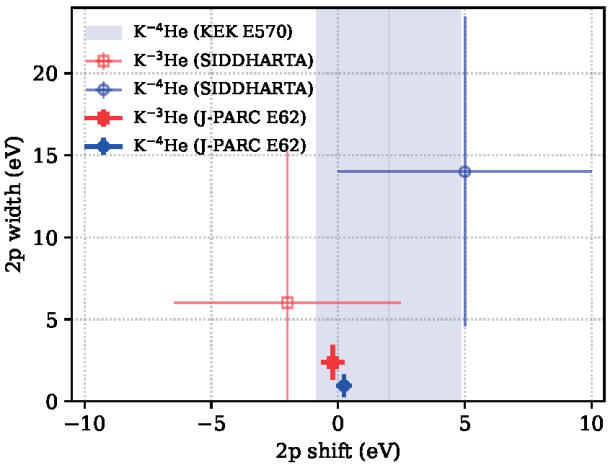

Fig. 2. Energy shift and width of 2p state of kaonic 3He (red) and 4He(bule) atoms determined by J-PARC E62. Previous measurements are also plotted.

References

[1] T. Hashimoto *et al.*, Phys. Rev. Lett. **128**, 112503 (2022).

Kaon Decay Experiment

The KOTO experiment studies the decay of a long-lived neutral kaon into a neutral pion (π^0) and a pair of neutrinos. The process breaks CP symmetry directly and its branching fraction is theoretically well predicted in the Standard Model as $(3.0 \pm 0.3) \times 10^{-11}$. The detection of this decay is challenging because only two photons from π^0 are observable, and the decay mode has not been observed. By examining this ultra-rare decay, a new source of CP symmetry breaking that can explain the matter-antimatter asymmetry in the universe may be revealed.

One of the important issues in studying a rare process is to control backgrounds that come from ordinary processes. In the analysis of the data accumulated in 2016-18, KOTO found that even O(10^{-5}) contamination of charged kaons in the neutral beam can cause backgrounds at the sensitivity level of 7×10^{-10}. In order to reduce this background, KOTO had installed a counter to detect charged particles at the entrance of the KOTO detector, called Upstream Charged Veto (UCV), first in 2020 and upgraded it for a better performance in early 2021. KOTO continued accumulating data with new UCV in May-June 2021. Data analysis is underway.

In parallel to the analysis efforts, KOTO is preparing for the next run. One is the upgrade of the data acquisition system to accommodate a higher beam power. The other is the further upgrade of UCV, aiming for a less material in the beam and a better radiation tolerance. These upgrades will be finished before the next beam time in FY2022. In addition, the design of a permanent magnet, which is installed at the end of the neutral beam line and sweeps out the charged kaons, is in progress for further background rejection toward a future sensitivity.

Search for Charged Lepton Flavor Violation

COMET aims to identify muon-to-electron conversion with a sensitivity higher than 10^{-14}. Intensive research and development were conducted in FY2021.

The cylindrical drift chamber performance was studied in details using cosmic-ray muons. The detector will be transported to J-PARC in 2022 for the final conditioning before installation to the COMET experiment area. The construction of a straw tube tracker and the installation of lutetium yttrium orthosilicate (LYSO) crystals for the electron calorimeter is currently in progress.

The construction of a capture solenoid (CS), which is used to acquire and transport pions / muons produced by the COMET primary proton target is in progress. The construction of the CS cryostat was successfully completed in 2021, followed by installation of the coil to the cryostat in 2022. The cryogenics system preparation has taken a great step forward; a liquid helium transfer tube containing super-conducting cable power lines was installed and connected to a muon transport solenoid (MTS). The MTS excitation test will be conducted before summer 2022.

COMET beam line construction completed in FY2021 and starts beam operation in early 2023 to carry out an engineering run. The proton beam at 8 GeV will be transported to the COMET primary beam line area and produce pions / muons on a production target made of a thin graphite plate. Pions and muons, decay products of the pions, will be transported to the COMET experiment area through MTS. A set of diagnostic detectors is installed to measure the beam phase space and background.

In parallel to these activities COMET carried out a proton beam extinction factor measurement in May 2021 at the K1.8BR beam line in Hadron Hall. A new beam injection scheme to MR from RCS was employed to confirm the beam extinction factor better than 10^{-10}.

Discussion for Future Plan of HEF

Several workshops both domestic and international were organized by HEF user community, Hadron Hall Users' Association (HUA). The workshops aim to discuss the future plan of HEF, namely HEF Extension Project, from both physics and facility design sides. Lists of the workshops are found in HUA web page [2]. Discussions are summarized in the 3rd White Paper on HEF Extension Project [3].

The project was reviewed by the international review committee formed under the J-PARC PAC and Institute of Particle and Nuclear Studies (IPNS), KEK. The meeting on the focused review was held on August 10, 11, and 18. High evaluation for the project was obtained.

References

[2] http://www.rcnp.osaka.u.ac.jp/~jparchua/en/hefextension.html

[3] arXiv:2110.04462 [nucl-ex] 9 Oct. 2021

Precise Measurements with Muons

The precision measurements of the anomalous magnet moment (g−2) and electric dipole moment (EDM) of muons are in preparation at J-PARC MLF. The collaboration continued the development of the room-temperature muon source, linear accelerators, beam injection beamline, storage magnet, and positron detector. The engineering design of the exterior preparation of the construction site was completed. The major achievements in this fiscal year are the first beam delivery of surface muon beam in H-line, successful start of the muoninum ionization tests at the S2 area, fabrication of the full IH-DTL cavity, and fabrication of rotating quadrupole for the injection beamline.

The virtual workshop on the muon g−2 theory initiative in June 2021

Theory Group

The mission of the theory group at the J-PARC branch is to investigate the theoretical aspects of particle and nuclear physics in collaboration with the experimental groups. The group consists of three IPNS staff members and four visiting researchers.

Owing to the COVID-19 pandemic, the activities of the theory group were mainly conducted online. Seminar series on J-PARC heavy-ion project, and four international online workshops on "Physics of Omega Baryons at the J-PARC-K10 beam line", "GPDs and related topics at J-PARC", "First and Second International Workshop on the Extension Project for the J-PARC Hadron Experimental Facility," and two domestic workshops on "Physics at the J-PARC K10 Beam line" and "J-PARC Hadron 2022" were organized by the group members. More than fifteen research papers were published in 2021.

Technical Support Group (Esys-Tokai)

The electronic systems group constructs electronic systems for Institute of Particle and Nuclear Study, KEK and collaborates with other institutes through a framework known as "Open-It." Regarding the J-PARC experiments, A MPPC signal digitizer ASIC using 100MHz 10bit ADC was developed and shows good signal-to-noise ratio (Fig. 3). Figure 4 shows a SiC pixel sensor and its performance before irradiation of radiation. We plan to irradiate the SiC pixel sensor for evaluating its performance for radiation-tolerant applications.

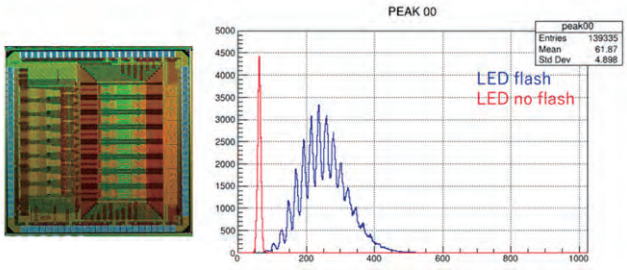

Fig. 3. A MPPC signal digitizer ASIC and ADC spectra with and without flash.

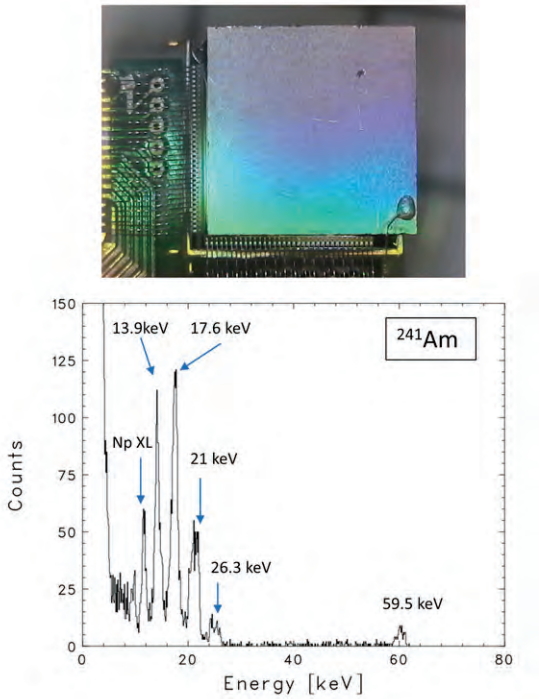

Fig. 4. A SiC pixel sensor and the measured spectrum for 241Am.

— Research Highlight —
Successfully obtained high-statistics Σ-proton scattering data at Hadron Experimental Facility

In order to elucidate nuclear force that acts between nucleons (*N*s) and forms atomic nuclei, baryon-baryon interaction by adding strange (*s*) to up (*u*) and down (*d*) quarks and extending Ns to octet baryons including hyperons (*Y*s) are intensively investigated at Hadron Experimental Facility (HEF). Scattering experiments are direct methods to investigate the interactions. For *NN* interaction, precise data on not only cross sections but also spin observables in wide angular and incident energy range were obtained by proton-proton (*pp*) or proton-neutron (*pn*) scattering experiments. Based on rich data, theoretical models have been constructed. So called "realistic nuclear force" predicted by these models is basic input for nuclear many-body calculations to study nuclei.

On the other hand, *YN* scattering experiments have been difficult and their data are very scarce. So far only data exist from bubble chamber experiments in 1960s and experiments using the scintillating fiber or scintillator target in late 1990s. In those experiments, number of hyperons were limited by their production rates and short lifetimes and scattered events were recorded and analyzed by the image-based methods. Carbon in the scintillation fiber also made backgrounds and degraded efficiency in the event identification. Consequently number of data points and their statistics were very limited. Recently high-statistics Σ hyperon-proton scattering experiment (J-PARC E40) was successfully carried out using high-intensity pion beam to produce Σ hyperons and modern detectors which can be operated under high-intensity beam circumstance.

Theoretically the Σ*N* interaction is predicted as strongly spin (S) and isospin (I) dependent. The only observed Σ hypernucleus ($^{4}_{\Sigma}$He) [1] is formed by the attraction in the S=1, I=1/2 channel. The spin- and isospin- averaged nuclear potential is known to be repulsive from the Σ quasi-free production spectra on several nuclei [2]. Therefore, details of the Σ*N* interaction should be investigated by the scattering experiments. The J-PARC E40 aims to study the Σ*N* interaction systematically by measuring differential cross sections of $\Sigma^- p$ [3] and $\Sigma^+ p$ [4] elastic and $\Sigma^- p \to \Lambda n$ [5] inelastic channels in the Σ momentum range of ~450 to ~800 MeV/*c*, where *P* and higher partial waves would contribute. Another interesting topic is the short-range repulsion in the $^3S_1$, I=3/2 channel ($\Sigma^+ p$). Due to the Pauli effect between quarks, larger repulsive core than that in the *NN* channel is expected in this channel, especially by the models based on quark picture and this may be one of keys to understand the origin of the repulsive core of nuclear force.

The experiment was carried out at K1.8 beam line of HEF from 2018 to 2020. The experimental setup and concept of the $\Sigma^- p$ scattering measurement are shown in Fig.1. Σ hyperons were produced via the $\pi^{\pm} p \to K^+ \Sigma^{\pm}$ reactions on a liquid hydrogen (LH_2) target. By measuring momenta of the beam π and the outgoing K^+ with Beam and KURAMA magnetic spectrometers, respectively, the production was identified and momentum of Σ was obtained. In total 1.62×10^7 Σ^- and 4.9×10^7 Σ^+ were accumulated.

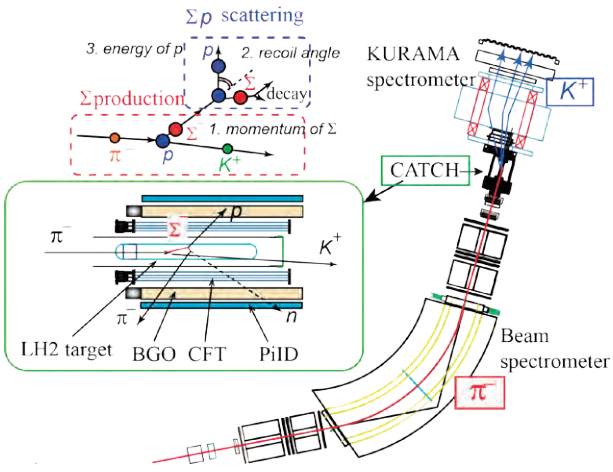

Fig. 1. The experimental setup and concept of the $\Sigma^- p$ scattering measurement are shown with an enlarged figure around the LH_2 target.

Scattering occurred between the running Σ and a proton in the LH_2 target was measured by CATCH detector [6] surrounding the LH_2 target. It consisted of a cylindrical scintillation fiber tracker (CFT), BGO calorimeter and scintillator hodoscope (PiID). The direction and energy of proton can be measured. But only direction can be measured for pion since pion may pass through

BGO. The events were identified by checking kinematical consistency. For example, in case of the $\Sigma^- p$ elastic scattering, the recoil proton was detected by CATCH. The proton kinematic energy can be calculated by assuming the kinematics of the elastic scattering at the scattering angle obtained from the Σ^- momentum vector and the proton direction and is compared with the measured one. Approximately 4500 $\Sigma^- p$ elastic, 2300 $\Sigma^- p$ inelastic, and 2400 $\Sigma^+ p$ elastic events were identified. These numbers are typically 100-times larger than those in the past experiments.

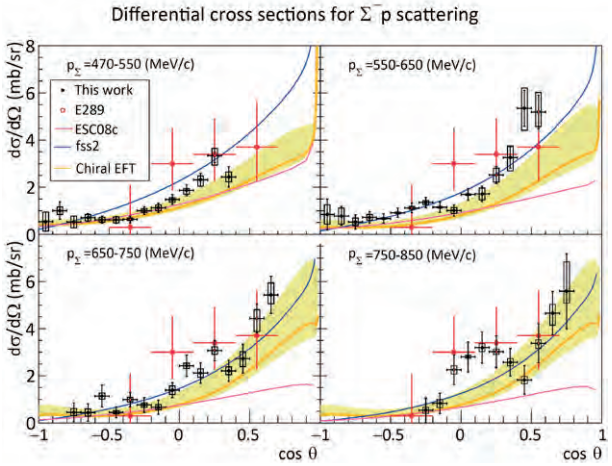

Fig. 2. Differential cross sections for $\Sigma^- p$ elastic channel obtained in J-PARC E40 (black points) [3]. The error bars and boxes show statistical and systematical uncertainties. The red points show the previous experimental data [7] (the same for all incident momenta). The dotted, dot-dashed, and solid lines present the prediction of theoretical models; Nijmegen ESC08 [8], fss2 [9], and χEFT with shadows for error bands [10], respectively.

Differential cross sections were obtained from numbers of the accumulated Σs and the identified events, the effective proton areal density with the correction by the Σ running path length in the LH_2 target, detection efficiencies, and solid angle acceptance of CATCH. Angular distribution of the differential cross sections for $\Sigma^- p$ elastic and inelastic channels are shown in Fig. 2 and 3, respectively, with the previous experimental data [7] and theoretical predictions by Nijmegen ESC08 / ESC16 based on meson-exchange [8], fss2 based on quark picture [9], and chiral effective field theory (χEFT) [10].

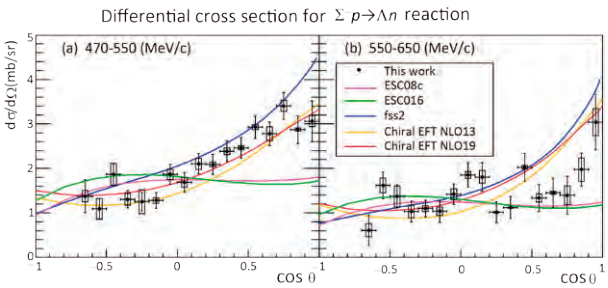

Fig. 3. Differential cross sections for $\Sigma^- p \rightarrow \Lambda n$.[5]

Obviously the data quality has improved drastically; smaller uncertainties and finer angular and incident momentum divisions for the $\Sigma^- p$ elastic channel and the first data for the $\Sigma^- p$ inelastic channel. The present data show forward peaked angular distribution as theoretical models predict, although small discrepancies are seen in some models. Theoretical models, however, can be improved using the present excellent data as inputs.

Experimental techniques developed in J-PARC E40 can be applicable for the Λp scattering experiment in near future. Recently three-body baryon force (3BF) is discussed in the context of neutron stars. In the study of 3BF, hyperon scattering experiments are also essential since they provide the basic information on 2-body baryon interactions in free space. The precious *YN* scattering data at present and in future will provide the better understanding of nuclear force and high-density nuclear matter inside neutron stars.

Reference

[1] T. Nagae *et al.*, Phys. Rev. Lett, **80**, 1605 (1998).

[2] P. Saha *et al.*, Phys. Rev. C**70**, 044613 (2004).

[3] K. Miwa *et al.*, Phys. Rev. C**104**, 045204 (2021).

[4] T. Nanamura *et al.*, Prog. Theor. Exp. Phys. **2022**, 093D01 (2022)

[5] K. Miwa *et al.*, Phys. Rev. Lett. **128**, 072501 (2021).

[6] Y. Akazawa *et al.*, Nucl. Instr. Meth. A**1029**, 166430 (2022).

[7] Y. Kondo *et al.*, Nucl. Phys. A **676**, 371 (2000).

[8] T. A. Rijken, M. M. Negels, and Y. Yamamoto, Prog. Theor. Phys. **185**, 14 (2016).

[9] Y. Fujiwara, Y. Suzuki, and C. Nakamoto, Prog. Part. Nucl. Phys. **58**, 489 (2007).

[10] J. Haidenbauer *et al.*, Nucl. Phys. A**915**, 24 (2013)

— Research Highlight —
Upgrades to the Neutrino Beamline Underway for T2K and Hyper-Kamiokande

The current T2K (2010—2027) and future Hyper-Kamiokande (HK) (2027—) long-baseline neutrino oscillation experiments rely on neutrinos produced at the J-PARC high-power neutrino facility. High statistics neutrino data are needed to achieve world-leading neutrino oscillation measurements [1,2].

The T2K and HK neutrino beams are produced by interactions of high-energy protons from the neutrino primary beamline with a long graphite production target in the neutrino secondary beamline. Outgoing particles from the target are then focused in three electromagnetic focusing devices, called *horns*, and allowed to decay into neutrinos. The number of neutrinos available for these experiments can be increased by increasing the number of protons, or by improving the focusing of the neutrino parent particles.

The proton beam power will be increased from 500 kW to 750 kW in 2021/2022, and 1.3+ MW in the future. Along with 2021/2022 upgrades to the J-PARC Main Ring (MR) accelerator towards a higher power proton beam, various upgrades to the neutrino beamline facility are also underway [3]. These upgrades will allow the neutrino facility to accept the upgraded high-power proton beam from the MR.

The most downstream end of the neutrino primary proton beamline has a high radiation level due to proton backscattering from and interactions with the neutrino production target. The radiation level is proportional to the proton beam power, such that upgrades towards semi-remote handling of irradiated beamline equipment are needed for later stages of T2K and early stages of HK. In 2021, the most downstream bending magnet in the neutrino primary beamline was replaced with a shorter, higher field magnet, as shown in Fig.1. New devices for quick maintenance of activated equipment in this region of the beamline were then installed in the additional space made available by the shorter bending magnet.

Upgrades to proton beam monitors are also underway. A prototype non-destructive proton beam profile monitor utilizing beam induced fluorescence was installed in the primary beamline, and final tests of the prototype monitor were carried out in 2021. Based on these test results, upgrades towards a full working monitor will be carried out in 2022. An Optical Transition Radiation monitor (OTR) continuously measures the proton beam position and profile directly upstream of the neutrino production target. In 2021, the spent most upstream horn (Horn 1) and OTR were removed from the beamline and various tests were performed on the old OTR system, as shown in Fig.2. An upgraded OTR system will be installed in 2022. This work is possible thanks to remote and onsite OTR experts from Canadian institutes.

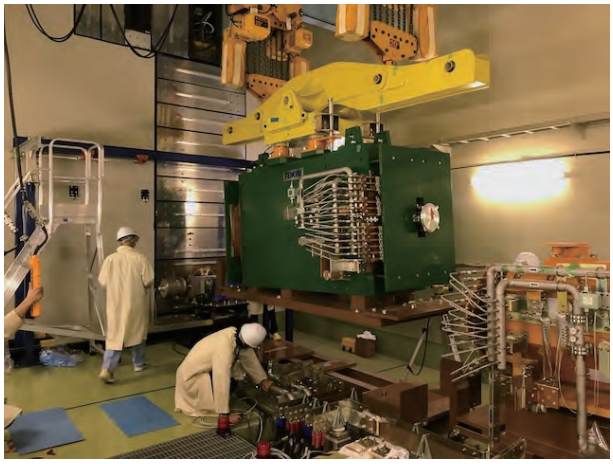

Fig. 1. New shorter bending magnet being installed at the downstream end of the neutrino primary beamline

In the secondary beamline, horns are used to focus hadrons of the correct charge sign produced by proton beam interactions with the target. At the same time, hadrons of the incorrect sign are defocused. This allows for production of a relatively pure beam of, for example, muon neutrinos, with a ~3% contamination of muon antineutrinos at the flux peak. Until 2021, the horns were run at a current of ±250 kA. A new, additional horn power supply has been installed, allowing the horns to be run at \(\pm\)320~kA from the next T2K data-taking period. This increased horn current will improve the focusing of neutrino parent particles, increasing the number of, for example, neutrinos by ~10%, and decreasing the number of antineutrinos by ~5%.

A new Horn 1 and Horn 2 (shown during fabrication in Fig.3) were produced at the University of Colorado in the United States and shipped to J-PARC. Design

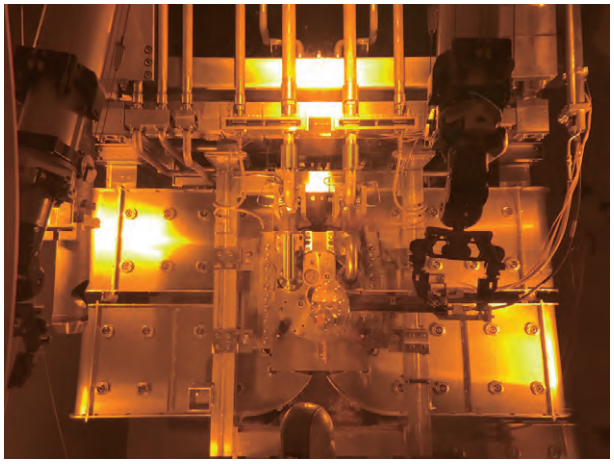

Fig. 2. Spent Horn 1 and OTR undergoing inspection in the neutrino secondary beamline facility maintenance area.

upgrades, especially for the cooling scheme of Horn 2, will allow these horns to be used at higher proton beam powers. Preparation work to install the new horns has been ongoing, and the new horns will be installed in the secondary beamline in 2022.

At the same time, a new neutrino production target, produced at Rutherford Appleton Laboratory in the UK, will also be installed. An improved cooling system for the target, to allow the target to accept a higher power proton beam, has also been developed and will be installed in 2022.

It is essential to properly handle radioactive water generated during the neutrino beam production process. Improvements in the facility for handling radioactive cooling water are also underway, and a new dilution tank, which will increase the water processing capacity by a factor of >5, is under construction.

These J-PARC neutrino facility upgrades to >750 kW will be completed in 2022, and then the neutrino beamline will be ready to accept the upgraded MR proton beam. Further upgrades towards 1.3 MW will be completed for the HK experiment.

Fig. 3. New Horn 2 under production at the University of Colorado.

Reference

[1] K. Abe *et al.* (T2K Collaboration), Nature **580**, 339 (2020).

[2] K. Abe *et al.*, (HK proto-collaboration), arXiv:1805.04163 (2018).

[3] Abe *et al.*, arXiv:1908.05141 (2019).

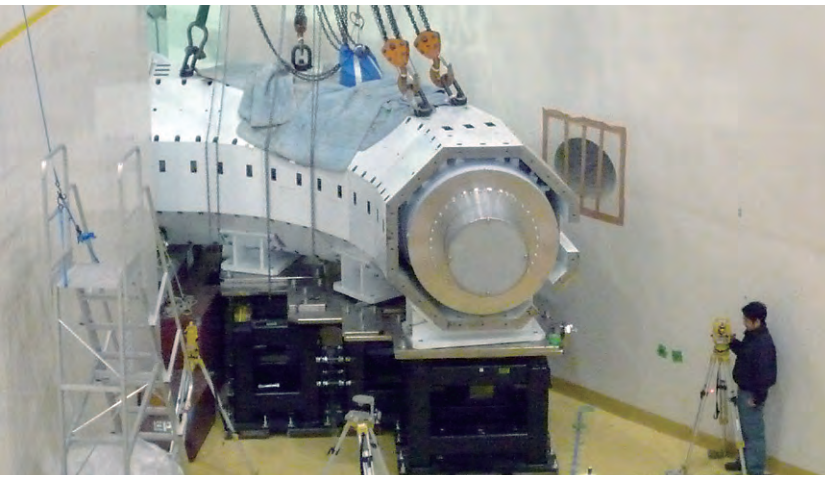

Cryogenics Section

Overview

The Cryogenics Section supports scientific activities in applied superconductivity and cryogenic engineering, carried out at J-PARC. It also supplies cryogen of liquid helium and liquid nitrogen. The support work includes maintainance and operation of the superconducting magnet systems for the T2K neutrino beamline and the muon beamlines at the Materials and Life Science Experimental Facility (MLF) and construction of the magnet systems at the Hadron Experimental Facility (HEF). It also actively conducts R&D works for future projects at J-PARC.

Cryogen Supply and Technical Support

The Cryogenics Section provides liquid helium cryogen for physics experiments at J-PARC. The used helium is recycled by the helium gas recovery facility at the Cryogenics Section. Figure 1 summarizes the liquid helium supply in FY2021.

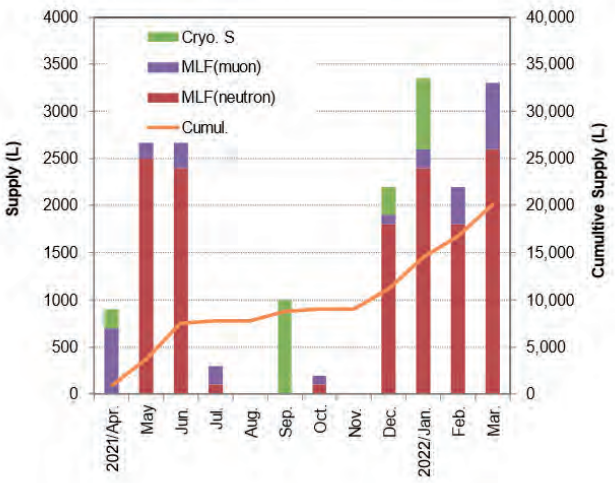

Fig. 1. Liquid helium supply at J-PARC from April 2021 to March 2022.

Liquid nitrogen was also supplied to the users for their convenience. Its amount in FY2021 is summarized in Fig. 2. The MR has been shut down for more than a year for the upgrade, so the amount of liquid nitrogen usage has decreased compared with the last year.

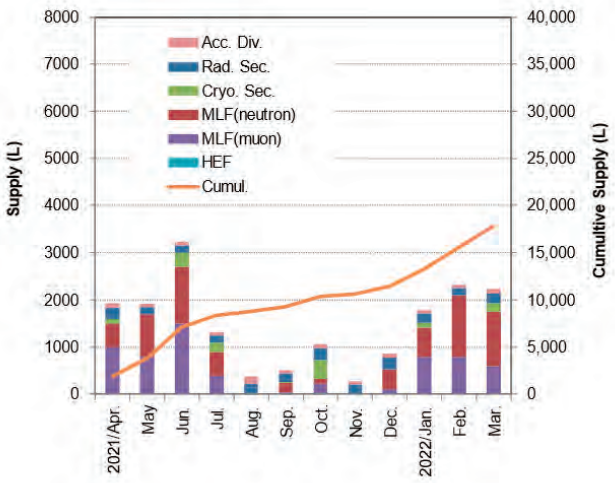

Fig. 2. Liquid nitrogen supply at J-PARC from April 2021 to March 2022.

Superconducting Magnet System for T2K

The superconducting magnet system for the T2K experiment operated during the periods shown in Table 1. The system worked well without disturbing the beam time. The operation time was only 27 days in April and regular maintenance works were carried out in the autumn. Figure 3 summarizes the incidents in the refrigeration system from FY2009. Recent troubles in FY2021 were caused by wrong stratus signals from a power source for the magnet to the T2K beam control system. Fortunately, they did not cause any hardware damages and the beam time was not suspended.

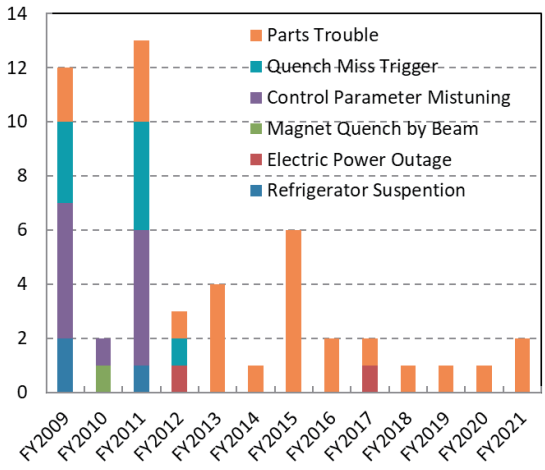

Fig. 3. Summary of incidents in the Refrigerator

Table 1. Operation history of the T2K superconducting magnet system.

	2021									2022			
	April	May	June	July	Aug.	Sept.	Oct.	Nov.	Dec.	Jan.	Feb.	Mar	April
Operation	⟷ 4/3-4/30												
Maintenance							⟷						

Superconducting Magnet Systems at the MLF

The Cryogenic Section contributes to the operation and maintenance of the superconducting magnet systems at the Muon Science Facility (MUSE) in the MLF. The superconducting solenoid in the Decay Muon Line (D-line) was operated from January 6 to July 22 2021. Annual maintenance, such as exchange of the oil separation filter, safety valve maintenance and so on, was performed from July to the end of November. One of the major maintenance works was an overhaul of the He compressor (Fig. 4). The cryogenic operation was restarted on January 11, 2022, because of the delay of the exchange work of the neutron target.

Fig. 4. Uninstalled LHe compressor.

Superconducting Magnet Systems at the HEF

The COMET experiment is under construction in the Hadron South Experimental Hall (HDS) of the Hadron Experimental Facility (HEF). The Cryogenics Section was involved in the construction of the cryogenic system and superconducting magnets.

Production of the superconducting solenoid magnet for the muon beamline is in progress. The pion capture solenoid (PCS) is under construction in the factory. A photograph of the fabricated cold masses and thermal shields of the PCS is shown in Fig. 5. Helium cooling pipe is welded on the support shell structure of the coils and the thermal shield made of 5 mm-thick aluminum plate. Fabrication of the superconducting magnet (the Bridge Solenoid) to tune the magnetic field at the exit of the muon beamline was finished and is waiting for cooldown test at J-PARC (Fig. 6).

Fig. 5. Photograph of the fabricated cold masses and thermal shields of the PCS.

The magnets are designed to be cooled by a two-phase flow of liquid helium which is supplied by a helium refrigeration system built in HDS. The current lead box (CLB) for the PCS was fabricated and installed in the HDS in FY2020. Five High Temperature Superconductor (HTS) current leads for 3 kA, 500 A and 250 A are installed. They are cooled not only by cryocoolers but also by the shield helium gas with 40 K supplied from a helium refrigerator. Figure 7 shows the insert of the PCS CLB. The cooling and current test of the capture CLB was carried out three times in total. It was confirmed that the capture CLB could be cooled well excitation of 2916 A and that various interlocks and the control system also worked well.

The surface equipment, such as cold box and

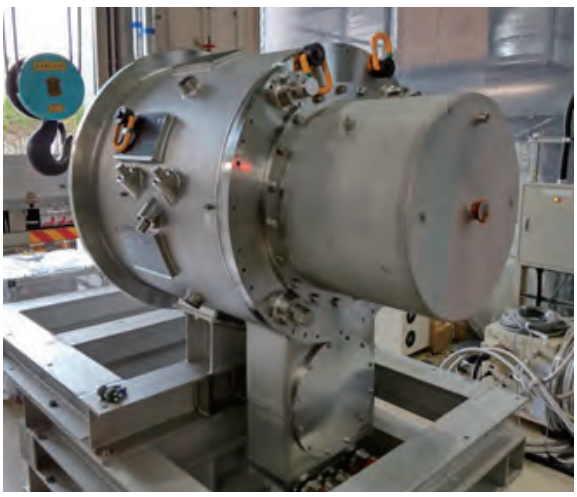

Fig. 6. Picture of the Bridge Solenoid delivered at J-PARC

current lead boxes for PCS and MTS, and the underground equipment (MTS, TRT) were finally connected from the view point of vacuum, electric and helium coolant shown in Fig.8. Cooling and excitation test for the MTS cooling system will be done in FY2022.

Fig. 7. Insert of the PCS CLB

Fig. 8. MTS cooling system

R&D for the Future Projects at J-PARC

The g-2/EDM project aims for the precise measurement of the anomalous magnetic moment and the electric dipole moment of muons. This experiment was proposed at the MUSE H-Line. A superconducting solenoid with a high field homogeneity, better than 1 ppm locally, plays a very important role as a muon storage ring. The numerical study of the magnet system on vibration conduction was carried out to evaluate the dynamic magnetic field fluctuation. The simulation study of the frequency response analysis using FEM software shows that the vibration caused by the cryocoolers on the cold box was not conducted to the superconducting coils at all, thanks to the good vibration isolation system of the cold box, indicating that the magnetic field error caused by the cryocooler vibration could be ignored.

A muonium hyperfine structure measurement, called MuSEUM experiment, has been proposed for the same beam line as the g-2/EDM project. In the experiment, the energy state transition in muonium will be observed under a static magnetic field with local homogeneity of 1 ppm. A magnetic field distribution measurement system has been developed. Figure 9 shows the prototype of the system.

NMR probes using pure water are used as standard probes for magnetic fields with sufficient accuracy. The possibility of systematic errors omitted from the evaluation cannot be eliminated if only one nuclide is used. In addition, due to the temperature dependence of the magnetic susceptibility, we are working on the development of NMR probes using ^{3}He gas as the other nuclide.

The advantages of ^{3}He are that its magnetic susceptibility is smaller than that of pure water and its temperature dependence is negligible, and its

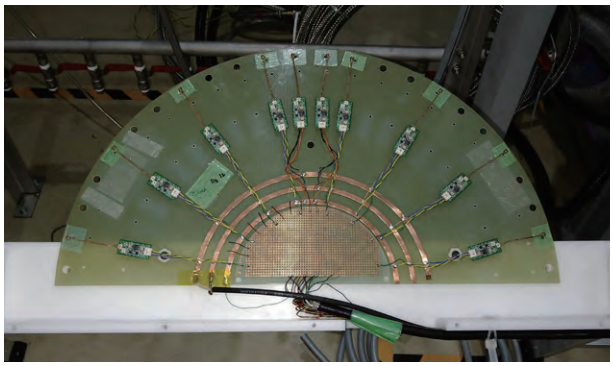

Fig. 9. Prototype of magnetic field distribution measurement system.

monatomic molecular structure is less indefinite. The disadvantage is that the density is smaller than that of pure water and the polarization due to the magnetic field alone is also smaller, so it is necessary to promote the polarization of the nuclei by other means to increase the signal intensity.

^{3}He is polarized by a method called MEOP (Metastability Exchange Optical Pumping). First, electrons are excited to a metastable state by applying radio frequency. The excited electrons are then irradiated with a circularly polarized laser beam at 1083 nm to polarize the electron spins. Finally, the electrons are polarized by transferring their polarization to another ground state, 3He nucleus.

The glass cell was cleaned with acetone and ethanol to avoid impurities, baked, evacuated to 10^{-7} Pa, and filled with ^{3}He. The spectra were obtained by applying radio frequency to the glass cell (Fig.10), and it was confirmed that the transition to the metastable state had occurred.

The glass cell should be perfectly spherical to maintain the polarizability and to suppress the indeterminacy of the magnetic field measurement due to its shape. The same is true for pure water. However, protrusions remain due to vacuuming and gas sealing. If it is possible to fabricate a perfectly spherical cell, the measurement accuracy can be expected to improve.

We are currently preparing a laser facility, and as soon as the polarization is confirmed, we will begin development of the NMR probe as an NMR probe, aiming for accuracy equivalent to or better than that of the pure water probe.

Applied research based on REBCO (rare-earth barium copper oxide) exhibiting high temperature superconductivity is underway to realize the future pion capture system for the muon beamline of MLF second target station (TS2-PCS). The irradiation effect on REBCO coated conductors has been studied for the assumption of PCS operation under an extremely high radiation environment with doses higher than 100 MGy. No significant degradation of critical current of superconductivity (I_C) in REBCO samples was confirmed by ^{60}Co gamma-ray irradiation up to 27.4 MGy. The superconductivity of REBCO samples disappeared at neutron irradiation fluence above 4.11×10^{22} n/m^2. Degradation of the superconducting transition temperature and critical current was observed at 8.23×10^{21} n/m^2. The relationship between the degradation rate of IC at 8.23×10^{21} n/m^2 relative to the unirradiated value I_{C0}, and the measurement temperature is shown in Fig. 11. The I_C/I_{C0} changes depending on the measurement temperature. Irradiation studies of conductors and magnet components will continue to be carried out to understand the effects and design the TS2-PCS.

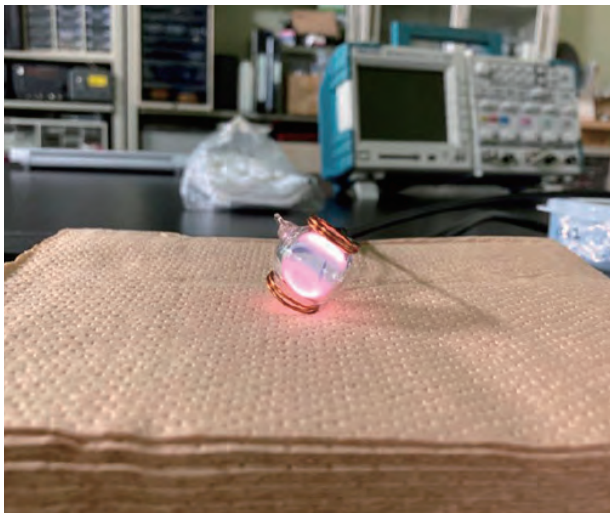

Fig. 10. ^{3}He glass cell that emits light by applying high frequency.

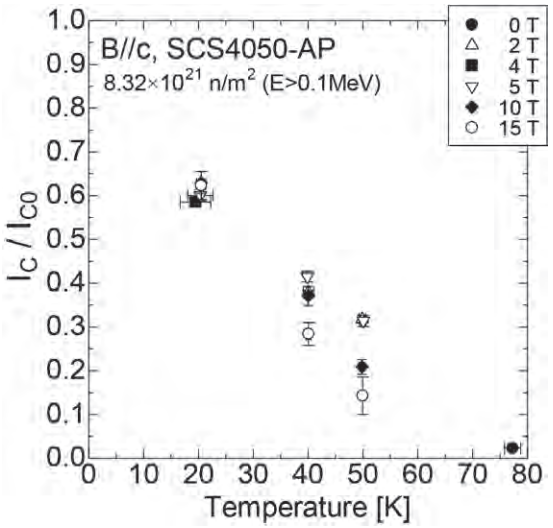

Fig. 11. Relationship between degradation ratio (I_C/I_{C0}) and measurement temperature

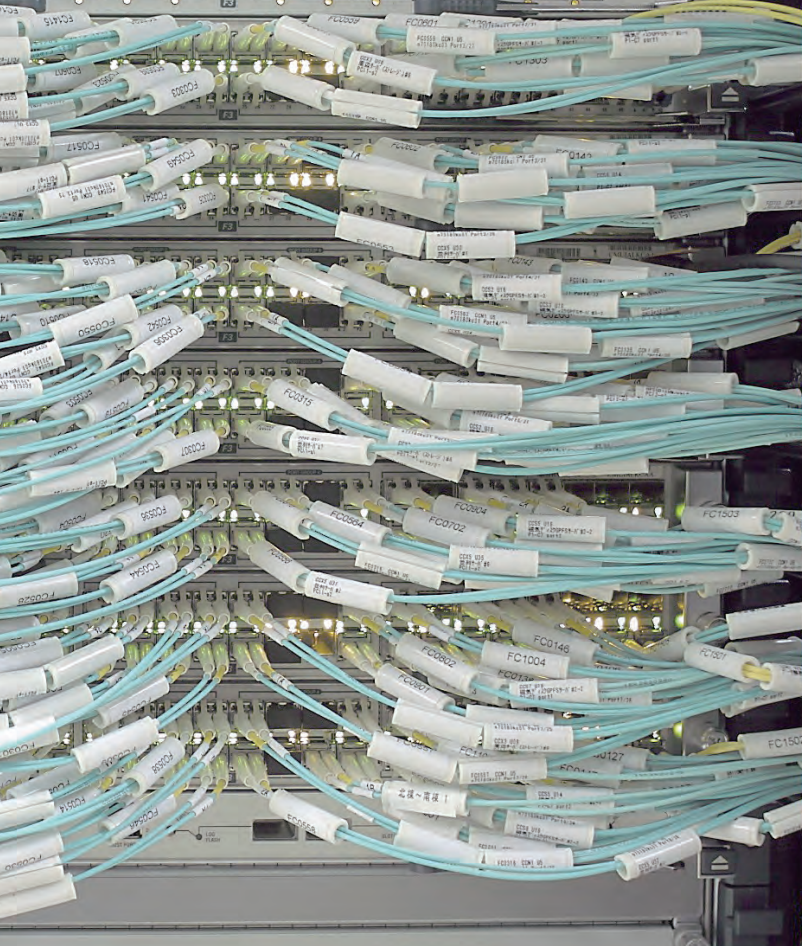

Information System

Overview

The Information System Section plans, designs, manages, and operates the network infrastructure of J-PARC and also provides support to ensure its information security. In terms of computing, until now, J-PARC has owed its major computer resource for analyzing and archiving data from neutrinos, nuclear physics and MLF experiments to the KEK central computer system on Tsukuba Campus. The section connects the J-PARC network to the KEK central computing system directory and helps the users to utilize the system effectively.

Status of Networking

Since 2002, the J-PARC network infrastructure, called JLAN, has been operated independently from KEK- and JAEA-LAN in terms of logical structure and operational policy. In 2021, the total number of hosts on JLAN exceeded 5,700, which was a 102% increase compared to the previous year. The growth curve of edge switches, wireless LAN access points and hosts (servers and PCs) connected to JLAN are shown in Figure 1.

SINET is not only a gateway from JLAN to the internet but also an important connection between the Tokai- and the KEK Tsukuba-sites in J-PARC. In April 2022, the

National Institute of Informatics (NII) will upgrade SINET (Japan Science Information Network https://www.sinet.ad.jp) from version 5 to 6, and the bandwidth capacity between the Tokai- and KEK Tsukuba-sites will be increased from 10 Gbps to 20 Gbps.

Figures 2 and 3 show the network utilization of the internet from/to JLAN. Since the bandwidth capacity for the internet through the SINET is 10 Gbps, it is clear that there is enough space for additional activity. Figures 4 and 5 show the statistics of data transfer between the Tokai- and the Tsukuba-sites through L2VPN provided by SINET. This shows that the usage level has been approaching a half of its capacity, especially during the period when the Hadron facility was running. At the end of FY2021, in March 2022, the peak value increased suddenly to 8Gbps, because data transfer was carried out by the g-2 experiment group.

Figure 6 shows the 5 minutes peak values of the network traffic for the recent years. The peak value of data transfer between Tokai- and Tsukuba-sites through L2VPN is continuously increased, and since the value will exceed 10G in near future, we decided to increase the bandwidth between Tokai and Tsukuba.

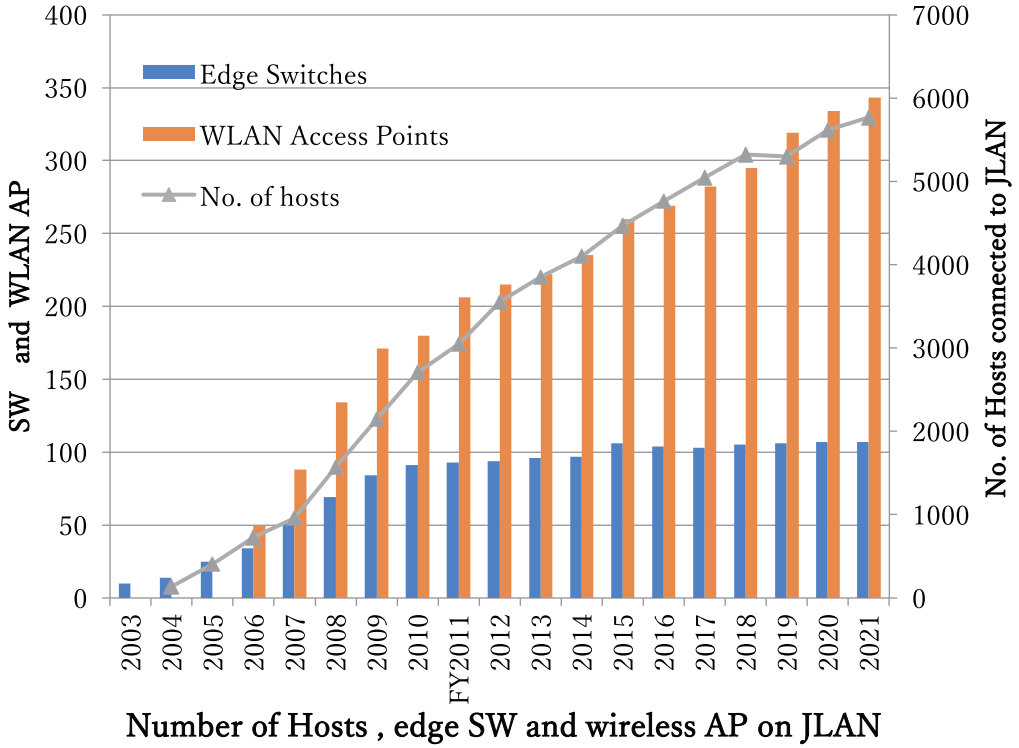

Fig. 1. The number of hosts, edge switches and wireless access points on JLAN..

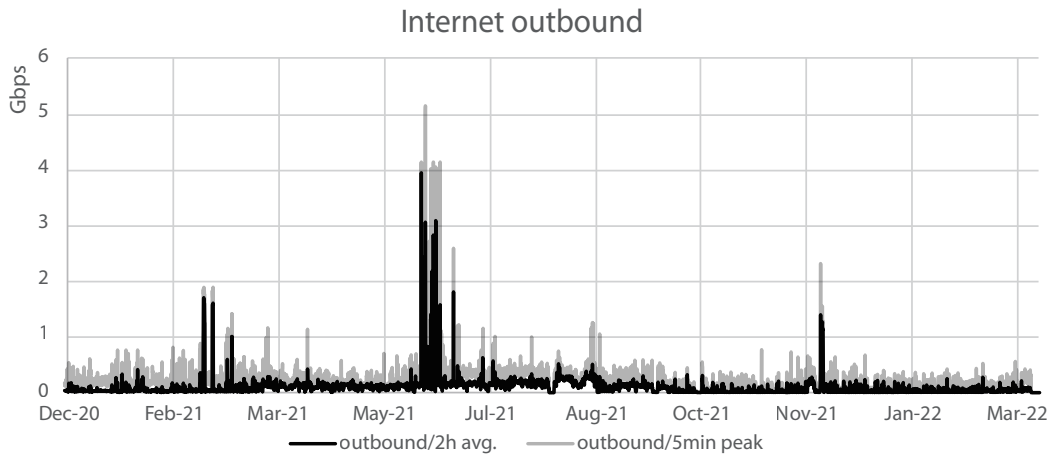

Fig. 2. Network traffic from JLAN to the internet (2 hours average and 5 minutes peak values).

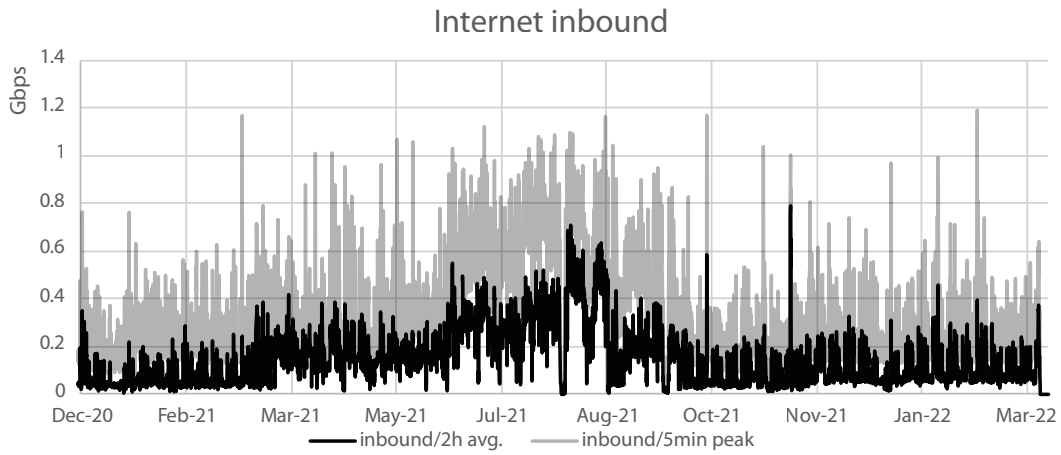

Fig. 3. Network traffic from the internet to JLAN (2 hours average and 5 minutes peak values).

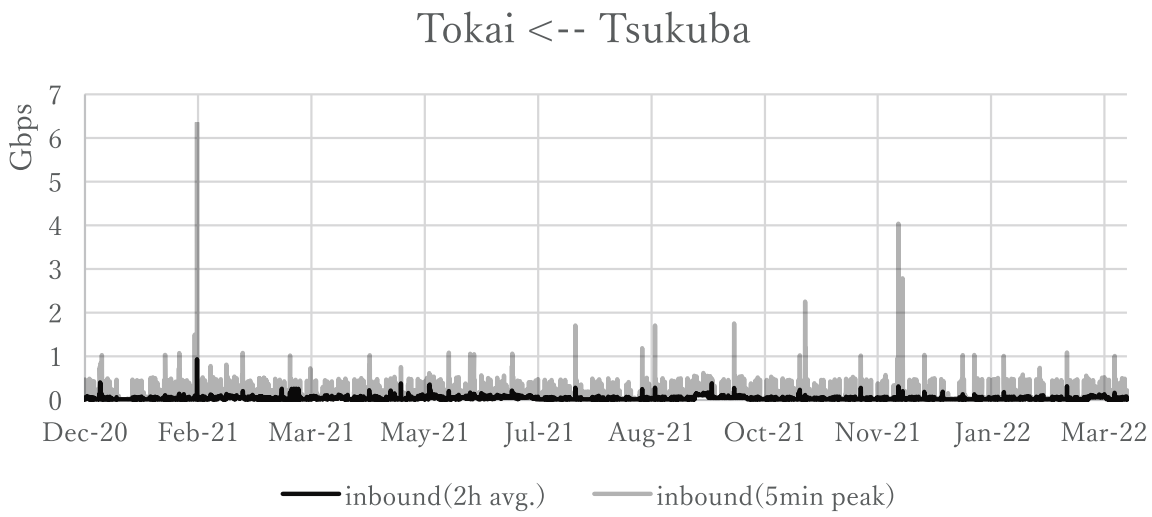

Fig. 4. Network traffic form the Tsukuba to Tokai sites.

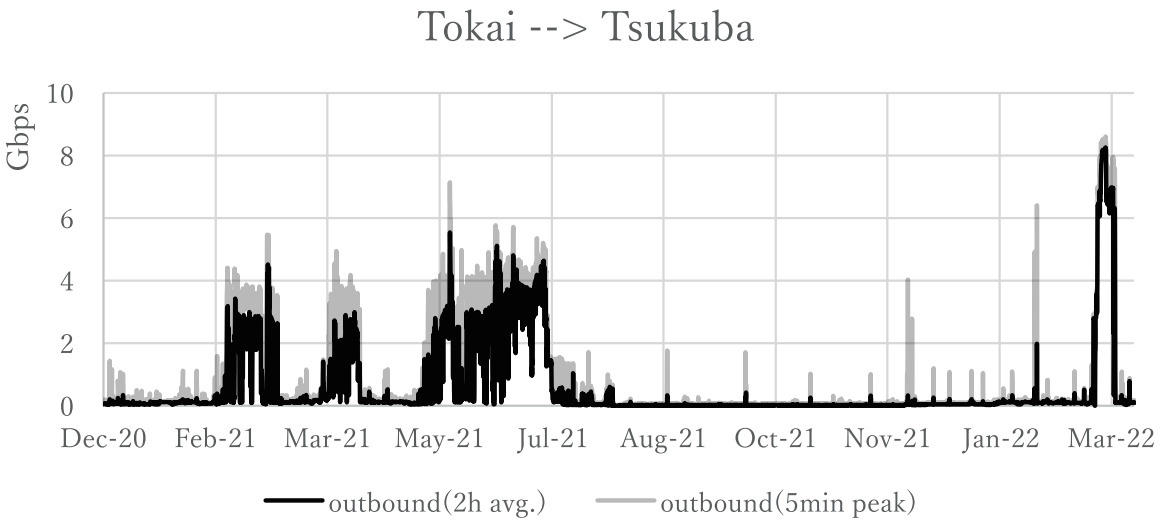

Fig. 5. Network traffic form the Tokai to Tsukuba sites.

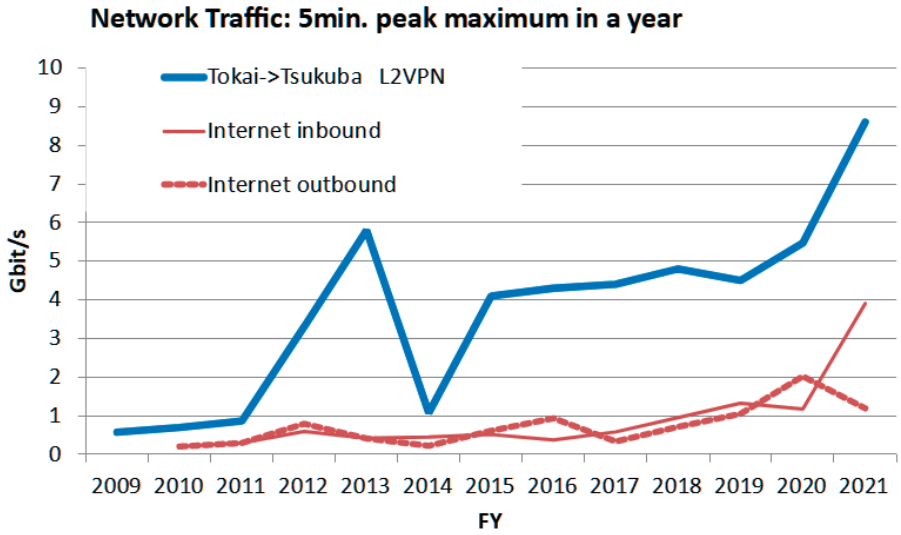

Fig. 6. 5 minutes peak values of network traffic for the recent years.

Internet Connection Services for Visitors and Public Users of J-PARC

Since 2009, J-PARC has offered a Guest network (GWLAN) service, which is a wireless internet connection service for short-term visitors, available in almost all J-PARC buildings. In the end of 2014, additional network service called User LAN has started. To use the GWLAN, users are required to receive a password at the J-PARC Users Office beforehand, while in the User LAN, they are authenticated by the same ID and password for the User Support System, which is also used for dormitory reservation and so on. From March 2016, a new service called "eduroam" has been introduced. The eduroam (https://www.eduroam.org/) is a secure roaming access service developed for the international research and education community and mutually used among a huge number of research institutes, universities, and other institutions around the world. The eduroam service will be a convenient third option of internet connection service for J-PARC visitors. Figure 7 shows this fiscal year's usage statistics of GWLAN, User LAN and the newly introduced eduroam service.

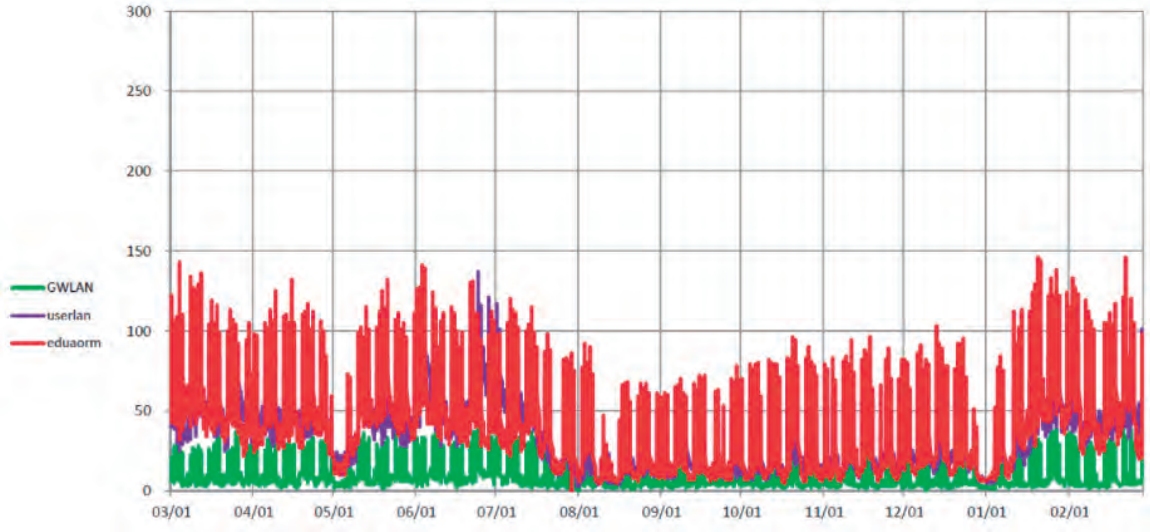

Fig. 7. Usage trends of GWLAN, User LAN and eduroam.

Status of Computing

Since J-PARC does not have computing resources for physics analysis and data archive, starting from 2009, the KEK central computing system (KEKCC) at the KEK Tsukuba campus has been mainly used for these purposes. KEKCC is shared by most of the research groups of KEK, including J-PARC. At the Neutrino (T2K), Hadron and Neutron (MLF) experiments, the data taken in J-PARC are temporarily saved at their facilities and then promptly transferred, stored, and analyzed at the system in Tsukuba. The storage of the system is also utilized as a permanent data archive for their data. The third upgrade of the system was completed in 2020, and the computing resources are shown in Table 1. Figures 8-10 show the utilization statistics of the computing resources in FY2021. The main users who used the CPU and storage constantly were from the Hadron and Neutrino experiment groups. The MLF group also started to store data to tapes on the system.

Table 1. Computing resources in the KEKCC.

CPU (Intel Xeon Gold 6230)	15000 cores
RAID Disk (GPFS)	25.5 Peta Bytes
Tape Library (HSM)	100 Peta Bytes

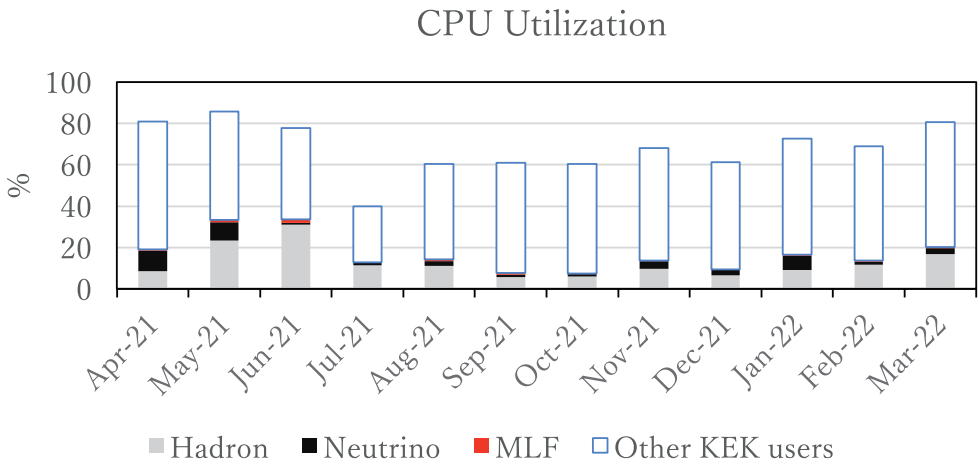

Fig. 8. CPU usage statistics of KEKCC in FY2021.

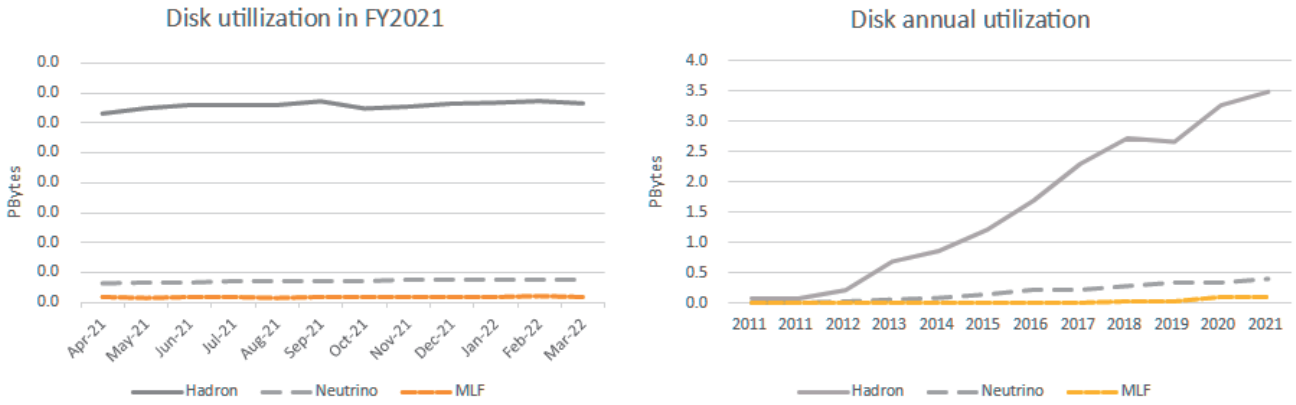

Fig. 9. Disk usage statistics (left: trend of FY2021, right: annual trend).

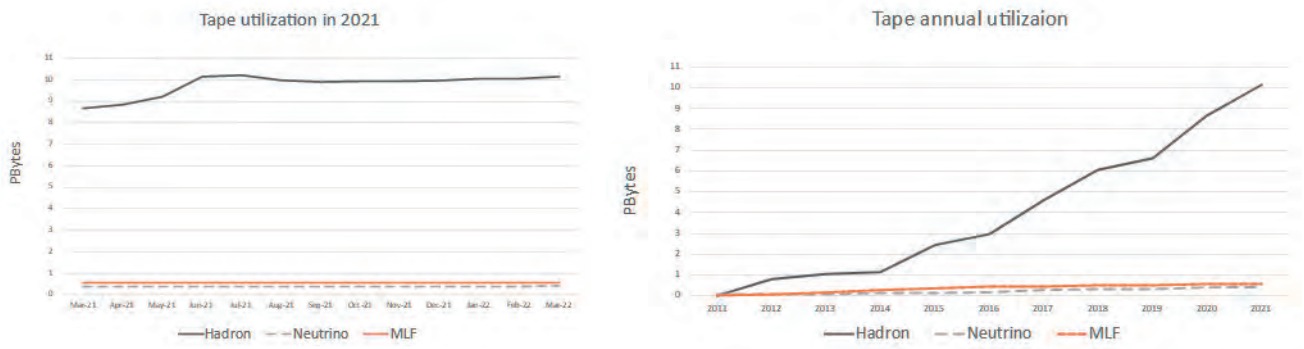

Fig. 10. Tape library usage statistics (left: trend of FY2021, right: annual trend).

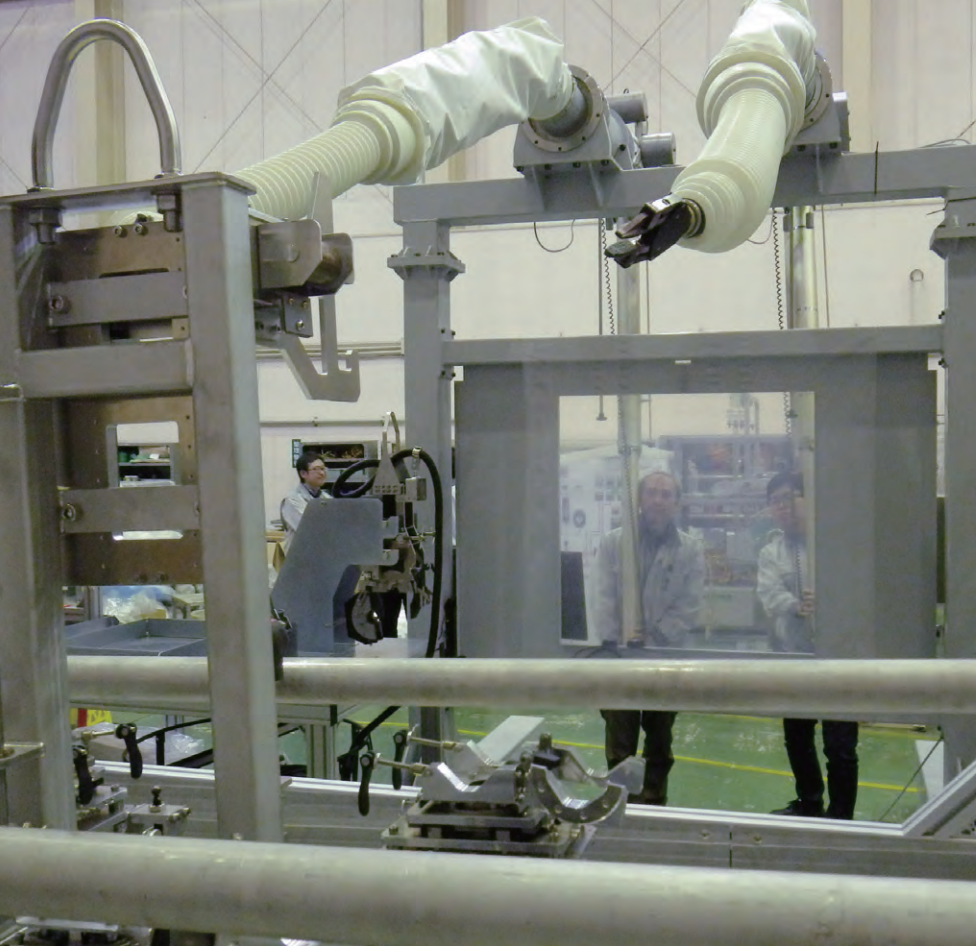

Transmutation Studies

Overview

We are developing nuclear transmutation technology with accelerator-driven systems (ADS) using the J-PARC's research resources and expertise in high-power accelerator and target technologies. The ADS is an effective nuclear system for volume reduction and mitigation of harmfulness of high-level radioactive waste produced in nuclear reactors. We believe that the ADS is one of the most beneficial applications of high-power accelerators for contributing to human society.

We have developed the J-PARC Transmutation Experimental Facility (TEF) which consists of two individual facilities: the ADS Target Test Facility (TEF-T) for irradiation of beam window materials, and the Transmutation Physics Experimental Facility (TEF-P) for reactor physics study on proton beam driven subcritical cores with bearing minor actinide fuels. The baseline design of TEF-T and TEF-P is available in the design reports JAEA-Technology 2017-003 and JAEA-Technology 2017-033, respectively.

In 2021, the Partitioning and Transmutation (P-T) Technology Evaluation Task Force (TF) was established by the Ministry of Education, Culture, Sports, Science and Technology (MEXT). The R&D activities on the P-T technology with ADS were discussed to formulate the next JAEA's mid- to long-term plan (MLTP) for JFY2022-2028. In December 2021, the TF made public the discussion results, "On evaluation of the P-T technology". One section of the report covers the future direction of J-PARC TEF, and two important policies are included in it.

- It is appropriate to review the experimental facility with an emphasis on the TEF-T function.
- In addition to challenging the engineering issues of ADS, it is desirable to consider the specifications of

the facility with seeking possibilities of benefiting to versatile needs of potential users.

According to the policies, the JAEA's MLTP states that "Regarding the J-PARC TEF program, JAEA reframes the facility plan based on the results of related R&D and versatile needs to the facility in addition to nuclear transmutation research."

We are reframing the concept of the facility to comply with the policies and the MLTP. The main purpose of the facility continues to be its TEF-T function, i.e., irradiation of ADS's structural materials by impinging the proton beam to an LBE target. Hence the facility is a kind of a proton irradiation facility (Fig. 1). In addition, we are exploring how the facility can contribute to versatile needs other than the ADS development. Some ideas of the versatile needs are as follows:

- Irradiation of materials used in high-energy accelerator facilities, such as J-PARC, fusion reactors and fission reactors,
- testing of the soft-error of semi-conductor devices by utilizing high-energy neutrons generated in the LBE target,
- production of radioisotopes for medical use, and so on.

As for the R&D activities on the lead-bismuth eutectic (LBE) target technology, the third campaign of materials corrosion test for 7,000 hours under oxygen concentration controlled high-temperature LBE flowing using the OLLOCHI loop is in progress. As of the end of March 2022, the test has reached about 3,000 hours.

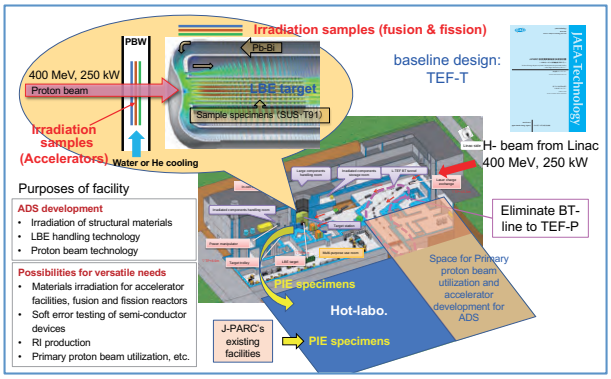

Fig. 1. Rough image of the current idea of the proton irradiation facility.

As for the R&D activities on the proton beam technology, a series of measurements of neutron production yields from iron, lead and bismuth targets bombarded by a 107-MeV proton beam provided by the FFAG accelerator at Kyoto University has been mostly completed. Assembling of a superconducting spoke cavity for ADS's linac by electron beam welding has started.

In February 2022, the eighth TEF Technical Advisory Committee (T-TAC) was held online. This year, the T-TAC was specifically asked to advice on concrete approach to implement the R&D activities in line with the next JAEA's MLTP. The main conclusion was as follows: *"It is recommended to carefully set the priorities of the proposed activities given the available resources from FY 2022 on."*

Research and development

Management of the lead-bismuth eutectic is one of the key issues of the ADS. At J-PARC, various research activities, such as operation of a corrosion test loop "OLLOCHI", operation of a spallation target mockup loop "IMMORTAL", and development of various sensors for LBE are underway. In addition, we published technical reports on the two test loops [1-2].

OLLOCHI

After the first campaign of corrosion test in OLLOCHI (Oxygen-controlled LBE LOop Corrosion tests in HIgh-temperature) [1], we started the second campaign of corrosion test in April 2021 and finished in July 2021. The total operation period was about 2,000 hours. In the second campaign, to confirm the effect of pre-oxidation of steel specimens, one of two specimen holders was held at 430˚C for 100 hours in LBE at saturated oxygen concentration (OC) prior to testing. The OC was then adjusted to 1×10^{-6} wt% and the other specimen holder was loaded in LBE. Test conditions were the same as those in the first campaign; maximum temperature and temperature difference were 450˚C

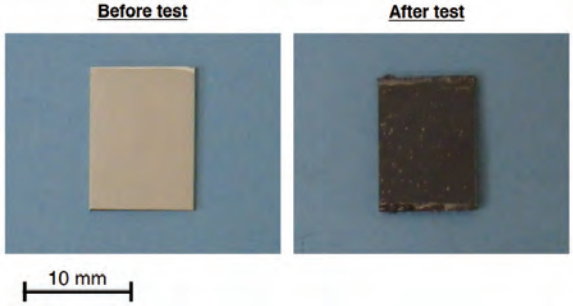

Fig. 2. Outline of specimen before and after the corrosion test.

and 100˚C, respectively. The flow rate was about 1 m/s at the specimen position. The tested specimens were taken out from the specimen holders shown in Fig. 2 and are being observed.

The third campaign of long-term corrosion test for 7,000 hours, which corresponds to the yearly operating hours of the ADS, started in November 2021 and will be completed in the fall of 2022.

IMMORTAL

IMMORTAL [2] is a mockup loop of LBE spallation target in TEF-T. In the loop, LBE, pressurized water, and atmospheric water were employed as coolants for primary, secondary, and ternary systems, respectively. The ternary system is equipped with a water-cooled chiller with a capacity equivalent to the rated output (50 kW max.) of a heater module (HM) installed in the primary (LBE) system. To further improve the stability of the heat balance between each cooling system, the chiller in the ternary system was replaced with an air-cooled heat exchanger.

Figure 3 shows the measured heat balance in the primary system after replacement of the ternary cooling system. Averaged heat exchange was 18.7 kW. It can be confirmed that the heat input at HM and heat removal at PHX are almost identical and stable. Previously, the values of HM and PHX were more unstable and sometimes differed due to the unstable performance of the chiller. The renewal of the equipment has made it possible for both to remain at approximately the same value, thus enabling IMMORTAL to operate in a stable heat balance. In the future, measurement of single tube heat-transfer of LBE and experiment of transient behavior, such as a Loss of flow accident, will be performed.

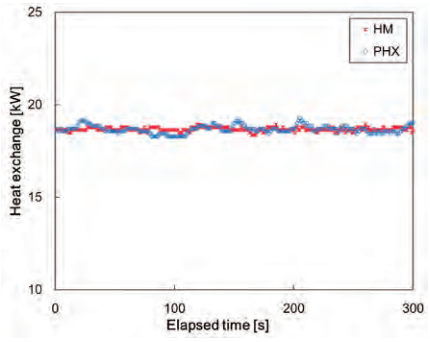

Fig. 3. Measured heat balance in the primary cooling system of IMMORTAL.

References

[1] S. Saito, *et al*., Development of High Temperature LBE Corrosion Test Loop "OLLOCHI", JAEA-Technology 2021-034, (2022), 94p. DOI:10.11484/jaea-technology-2021-034

[2] H. Obayashi, *et al*., Development of Mock-up Test Loop (IMMORTAL) for LBE Spallation Target, JAEA-Technology 2021-035, (2022), 66p. DOI:10.11484/jaea-technology-2021-035

EM flow velocity probe development

Local velocity measurement in the LBE under the operation temperature conditions of the LBE spallation target or ADS is important to evaluate validity of the numerical flow field analyzed by the existing CFD codes. The temperature range assumed in the LBE flowing in these facilities reaches 250˚C and up to about 450˚C. Due to lack of heat resistance of the existing measurement methods, the velocity measurement in such temperature range so far is still difficult. In JAEA, an electromagnet flow velocity probe (EM probe) which can be applied to the LBE temperatures up to 500˚C and is equipped with constant sensitivity for the velocities, regardless of the various temperatures, has been continuously developed.

Prototype EM probe was applied to high temperature LBE up to about 500˚C in FY2020, by using NALTO (**N**imble velocity measurement **A**pparatus in **L**BE with controlled **T**emperature and **O**xygen potential) which is a functional test apparatus utilizing a rigid body rotation characteristic of the LBE. As a result, we successfully confirmed a clear linearity between the velocity and the output voltage of the probe. However, we also recognized attenuation of the voltage signal due to demagnetization of the core for the electromagnet, depending on the LBE temperature. Hence, as shown in Fig. 4, an EM probe without the core material was manufactured as a new prototype sensor in FY2021. Then, we started to accumulate experimental results to check the probe's performance.

Furthermore, we have also performed static corrosion test to upgrade durability of electrodes for the EM probe. Three tested materials and a reference material were W, Mo, Zr and SS316L, respectively. In the test, the LBE temperature was set at 450˚C. Oxygen concentration was kept at 1×10^{-6} wt%. The total test period was

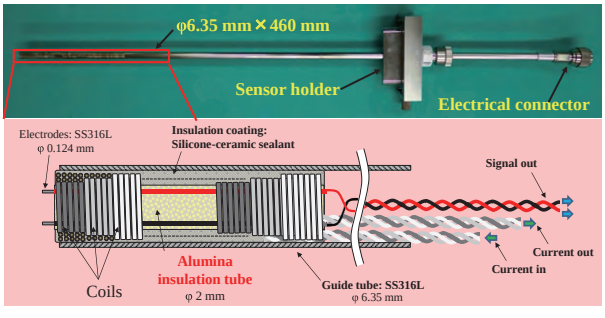

Fig. 4. Details of a new prototype EM probe.

1000 h. As a result, no significant corrosion to the materials was observed. Detailed evaluation of the candidate materials is continuously needed.

Beam transport to the target

After developing the reference design for the JAEA-ADS linac, the next step is the design of the beam transport to the target (BTT) that carries the beam from the end of the linac to the beam window and onto the spallation target, with a specified beam profile, current density, and beam loss.

The JAEA-ADS BTT has to transport efficiently a 30-MW beam with high beam power stability and low peak density to ensure beam window integrity, which is a primary concern for the ADS. Additionally, the design of the BTT must be compatible with the established reactor design, and the elements that comprise the BTT must facilitate the maintenance and replacement of the fuel and the beam window. To this end, a robust-compact BTT design was developed through massive multiparticle simulations.

Figure 5 shows the schematic view of the BTT and the radial distribution of the proton beam for an error study comprising element errors (e.g., misalignment) and input beam errors, such as emittance growth. The BTT smoothly increased the transverse beam size to decrease the peak beam current density at the target and confined the beam loss inside the reactor section, which has the proper shielding and cooling. The analysis confirms that the BTT design satisfies the stability requirements for the JAEA-ADS system. In future work, nonlinear optics will be studied to reduce the peak beam current density and decrease the beam loss.

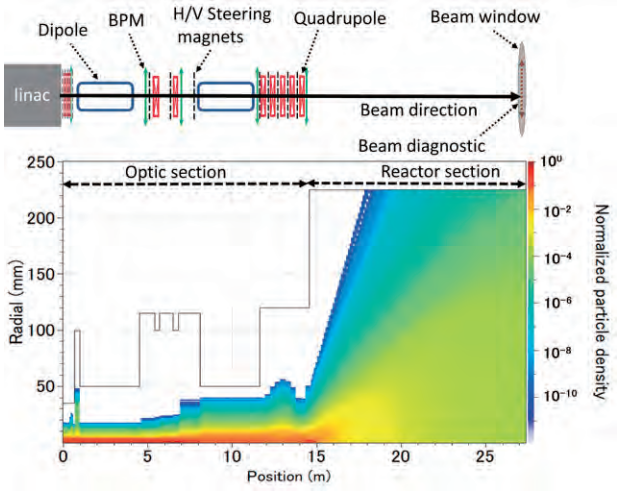

Fig. 5. Schematic view and radial distribution for beam error studies of the JAEA-ADS BTT.

Measurement of nuclide production cross sections

In the analyses of induced radioactivity and radiation shielding of the ADS, in-depth cross-section data of radioactive nuclides produced from the nuclear reactions are required. So far, we have obtained the nuclide-production cross section data for a wide range of target nuclei (e.g., Be, Al, Mn, Co, Bi, and Pb) using the J-PARC proton beams. In FY2021, we measured the nuclide-production cross sections for Si, which represents the important material of the ADS beam monitor.

In this experiment, nuclide-production cross-section data at incident proton energies of 0.4, 1.2, and 3.0 GeV were successfully acquired with an experimental uncertainty of <4%. Figure 6 compares the obtained ^{22}Na production cross section with the evaluated cross sections contained in the evaluated nuclear data library, JENDL/HE-2007, and experimental data measured by Michel et al. The result demonstrated that our data are generally in line with those by Michel et al. and that JENDL/HE-2007 fails to reproduce the experimental data. Note that our data are more precise than those by Michel et al.

For further validation of the evaluated data, the nuclide-production cross-section measurements will be continued, and then the evaluation of nuclide-production cross sections will be improved based on the measured data and results obtained.

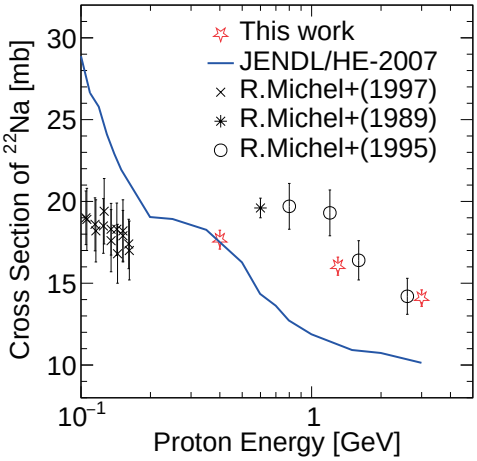

Fig. 6. Proton-induced ^{22}Na production cross section for Si.

Measurement of thick-target neutron yields

For the research and development of ADS and fundamental research on the ADS reactor physics using the Kyoto University Critical Assembly (KUCA) combined with the Fixed-Field Alternating Accelerator (FFAG) accelerator, an experimental program to measure nuclear data related to the ADS has been conducted,

entrusted by MEXT (FY2019 – FY2022). Under this framework, we measured proton-induced neutron-production double-differential thick target neutron yields (TTNYs) for Fe, Pb, and Bi targets, which represent important materials for the ADS beam window and spallation target, with the time-of-flight method using the 107-MeV proton beam accelerated from the FFAG accelerator at Kyoto University.

Figure 7 shows the 107-MeV proton-induced TTNYs for Pb measured at detector angles of 5°, 60°, 90°, and 120° in comparison with calculation results using different types of nuclear reaction models implemented in the Monte Carlo particle transport code system, PHITS (i.e., current and former default models). For both models, the results revealed distinctive discrepancies between the calculation results and the measured data for high energy neutrons. The obtained TTNYs for Pb and Bi are the world's first data in the energy domain of ~100 MeV. The data and findings obtained in this experiment are expected to help improve the nuclear reaction models.

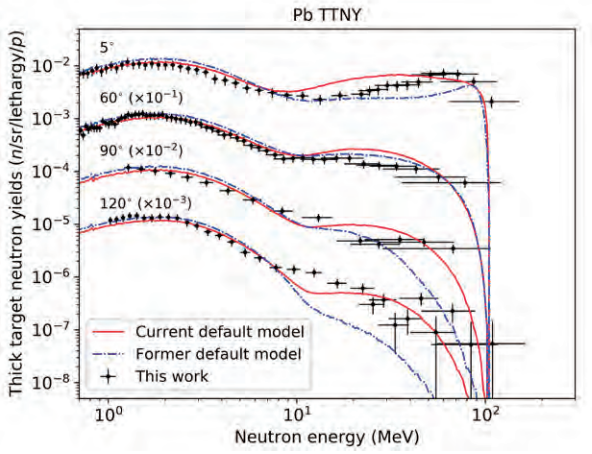

Fig. 7. 107-MeV proton-induced TTNY for Pb.

Benchmarking Experimental Data Obtained to Validate Nuclear Data for ADS

A fast neutron system dedicated to transmutation (accelerator-driven system: ADS) has been investigated to reduce the environmental burden of high-level radioactive waste (HLW). ADS is capable of converting partitioned long-lived nuclides with strong radiotoxicity into stable or short-lived nuclides by fission reaction with neutrons. The top candidate for ADS coolant is lead bismuth, which is chemically stable and very safe. However, Japan has no experience with the use of lead bismuth as a nuclear reactor coolant, and the characteristics of the nuclear reaction (nuclear-reaction cross section) of lead and bismuth have not been sufficiently verified. Hence, the new experimental data (multiplication factor and lead/void reactivity worth) were obtained to validate the nuclear-reaction cross section of lead in fast neutron systems using a critical assembly in the United States [1]. In this study, the multiplication factor (k_{eff}) of the experiment was benchmarked [2]. This benchmark provides a reference (Ref) configuration and three different voided ones (2V, 3V, 4V). In Ref configuration, the core consists of high-enriched uranium, natural uranium, and lead. In the voided ones, the amount of lead gradually decreases from 2V to 4V. Table 1 shows the benchmark k_{eff} with evaluated experimental uncertainty Δk.

Table. 1. Benchmark k_{eff}

Configuration	Benchmark k_{eff}
Ref	1.00269 (+0.00075/-0.00113)
2V	1.00302 (+0.00078/-0.00113)
3V	1.00334 (+0.00079/-0.00117)
4V	1.00359 (+0.00080/-0.00116)

The relatively larger uncertainty in the k_{eff} arises from the uncertainty in tolerance of lead material, thickness of each material, and mass and gap of copper reflectors.

These measurements were compared with the calculation values using nuclear-reaction cross section data (nuclear data) developed in Japan (JENDL-4.0) and the United States (ENDF/B-VIII.0). As shown in Table 2, the calculation results using ENDF/B-VIII.0 well reproduced the experimental ones, whereas that using JENDL-4.0 underestimated them outside the range of experimental uncertainty (around -115 per cent mille (pcm)).

Table. 2. Resulting (C-E)/E

Configuration	(C – E)/E (pcm)	
	ENDF/B-VIII.0	JENDL-4.0
Ref	-67	-147
2V	-66	-145
3V	-68	-144
4V	-67	-141

These benchmarks have passed the rigorous examination of the International Handbook of Evaluated Criticality Safety Benchmark Experiments Project (ICSBEP) belonging to the Nuclear Science Committee of Nuclear Energy Agency of Organization for Economic Co-operation and Development (OECD/NEA/NSC) and will be registered in the 2022 version of ICSBEP.

References

[1] M. Fukushima, J. Goda, A. Oizumi *et al*., Nuclear Science and Engineering, 194(2), pp.138-153 (2020).

[2] A. Oizumi, M. Fukushima, S. Gunji *et al*., International Handbook of Evaluated Criticality Safety Benchmark Experiments, IEU-MET-FAST-025, OECD/NEA/NSC (2022).

International and Domestic Cooperation

In spite of the severe restrictions due to COVID-19, we proceeded steadily with the international and domestic cooperation.

We are collaborating closely with the Belgian Nuclear Research Centre (SCK CEN) for the ADS development under the collaboration arrangement between SCK CEN and JAEA. SCK CEN is promoting the MYRRHA (Multi-purpose hYbrid Research Reactor for High-tech Application) project, which is the world's first large scale ADS project at power levels scalable to industrial systems. In November 2021, the collaboration arrangement was extended for another five-year period. One of the three specific topics of cooperation (STC) is for R&D on ADS. The STC was renewed for the same period. Five research topics were included in the STC: (1) accelerator technology for ADS, (2) Nuclear data, high energy physics, subcriticality monitoring and fuel cycle analysis, (3) Materials R&D, (4) LBE coolant chemistry control and purification and (5) LBE instrumentation for thermal-hydraulic analyses.

We continued the collaboration with Karlsruhe Institute of Technology in Germany on the LBE technology. We are participating with the eighth Spallation Target Irradiation Program (STIP-8) at Paul Scherrer Institute in Switzerland, and a proton-beam irradiation program of steel samples including JAEA's ones has been completed.

We are also collaborating with universities in Japan. One of the collaborations is with the University of Fukui on behavior of spallation and corrosion products in LBE. We are developing the Transport of RAdionuclides In Liquid metal systems (TRAIL) code. We continued the experimental study on the evaporation behavior of volatile elements from LBE.

Another collaboration is with Tokyo Institute of Technology (TIT). Several steel specimens were provided by TIT, and a materials corrosion behavior of these specimens in the flowing LBE in the OLLOCHI loop was investigated.

Safety

Safety

1. Major events on safety culture and safety activities in J-PARC

Through our experiences of the various accidents and incidents, J-PARC has reaffirmed that "The safety of the facility is achieved by the efforts of every person involved", and we actively implement safety culture development activities to upgrade the safety awareness and skills of each person. Our efforts to enforce the safety culture in J-PARC include sharing safety information, enhancement of safety awareness, education and training, etc. For these purposes, new approaches are being introduced sequentially. In addition, these activities are being reviewed internally and by external experts to ensure continuous improvement.

In FY2021, we established a safety policy of "risk awareness and sharing risk information". Specifically, the following is required: 1) workers should look at the work site with a fresh perspective, free from biases caused by experience, and become aware of new risks; 2) workers should communicate the risks to the person in charge, the section leaders, etc.; 3) the person in charge, section leader, etc., inform newcomers to J-PARC of the potential risks at the facility. By sharing and dealing with risks in this way, we aimed to improve the safety capability of J-PARC.

Table 1 lists the major events on safety culture and safety activities at J-PARC.

In order not to forget the radioactive material leak incident that occurred on May 23, 2013, the J-PARC sections exchange safety information with each other and a workshop for fostering safety culture is held every year around May 23. The Safety Day in FY2021 was held on May 28 via online meeting. Some good practices received awards from the director, and work management in the Rapid Cycling Synchrotron (RCS) facility was introduced. Following these programs, the main talk entitled "Assertion culture supporting safety at the engineering and maintenance department, ANA" was given by Mr. Satoru Nabeshima, ALL NIPPON AIRWAYS CO., LTD. Further, an updated video material on the radioactive material leak incident in 2013 was presented.

The 8th Symposium on Safety in Accelerator Facilities was held on August 27 via online meeting, and 121 participants exchanged information on safety issues at accelerator facilities. Six presentations from accelerator facilities were made on the recent situation of each facility and safety activities under the novel coronavirus pandemic. Circumstances and difficulties concerning the application for a license for the accelerator operation at each facility were also shared.

An emergency drill was conducted on November 21 at RCS in cooperation with the Nuclear Science Research Institute of the Japan Atomic Energy Agency. It was assumed that a worker was left in the tunnel of RCS and exposed to radiation when the beam operation started. The drill included transportation and decontamination of the exposed worker, an estimation of the exposure doses, setup of the command post and communication with the accident site, report to the headquarters via TV conference, and simulated press release.

The J-PARC safety audit in fiscal year 2021 was conducted by two auditors on December 20. They reviewed the following points: 1) Compliance initiatives, 2) Organization for safety management, and 3) Safety management in works. The auditors gave us valuable recommendations, such as ideas for effective improvements of the rad-work permit processes, scheduling maintenance works with a proper margin, review and improvement of all activity, including maintenance works.

2. Radiological license update and facility inspection

Applications to update the radiological license were submitted to the Nuclear Regulation Authority on February 16, 2022. Table 2 lists the main changes in the applications. The permit for the applications was issued on August 24, 2022.

On January 11, 2022, "The new construction plans" for new and additional facilities for the Materials and Life Science Experimental Facility, Hadron Experimental Facility, and Neutrino Experimental Facility were submitted to the Ibaraki prefecture for preliminary approval by the local government in accordance with the Ibaraki Prefecture Nuclear Safety Agreement.

The facility inspection for the new fast muon experimental facility (H line) and the extension of the slow muon experimental facility (S line) at the Materials and Life Science Experimental Facility, which was applied for on October 5, 2020, and approved on June 9, 2021, was conducted by the Radiation Management Research Institute, Inc., registered inspection agency, on January 25, 2022.

3. Meeting of the committee on the radiation safety matter

The J-PARC Radiation Safety Committee is organized as an advisory committee to both JAEA and KEK to discuss policy on radiation safety in J-PARC. Meanwhile, the Radiation Safety Review Committee has been established to discuss specific subjects of radiation safety at J-PARC.

In FY2021, the J-PARC Radiation Safety Committee met twice, and the Radiation Safety Review Committee met four times. Table 3 lists the major issues tackled by the committees.

4. Radiation exposure of radiation workers

The number of persons subject to annual measurement of external exposure in FY2021 was 3090.

Table 4 lists the distribution of annual exposed doses for each category of workers. There was no exposure exceeding the dose limit specified in the local radiation protection rule for J-PARC and the administrative dose limits (7 mSv/year) specified in the detailed rule of local radiation protection rule for J-PARC. The total annual effective dose was 33.9 person·mSv, and the maximum effective dose was 1.2 mSv.

Table 1. List of major events on safety in FY2021.

Day	Events
May 28, 2021	Safety Day (Meeting to exchange safety information between each section, Workshop for fostering safety culture)
July 2, 2021	Liaison committee on safety and health for contractors
August 27, 2021	The 8th Symposium on Safety in Accelerator Facilities
October-December	Refresher course on radiation safety for in-house staff (e-learning)
November 21, 2021	Emergency drill assuming that the beam operation started while a worker was in the tunnel of the Rapid Cycling Synchrotron, , causing massive exposure
December 20, 2022	FY2021 J-PARC Safety Audit

Table 2. Major application items of the radiological license

Facility	Items of an application
Li	• Change in the maximum number of accelerated particles • Appropriateness of description
RCS	• Change in the maximum number of accelerated particles • Appropriateness of description
MR	• Change in the maximum number of accelerated particles • Appropriateness of description
MLF	• Installation of the Muon accelerator • Modification of the exhaust purification system (a gas waste treatment facility) • Appropriateness of description
HD	• Change in the maximum number of accelerated particles • Expansion of the room for radiation generator use (installation of a new primary beamline (C-line)) • Modification of the exhaust system, addition of exhaust and drainage facilities • Appropriateness of description
NU	• Change in the maximum number of accelerated particles • Addition of entrance for the radiation-controlled area • Modification of the air exhauster

Table 3. Radiation Safety Committee (RSC) and Radiation Safety Review Committee (RSRC) in FY2021

No.	Date	Major Issues
The Radiation Safety Committee		
37th	July 19, 2021	• Change of the plan for radiological license update in FY2021
38th	March 29, 2022	• The plan for radiological license update in FY2022
The Radiation Safety Review Committee		
30th	July 14, 2021	• Installation of an X-ray generator • Revision of the detailed rule of local radiation protection rule for J-PARC • Re-evaluation of radioactivity in cooling water
31st	September 2, 2021	• Next radiological license update
32nd	November 8, 2021	• Revision of the accident reporting regulations and the guidelines for accident countermeasure activities • Revision of J-PARC Center reporting standards • Revision of the operation manual for J-PARC
33rd	February 1, 2021	• Partial revision of Rules and Regulations accompanying changes in organizational structure (as of April 1, 2022)

Table 4. Annual exposure doses in FY2021

	# of workers	Dose range x (mSv)				Collective dose (person · mSv)	Maximum dose (mSv)
		ND	0.1≤ x ≤1.0	1.0< x ≤5.0	5.0< x		
In-house staff	688	661	27	0	0	8.2	1.0
Users	929	929	0	0	0	0.0	0.0
Contractors	1,481	1,389	91	0	0	25.7	1.2
Total	3,090	2,971	118	0	0	33.9	1.2

*If the same worker changed the worker classification during the fiscal year, the worker was counted as one worker per the classification. Therefore, the total number does not match the sum of the respective classification.

User Service

Users Office (UO)

Outline

The J-PARC Users Office (UO) was established in 2007. In December 2008, it opened an office on the first floor of the IBARAKI Quantum Beam Research Center in Tokai-mura. UO maintains the Tokai Dormitory for the J-PARC Users. UO provides on-site and WEB support with one-stop service for the utilization of the J-PARC. As of March 31, 2021, UO had 11 staffs and 5 WEB Support SE staffs in the Users Affairs Section. The J-PARC Users, after the approval of their experiment, follow the administrative procedures outlined on the Users Office (UO) WEB Portal Site, related to the registration as a J-PARC User, radiation worker registration, safety education, accommodation, invitation letter for visa and other requirements. Then the UO staffs provide them with support by e-mail. After their arrival at the J-PARC, UO gives on-site assistance to the J-PARC Users, like receiving the J-PARC ID, glass badge, and safety training. Since 2015, UO had been doing its part to improve the J-PARC online experiment system and make it more user-friendly.

After the experiments UO may return the experiment samples at User's cost after cooling the radioactive activities.

Map to the J-PARC Users Office

Activities of the UO

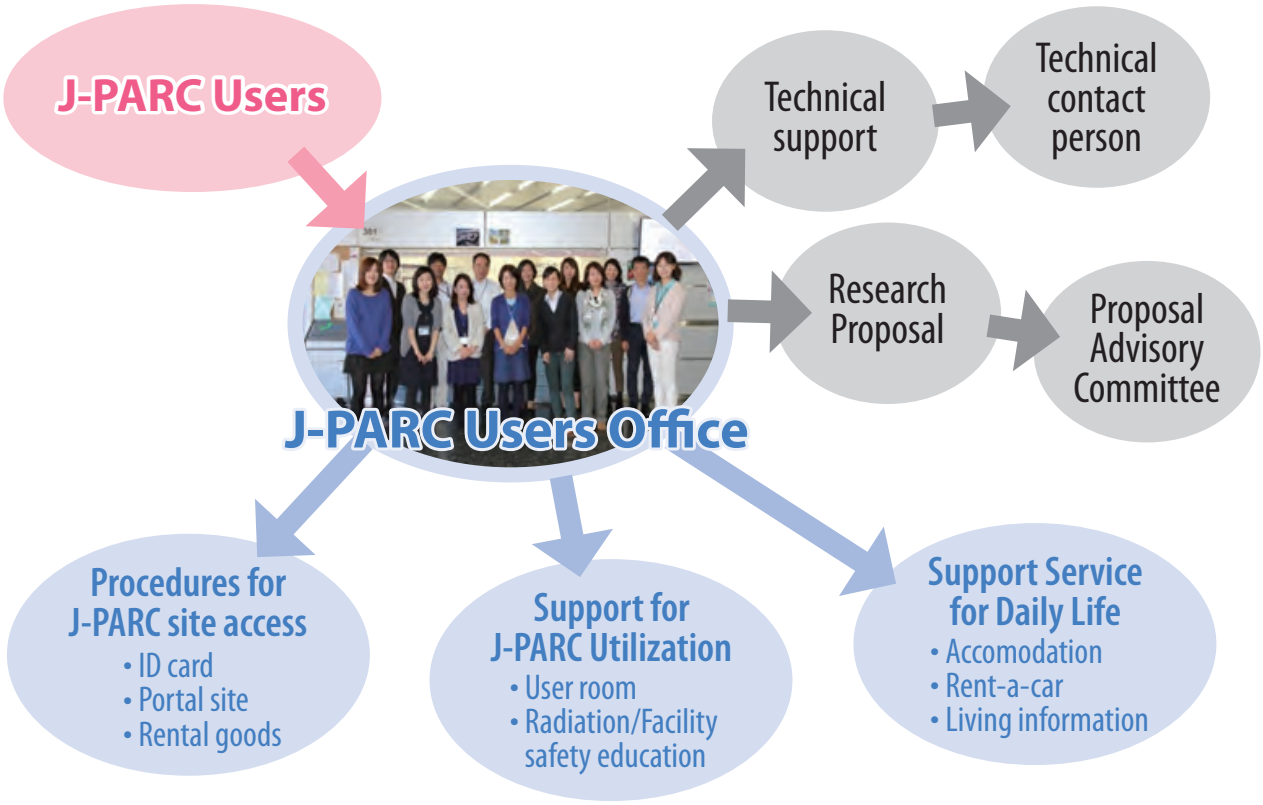

One stop service for J-PARC users

on the web

Step 1 User registration

New user: Getting user ID

Registered user: Annual registration, specifying of the visit

Approval of UO

Step 2-1 Obligatory application

Application form to visit J-PARC
Visit proposal (foreign nationality)
Reservation of safety training
On-line education video

Step 2-2 Optional application

J-PARC Card for facility access
Network registration
Radiation worker registration
Reservation of Dormitory
Invitation letter for Visa

on-site support

Step 3

Procedures upon arrival at the first day

Recieve J-Parc User ID card

Vehicle Permission pass

Safety education and dosimeter

Rental goods
Bicyle
PHS
Cafeteria card
Locker key
Office key

Step 4 J-PARC Experiment and meeting

Step 5 Leaving procedures

Retern all cards, keys, rental goods UO (office hours) or return box!

Users Office at IQBRC
Office hours(9:00-17:00, Mon.-Fri.)

Rental bicycle

Return box at IQBRC

User Statistics

Users in 2021 (Japanese/Foreigners, person-days)

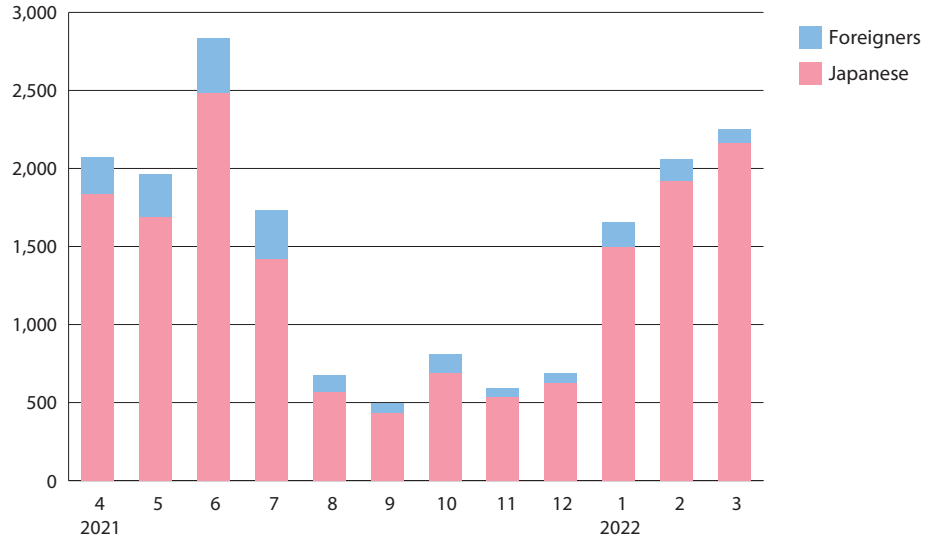

Users in 2021 (according to facilities, person-days)

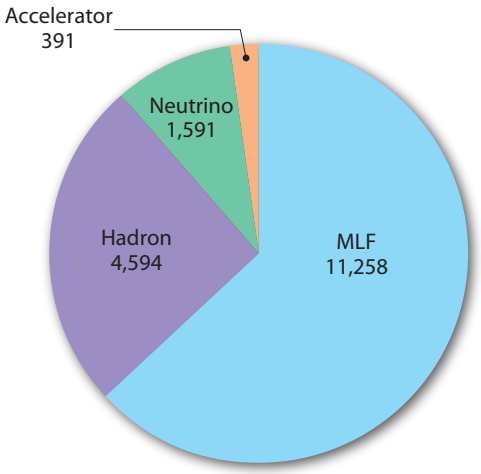

Users in 2021 (according to organizations, person-days)

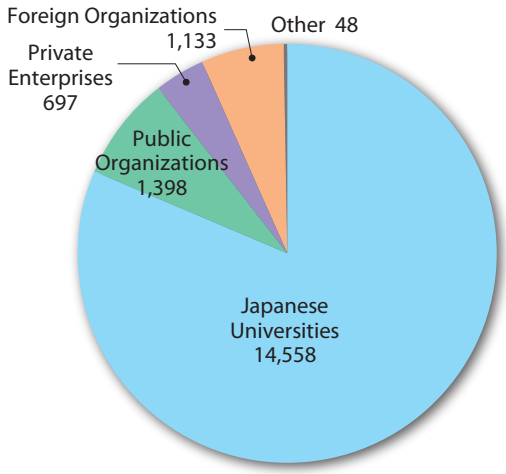

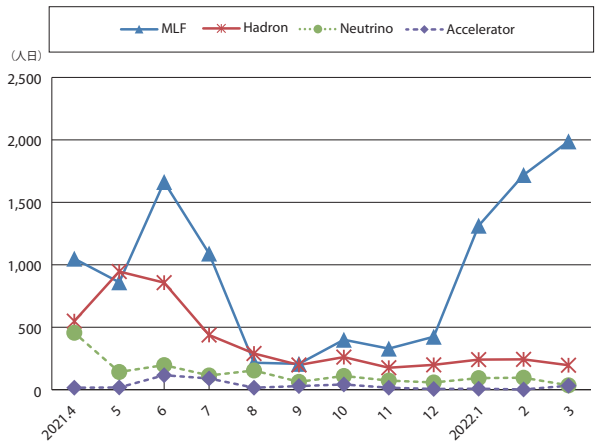

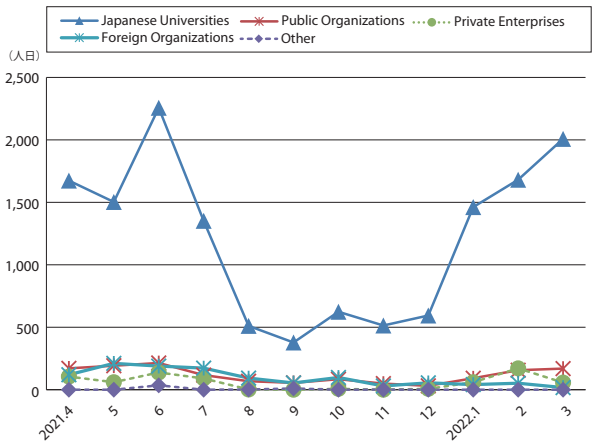

MLF Proposals Summary - FY2021

The proposals for 2021A are not included in Table 1. Due to the COVID-19 situation, 2020B and 2021A were combined into one proposal round. The operations period for the proposals for "2020B+2021A" was from December 2020 to July 2021. Therefore, the proposals for 2021A were included in the FY2020 data as they cannot be counted separately.

Table 1. Number of Proposals by Beamline

Beam-line	Instrument		2021B		Full Year			
			Submitted	Approved	Submitted	Submitted	Approved	Approved
			GU	GU	PU/S	IU	PU/S	IU
BL01	4D-Space Access Neutron Spectrometer - ***4SEASONS***		24(0)	8(0)	0	2	0	2
BL02	Biomolecular Dynamics Spectrometer - ***DNA***		26(2)	7(2)	2	3	2	3
BL03	IBARAKI Biological Crystal Diffractometer - ***iBIX***	(100-β)‡	3	3	0	0	0	0
		(β)†	1	1	45 ※	0	44 ※	0
BL04	Accurate Neutron-Nucleus Reaction Measurement Instrument - ***ANNRI***		10	5	2	1	2	1
BL05	Neutron Optics and Physics - ***NOP***		8	6	1	0	1	0
BL06	Village of Neutron Resonance Spin Echo Spectrometers - ***VIN ROSE***		2	2	1	0	1	0
BL08	Super High Resolution Powder Diffractometer - ***SuperHRPD***		9	5	1	0	1	0
BL09	Special Environment Neutron Powder Diffractometer - ***SPICA***		4	4	1	0	1	0
BL10	Neutron Beamline for Observation and Research Use - ***NOBORU***		16	4	2	1	2	1
BL11	High-Pressure Neutron Diffractometer - ***PLANET***		18(0)	7(0)	0	2	0	2
BL12	High Resolution Chopper Spectrometer - ***HRC***		7	4	1	0	1	0
BL14	Cold-Neutron Disk-Chopper Spectrometer - ***AMATERAS***		47	7	1	1	1	1
BL15	Small and Wide Angle Neutron Scattering Instrument - ***TAIKAN***		36(2)	12(2)	2	3	2	3
BL16	Soft Interface Analyzer - ***SOFIA***		17	5	0	1	0	1
BL17	Polarized Neutron Reflectometer - ***SHARAKU***		17(2)	10(2)	3	3	3	3
BL18	Extreme Environment Single Crystal Neutron Diffractometer - ***SENJU***		22(1)	7(1)	1	1	1	1
BL19	Engineering Materials Diffractometer - ***TAKUMI***		27	12	2	1	2	1
BL20	IBARAKI Materials Design Diffractometer - ***iMATERIA***	(100-β)‡	8	7	0	0	0	0
		(β)†	22	22	28	0	26	0
BL21	High Intensity Total Diffractometer - ***NOVA***		19	15	1	0	1	0
BL22	Energy Resolved Neutron Imaging System - ***RADEN***		19(2)	8(2)	0	2	0	2
BL23	Polarized Neutron Spectrometer - ***POLANO***		4	4	1	0	1	0
D1	Muon Spectrometer for Materials and Life Science Experiments - ***D1***		21(1)	10(0)	1	1	1	1
D2	Muon Spectrometer for Basic Science Experiments - ***D2***		11(4)	4(2)	1	1	1	1
S1	General purpose μSR spectrometer - ***ARTEMIS***		41(0)	18(0)	1	1	1	1
S2	Muonium Laser Physics Apparatus - ***S2***		0	0	0	1	0	1
U1A	Ultra Slow Muon Microscope - ***U1A***		0	0	0	1	0	1
U1B	Transmission Muon Microscope - ***U1B***		0	0	0	1	0	1
H1	High-intensity Muon Beam for General Use - ***H1***		0	0	0	1	0	1
Total			***439***	***197***	***89***	***28***	***86***	***28***

GU : General Use **PU** : Project Use or Ibaraki Pref. Project Use **S** : S-type Proposals
IU : Instrument Group Use
† : Ibaraki Pref. Exclusive Use Beamtime (β = 80%)
‡ : J-PARC Center General Use Beamtime (100-β = 20%)
( ) : Number of proposals under the New User Promotion (BL01, BL02, BL11, BL15, BL17, BL18, BL22) or P-type proposals (D1,D2, S1) in GU

※ Operations period is held twice per year (for each of the A and B periods), with only the yearly total shown above.
The actual total number of proposals in each beamline named in the table does not match the number shown in the "Total" cell, because some proposals are submitted or approved across multiple beamlines.

Table 2. Number of Long-Term Proposals by Fiscal Year

Fiscal Year	Submitted	Approved
2019	9	4
2020	13	3
2021	0	0

Due to the COVID-19 situation, no Long-Term Proposals were called for FY2021.

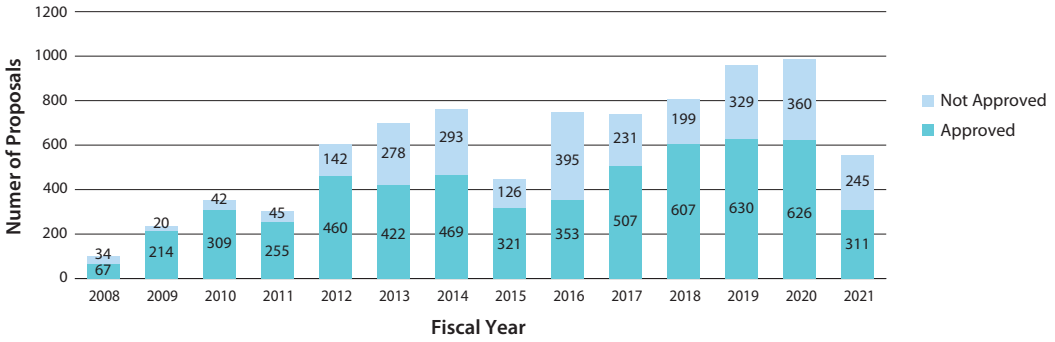

Fig. 1. Number of MLF Proposals over Time

After publishing J-PARC Annual Report 2020, additional Fast Track Proposals and Urgent Proposals were approved. Therefore, the number of proposals for FY2020 was changed in Figure 1.

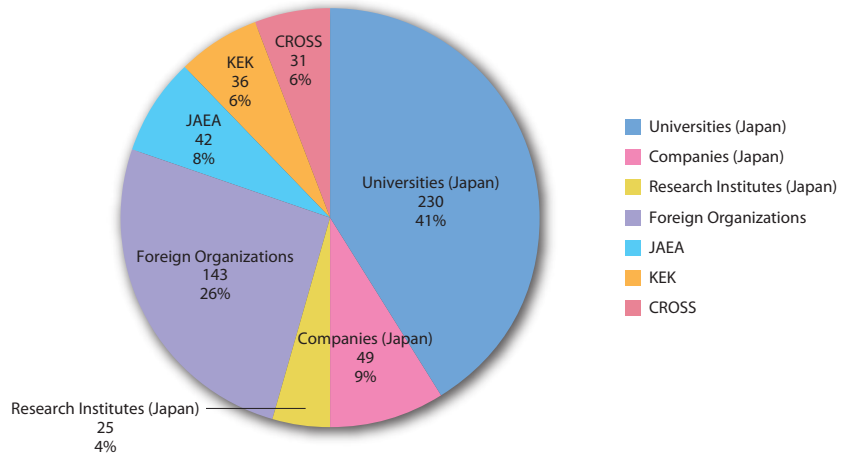

Fig. 2. Origin of Submitted Proposals by affiliation - FY2021

J-PARC PAC Approval Summary for the 2021 Rounds

	(Co-) Spokespersons	Affiliation	Title of the experiment	Approval status (PAC recommendation)	Beamline	Status
E03	K.Tanida	JAEA	Measurement of X rays from X^- Atom	Stage 2	K1.8	Data taking
P04	J.C.Peng, S.Sawada	U of Illinois at Urbana-Champaign; KEK	Measurement of High-Mass Dimuon Production at the 50-GeV Proton Synchrotron	Deferred	Primary	
E05	T.Nagae	Kyoto U	Spectroscopic Study of X-Hypernucleus, $^{12}_{X}$Be, via the ^{12}C(K^-, K^+) Reaction	Stage 2 New experiment E70 based on the S-2S spectrometer	K1.8	Finished
E06	J.Imazato	KEK	Measurement of T-violating Transverse Muon Polarization in $K^+ \to p^0 m^+ n$ Decays	E36 as the first step	K1.1BR	
E07	K.Imai, K.Nakazawa, H.Tamura	JAEA, Gifu U, Tohoku U	Systematic Study of Double Strangeness System with an Emulsion-counter Hybrid Method	Stage 2	K1.8	Finished Data analysis
E08	A.Krutenkova	ITEP	Pion double charge exchange on oxygen at J-PARC	Stage 1	K1.8	
E10	A.Sakaguchi, T.Fukuda	Osaka U, Osaka EC U	Production of Neutron-Rich Lambda-Hypernuclei with the Double Charge-Exchange Reaction (Revised from Initial P10)	Stage 2	K1.8	Li run finished, Be target run with S-2S
E11	A.K.Ichikawa, F.Sanchez	KEK	Tokai-to-Kamioka (T2K) Long Baseline Neutrino Oscillation Experimental Proposal	Stage 2	neutrino	Data taking
E13	H.Tamura	Tohoku U	Gamma-ray spectroscopy of light hypernuclei	Stage 2	K1.8	Finished
E14	T.Yamanaka	Osaka U	Proposal for $K_L \to p^0$ n n-bar Experiment at J-PARC	Stage 2	KL	Data taking
E15	M.Iwasaki, T.Nagae	RIKEN, Kyoto U	A Search for deeply-bound kaonic nuclear states by in-flight 3He(K-, n) reaction	Stage 2	K1.8BR	Finished
E16	S.Yokkaichi	RIKEN	Measurements of spectral change of vector mesons in nuclei (previously "Electron pair spectrometer at the J-PARC 50-GeV PS to explore the chiral symmetry in QCD")	Stage 2 for Run 0	High p	Data taking
E17	R.Hayano, H.Outa	U Tokyo, RIKEN	Precision spectroscopy of Kaonic ^{3}He 3d->2p X-rays	Registered as E62 with an updated proposal	K1.8BR	
E18	H.Bhang, H.Outa, H.Park	SNU, RIKEN, KRISS	Coincidence Measurement of the Weak Decay of $^{12}_{L}$C and the three-body weak interaction process	Stage 2	K1.8	
E19	M.Naruki	KEK	High-resolution Search for Q^+ Pentaquark in $p^-p \to K^-X$ Reactions	Stage 2	K1.8	Finished
E21	Y.Kuno	Osaka U	An Experimental Search for μ – e Conversion at a Sensitivity of 10^{-16} with a Slow-Extracted Bunched Beam	Phase-I Stage 2 PAC recommends producing a more detailed schedule to ensure a timely start.	COMET	
E22	S.Ajimura, A.Sakaguchi	Osaka U	Exclusive Study on the Lambda-N Weak Interaction in A=4 Lambda-Hypernuclei	Stage 1	K1.8	
T25	S.Mihara	KEK	Extinction Measurement of J-PARC Proton Beam at K1.8BR	Test Experiment	K1.8BR	Finished
E26	K.Ozawa	KEK	Search for w-meson nuclear bound states in the $p-+^AZ \to n+^{(A-1)}_{w}(Z-1)$ reaction, and for w mass modification in the in-medium $w \to p^0g$ decay	Stage 1	K1.8	
E27	T.Nagae	Kyoto U	Search for a nuclear Kbar bound state K^-pp in the d(p^+, K^+) reaction	Stage 2	K1.8	Fisnished
E29	H.Ohnishi	RIKEN	Search for f-meson nuclear bound states in the pbar + $^AZ \to f + ^{(A-1)}_{f}(Z-1)$ reaction	Stage 1	K1.1	
E31	H.Noumi	Osaka U	Spectroscopic study of hyperon resonances below KN threshold via the (K^-,n) reaction on Deuteron	Stage 2	K1.8BR	Finished Data analysis
T32	A.Rubbia	ETH, Zurich	Towards a Long Baseline Neutrino and Nucleon Decay Experiment with a next-generation 100 kton Liquid Argon TPC detector at Okinoshima and an intensity upgraded J-PARC Neutrino beam	Test Experiment	K1.1BR	Finished
P33	H.M.Shimizu	Nagoya U	Measurement of Neutron Electric Dipole Moment	Deferred	Linac	

	(Co-) Spokespersons	Affiliation	Title of the experiment	Approval status (PAC recommendation)	Beamline	Status
E34	T. Mibe	KEK, RIKEN	An Experimental Proposal on a New Measurement of the Muon Anomalous Magnetic Moment g-2 and Electric Dipole Moment at J-PARC	Stage 2	MLF	
E36	M.Kohl, S.Shimizu	Hampton U, Osaka U	Measurement of G(K^+ -> e^+ n)/G(K^+ -> m^+ n) and Search for heavy sterile neutrinos using the TREK detector system	Stage 2	K1.1BR	Finished Data analysis
E40	K.Miwa	Tohoku U	Measurement of the cross sections of Σp scatterings	Stage 2	K1.8	Finished Data analysis
P41	M.Aoki	Osaka U	An Experimental Search for μ – e Conversion in Nuclear Field at a Sensitivity of 10^{-14} with Pulsed Proton Beam from RCS	Deferred	MLF	Reviewed in MLF/ IMSS
E42	J.K.Ahn	Pusan National U	Search for H-Dibaryon with a Large Acceptance Hyperon Spectrometer	Stage 2	K1.8	Finished Data analysis
E45	K.H.Hicks, H.Sako	Ohio U, JAEA	3-Body Hadronic Reactions for New Aspects of Baryon Spectroscopy	Stage 2 PAC requests that the group further examine ways to reduce the total beam time requested and to find an efficient running scheme, including quick but careful beam tuning.	K1.8	
T46	K.Ozawa	KEK	EDIT2013 beam test program	Test Experiment	K1.1BR	Abandonded
T49	T.Maruyama	KEK	Test for 250L Liquid Argon TPC	Test Experiment	K1.1BR	Withdrawn
E50	H.Noumi	Osaka U	Charmed Baryon Spectroscopy via the (π, D^{*-}) reaction	Stage 1 The FIFC, IPNS, and E50 should investigate the beam-line feasibility	High p	
T51	S.Mihara	KEK	Research Proposal for COMET(E21) Calorimeter Prototype Beam Test	Test Experiment	K1.1BR	had to be stopped
T52	Y.Sugimoto	KEK	Test of fine pixel CCDs for ILC vertex detector	Test Experiment	K1.1BR	not performed yet
T53	D.Kawama	RIKEN	Test of GEM Tracker, Hadron Blind Detector and Lead-glass EMC for the J-PARC E16 experiment	Test Experiment	K1.1BR	not performed yet
T54	K.Miwa	Tohoku U	Test experiment for a performance evaluation of a scattered proton detector system for the Σp scattering experiment E40	Test Experiment	K1.1BR	not performed yet
T55	A.Toyoda	KEK	Second Test of Aerogel Cherenkov counter for the J-PARC E36 experiment	Test Experiment	K1.1BR	had to be stopped
E56	T.Maruyama	KEK	A Search for Sterile Neutrino at J-PARC Materials and Life Science Experimental Facility	Stage 2	MLF	Data taking
E57	J. Zmeskal	Stefan Meyer Institute for Subatomic Physics	Measurement of the strong interaction induced shift and width of the 1s state of kaonic deuterium at J-PARC	Stage 1	K1.8BR	in preparation
P58	M. Yokoyama	U. Tokyo	A Long Baseline Neutrino Oscillation Experiment Using J-PARC Neutrino Beam and Hyper-Kamiokande	Deferred	neutrino	
T59	A. Minamino	Kyoto U	A test experiment to measure neutrino cross sections using a 3D grid-like neutrino detector with a water target at the near detector hall of J-PARC neutrino beam-line	To be arranged by IPNS and KEK-T2K	neutrino monitor bld	Finished
T60	T. Fukuda	Toho U	Proposal of an emulsion-based test experiment at J-PARC	Arranged by IPNS and KEK-T2K	neutrino monitor bld	Finished
E61	M. Wilking	Stony Brook U	NuPRISM/TITUS	Superseded. E61 has been adopted in Hyper-K as IWCD. IWCD is reviewed by HK-PAC.	neutrino	
E62	R. Hayano, S. Okada, H. Outa	U. Tokyo, RIKEN	Precision Spectroscopy of kaonic atom X-rays with TES	Stage 2	K1.8BR	Finished
E63	H. Tamura	Tohoku U	Gamma-ray spectroscopy of light hypernuclei II	Stage 2	K1.1	BL not ready yet. Exp. in preparation
T64	Y. Koshio	Okayama U	Measurement of the gamma-ray and neutron background from the T2k neutrino/anti-neutrino at J-PARC B2 Hall	Arranged by IPNS and KEK-T2K	neutrino	

	(Co-) Spokespersons	Affiliation	Title of the experiment	Approval status (PAC recommendation)	Beamline	Status
E65	A.K.Ichikawa, F.Sanchez	Kyoto U	Proposal for T2K Extended Run	Stage-2	neutrino	
T66	T. Fukuda	Nagoya U	Proposal of an emulsion-based test experiment at J-PARC	Test Experiment	neutrino	
P67	I. Meigo	JAEA	Measurement of displacement cross section of proton in energy region between 3 and 30 GeV for high-intensity proton accelerator facility	Carry out the experiment within the framework of facility development	MR	
T68	T. Fukuda	Nagoya U	Extension of T60/T66 Experiment: Proposal for the Run from 2017 Autumn	Test Experiment	neutrino	
E69	A. Minamino	Yokohama National U	Study of neutrino-nucleus ineraction at around 1GeV using cuboid lattice neutrino detector, WAGASHI, muon range detectors and magnetized spectrometer, Baby MIND, at J-PARC neutrino monitor hall	Superseded. Merged with T2K.	neutrino	
E70	T. Nagae	Kyoto U	Proposal for the next E05 run with the S-2S spectrometer	Stage-2	K1.8	
E71	T. Fukuda	Nagoya U	Proposal for precise measurement of neutrinop-water cross-section in NINJA physics run	Stage-2	neutrino	Data taking
E72	K. Tanida	JAEA	Search for a Narrow Λ* Resonance using the p(K-, Λ)η Reaction with the hypTPC Detector	Stage-2	K1.8BR	
E73	Yue Ma	RIKEN	${}^{3}_{\Lambda}$H and ${}^{4}_{\Lambda}$H mesonic weak decay lifetime measurement with ^{3,4}He(K^-,π^0)${}^{3,4}_{\Lambda}$H reaction	PAC suggests Stage-2 approval	K1.8BR	
P74	A.Feliciello	INFN, Torino	Direct measurement of the 3ΛH and 4ΛH lifetimes using the 3,4He(π-,K0)3,4ΛH reactions	Rejected	K1.1	
E75	H.Fujioka	Tokyo Inst. Tech,	Decay Pion Spectroscopy of 5ΛΛH Produced by Ξ-hypernuclear Decay	PAC suggests Stage-2 approval	K1.8	
P76	H.M.Shimizu	Nagoya U	Searches for the Breaking of the Time Reversal Invariance in Polarized Epithermal Neutron Optics	Deferred	MLF	
T77	Yue Ma	RIKEN	Feasibility study for 3ΛH mesonic weak decay lifetime measurement with 3,4He(K-,π0)3,4ΛH reaction	PAC supoorts the ontinuation of T77 by an explorative run with the 3He target.	K1.8BR	Finished Data analysis
T78	H.Nishiguchi	KEK	8GeV Operation Test and Extinction Measurement	Test Experiment	K1.8BR	Finished
E79	T.Ishikawa	Tohoku U	Search for an I=3 dibaryon resonance	Stage-1	High p	
E80	F.Sakuma	RIKEN	Systematic investgatin of the light kaonic nuclei	Stage-1	K1.8BR	
T81	T.Fukuda	Nagoya U	Proposal of test experiment for technical improvements of neutrino measurements with nuclear emulsion detector	Test Experiment	neutrino	
E82	T.Maruyama	KEK	JSNS2-II	PAC suggests Stage-2 approval	MLF	
E83	J. H. Yoo	Korea U	Search for sub-millicharged particles at J-PARC	PAC suggests stage-1 status.	neutrino	
E88	H. Sako	JAEA	Study of in-medium modification of phi mesons inside the nucleus with phi->K^+K^- measurement with the E16 spectrometer	PAC suggests stage-1 status.	high-p	
P89	T. Yamaga	RIKEN	Investigation of fundamental properties of the KNN state	Deferred. PAC would like to see the detailed feasibility of P89 after E80's TDR.	K1.8BR	
E90	Y.Ichikawa, K.Tanida	JAEA	High resolution spectroscopy of the "ΣN cusp" by using the d(K^-, π^-) reaction	PAC suggests stage-1 status.	K1.8	
P91	Y.Morino	KEK	Proposal for study of charm component in the nucleon via J/ψ measurement with the J-PARC E16 spectrometer	Deferred.	high-p	
P92	F.Sakuma	RIKEN	Proposal for the E80 Phase-I Experiment:Investigation of the KNNN $^-$ Bound State Focusing on the Λd Decay	Deferred. PAC recommends that the proponents should carefully analyze the T77 data and seek further justification for the K-NNN bound state interpretation.	K1.8BR	
P93	K.Shirotori	Osaka U (RCNP)	Proposal of test experiment to evaluate performances of secondary beam mode at the high-momentum beam line	Deferred. PAC requests that the beamline modification part of the proposal be discussed with the Lab/Facility management. PAC also recommends the proponents make specific proposals.	high-p	

Organization and Committees

Organization Structure

J-PARC Center Management System Chart

as of April 1, 2021

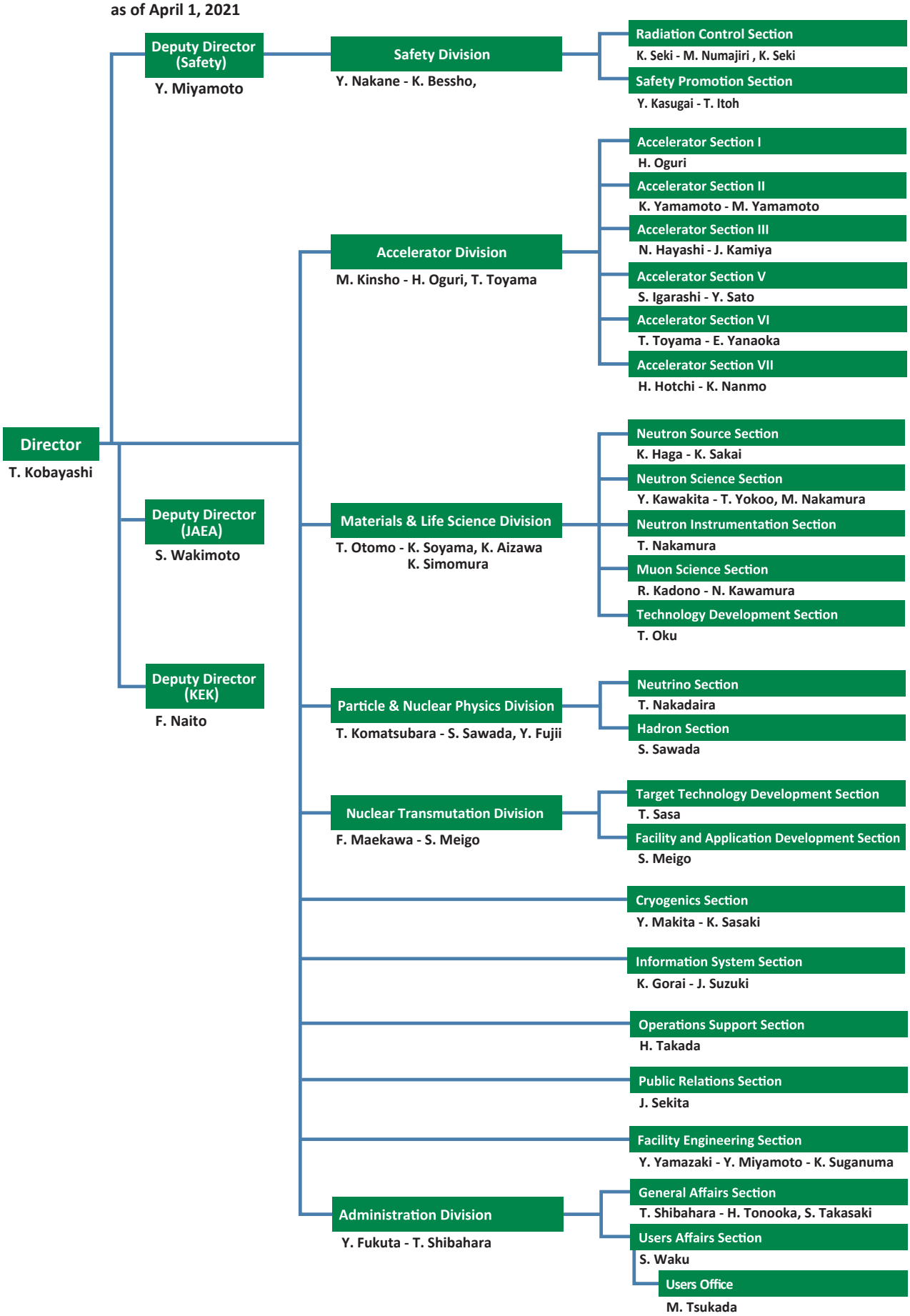

Members of the Committees Organized for J-PARC

(as of March, 2020)

1) Steering Committee (*) Chair

Junji Haba (*)	High Energy Accelerator Research Organization (KEK), Japan
Koki Uchimaru	High Energy Accelerator Research Organization (KEK), Japan
Naohito Saito	High Energy Accelerator Research Organization (KEK), Japan
Nobuhiro Kosugi	High Energy Accelerator Research Organization (KEK), Japan
Tadashi Koseki	High Energy Accelerator Research Organization (KEK), Japan
Hiroyuki Oigawa (*)	Japan Atomic Energy Agency (JAEA), Japan
Kenji Sudo	Japan Atomic Energy Agency (JAEA), Japan
Masayasu Takeda	Japan Atomic Energy Agency (JAEA), Japan
Toshiyuki Momma	Japan Atomic Energy Agency (JAEA), Japan
Akira Endo	Japan Atomic Energy Agency (JAEA), Japan
Takashi Kobayashi	J-PARC Center, Japan

2) International Advisory Committee (*) Chair

Thomas Prokscha	Paul Scherrer Institute (PSI), Switzerland
Yoko Sugawara	Toyota Physical and Chemical Research Institute, Japan
Paul Langan	Institut Laue-Langevin, France
Takeshi Egami	University of Tennessee, USA
Dan Alan Neumann	National Institute of Standards and Technology, USA
Robert McGreevy (*)	Science & Technology Facilities Council (STFC), UK
Jie Wei	Michigan State University, USA
John Thomason	Science & Technology Facilities Council (STFC), UK
Joachim Mnich	The European Organization for Nuclear Research(CERN), Switzerland
Dmitri Denisov	Brookhaven National Laboratory, USA
Angela Bracco	INFN, Istituto Nazionale di Fisica Nucleare, Italy
Reiner Kruecken	TRIUMF, Canada
Hamid Aït Abderrahim	Belgian Nuclear Research Centre (SCK CEN), Belgium
Akira Hasegawa	Tohoku University, Japan
Shinichi Kamei	Mitsubishi Research Institute, Japan
Hiromi Yokoyama	The University of Tokyo, Japan

3) User Consultative Committee for J-PARC (*) Chair

Masaki Ishitsuka	Tokyo University of Science, Japan
Hajime Nanjo	Osaka University, Japan
Shoji Asai	The University of Tokyo, Japan
Takeshi Komatsubara	High Energy Accelerator Research Organization (KEK), Japan
Satoshi Nakanura	Tohoku University, Japan
Tomofumi Nagae	Kyoto University, Japan
Fuminori Sakuma	RIKEN, Japan
Shinya Sawada	High Energy Accelerator Research Organization (KEK), Japan
Kouji Miwa	Tohoku University, Japan
Hiroyuki Kimura	Tohoku University, Japan
Toshio Yamaguchi (*)	Fukuoka University, Japan
Takashi Kamiyama	Hokkaido University, Japan
Takatsugu Masuda	The University of Tokyo, Japan
Kazuhisa Kakurai	Comprehensive Research Organization for Science and Society (CROSS), Japan
Toshiya Otomo	High Energy Accelerator Research Organization (KEK), Japan
Kenya Kubo	International Christian University, Japan
Tadashi Adachi	Sophia University, Japan
Koichiro Shimomura	High Energy Accelerator Research Organization (KEK), Japan
Yuko Kojima	Mitsubishi Chemical Corporation, Japan
Hiroyuki Kishimoto	Sumitomo Rubber Industries, Ltd. Japan
Hideto Imai	Nissan Analysis and Research Center, Japan
Masahiro Hino	Kyoto University, Japan
Hironori Kodama	Ibaraki Prefecture, Japan
Satoru Yamashita	The University of Tokyo, Japan
Cheol-Ho Pyeon	Kyoto University, Japan
Kazufumi Tsujimoto	Japan Atomic Energy Agency (JAEA), Japan

4) Accelerator Technical Advisory Committee (*) Chair

Wolfram Fischer	Brookhaven National Laboratory (BNL), USA
Mats Lindroos	European Spallation Source, ERIC, Sweden
John Thomason	Science and Technology Facilities Council (STFC), UK
Sheng Wang	Institute of High Energy Physics, CAS, China
Toshiyuki Shirai	National Institutes for Quantum and Radiological Science and Technology, Japan
Alexander Aleksandrov	Oak Ridge National Laboratory, USA
Jie Wei (*)	Michigan State University., USA
Robert Zwaska	Fermi National Accelerator Laboratory (FNAL), USA
Simone Gilardoni	European Organization for Nuclear Research (CERN), Switzerland

5) Neutron Advisory Committee (*) Chair

Phillip King	Rutherford Appleton Laboratory, UK
Bertrand Blau	Paul Scherrer Institut (PSI), Switzerland
Michael J Dayton	Oak Ridge National Laboratory (ORNL), USA
Guenter Muhrer	European Spallation Source(ESS), Sweden
Christiane Alba-Simionesco	Laboratoire Leon Brilloin (LLB) Sacley, France
Jamie Schulz (*)	Australian Nuclear Science and Technology Organization(ANSTO), Australia
Jon Taylor	European Spallation Source(ESS), Sweden
Sungil Park	Korea Atomic Energy Research Institute(KAERI), Korea
Yoshie Ohtake	RIKEN, Japan
Takahisa Arima	The University of Tokyo, Japan
Ken Anderson	Oak Ridge National Laboratory (ORNL), USA
Toyohiko Kinoshita	Japan Synchrotron Radiation Research Institute(JASRI), Japan

6) Muon Advisory Committee (*) Chair

Martin Månsson	KTH Royal Institute of Technology, Sweden
Thomas Prokscha (*)	Paul Scherrer Institut (PSI), Switzerland
Andrew MacFarlane	University of British Columbia, Canada
Klaus Kirch	ETH Zurich and Paul Scherrer Institute (PSI), Switzerland
Kenya Kubo	International Chiristian University, Japan
Tadayuki Takahashi	University of Tokyo, Japan
Nori AOI	Osaka University, Japan
Hiroshi Amitsuka	Hokkaido University, Japan

7) Radiation Safety Committee (*) Chair

Yoshitomo Uwamino (*)	Japan Radioisotope Association, Japan
Yoshihiro Asano	High Energy Accelerator Research Organization (KEK), Japan
Hiroshi Watabe	Tohoku University, Japan
Takeshi Iimoto	University of Tokyo, Japan
Takeshi Murakami	National Institutes for Quantum and Radiological Science and Technology (QST), Japan
Yukinori Kobayashi	High Energy Accelerator Research Organization (KEK), Japan
Toshiya Sanami	High Energy Accelerator Research Organization (KEK), Japan
Yoshihito Namito	High Energy Accelerator Research Organization (KEK), Japan
Akira Endo	Japan Atomic Energy Agency (JAEA), Japan
Takumi Nemoto	Japan Atomic Energy Agency (JAEA), Japan
Nobuyuki Kinouchi	Japan Atomic Energy Agency (JAEA), Japan

8) Radiation Safety Review Committee (*) Chair

Yukihiro Miyamoto (*)	Japan Atomic Energy Agency (JAEA), Japan
Yoshihiro Nakane	Japan Atomic Energy Agency (JAEA), Japan
Masaharu Numajiri	High Energy Accelerator Researchi Organization (KEK), Japan
Hidetoshi Kikunaga	Tohoku University, Japan
Hiroshi Yashima	Kyoto Univaersity, Japan
Kanenobu Tanaka	Institute of Physical and Chemical Research (RIKEN), Japan
Nobuyuki Chiga	National Institute for Quantum and Radiological Science and Technoloty (QST), Japan
Toshiro Itoga	Japan Synchrotron Radiation Research Institute (JASRI), Japan
Koji Kiriyama	Comprehensive Reserch Organization for Science and Society (CROSS), Japan
Akira Hirose	Japan Atomic Energy Agency (JAEA), Japan
Makoto Kobayashi	Japan Atomic Energy Agency (JAEA), Japan
Kaiichi Haga	High Energy Accelerator Researchi Organization (KEK), Japan
Kazuyoshi Masumoto	High Energy Accelerator Researchi Organization (KEK), Japan
Michikazu Kinsho	Japan Atomic Energy Agency (JAEA), Japan
Yoshiaki Fujii	High Energy Accelerator Researchi Organization (KEK), Japan
Takeshi Komatsubara	High Energy Accelerator Researchi Organization (KEK), Japan
Kazuya Aizawa	Japan Atomic Energy Agency (JAEA), Japan

9) MLF Advisory Board (*) Chair

Takahisa Arima (*)	The University of Tokyo, Japan
Taku Sato	Tohoku University, Japan
Osamu Yamamuro	The University of Tokyo, Japan
Takashi Kamiyama	Hokkaido University, Japan
Yoshiharu Sakurai	Japan Synchrotron Radiation Research Institute(JASRI), Japan
Hiroshi Amitsuka	Hokkaido University, Japan
Yoko Sugawara	Toyota Physical and Chemical Research Institute, Japan
Tadashi Adachi	Sophia University, Japan
Hiroyuki Kishimoto	Sumitomo Rubber Industries, Japan
Yoshie Otake	RIKEN, Japan
Jun Takahara	Kyusyu University, Japan
Masahiro Hino	Kyoto University, Japan
Yasuhiro Iye	Chubu University, Japan
Toshiya Otomo	High Energy Accelerator Research Organization (KEK), Japan
Kazuhiko Soyama	Japan Atomic Energy Agency (JAEA), Japan
Kazuya Aizawa	Japan Atomic Energy Agency (JAEA), Japan
Koichiro Shimomura	High Energy Accelerator Research Organization (KEK), Japan
Yukinobu Kawakita	Japan Atomic Energy Agency (JAEA), Japan
Ryosuke Kadono	High Energy Accelerator Research Organization (KEK), Japan
Shinichi Itoh	High Energy Accelerator Research Organization (KEK), Japan
Masayasu Takeda	Japan Atomic Energy Agency (JAEA), Japan
Kenji Nakajima	Japan Atomic Energy Agency (JAEA), Japan
Jun-Ichi Suzuki	Comprehensive Research Organization for Science and Society (CROSS), Japan

10) Program Advisory Committee (PAC) for Nuclear and Particle Physics Experiments at the J-PARC 50Gev Proton Synchrotron

(*) Chair

Ichiro Adachi	High Energy Accelerator Research Organization (KEK), Japan
Motoi Endo	High Energy Accelerator Research Organization (KEK), Japan
Yoshitaka Itow	Nagoya University, Japan
Takahiro Kawabata	Osaka University, Japan
Hiroaki Ohnishi	Tohoku University, Japan
Akira Ohnishi	Kyoto University, Japan
Kohei Yorita	Waseda University, Japan
Patrick Achenbach	Mainz University, Germany
Monika Blanke	Karlsruhe Institute of Technology, Germany
Laura Fields	Fermi National Accelerator Laboratory (FNAL), USA
David Jaffe	Brookhaven National Laboratory (BNL), USA
Francois Le Diberder	The French National Institute of Nuclear and Particle Physics (IN2P3), France
Kam-Biu Luk	University of California at Berkley, USA
Anthony William Thomas	University of Adelaide, Australia
Nu Xu	Lawrence Berkeley National Laboratory, USA
Rikutaro Yoshida (*)	Argonne National Laboratory, USA

11) TEF Technical Advisory Committee

(*) Chair

Marc Schyns (*)	Belgian Nuclear Research Center(SCK • CEN), Belgium
Michael Butzek	Forschungszentrum Jülich, Germany
Thierry Stora	European Organization for Nuclear Research (CERN), Switzerland
Yukinobu Watanabe	Kyushu University, Japan
Kazuo Hasegawa	National Institutes for Quantum and Radiological Science and Technology (QST), Japan
Georg Müller	Karlsruhe Institute of Technology, Germany
Kei Ito	Kyoto University, Japan

Main Parameters

Present main parameters of Accelerator

Linac	
Accelerated Particles	Negative hydrogen
Energy	400 MeV
Peak Current	50 mA
Pulse Width	0.385 ms for MLF 0.50 ms for MR-FX 0.20 ms for MR-SX
Repetition Rate	25 Hz
Freq. of RFQ, DTL, and SDTL	324 MHz
Freq. of ACS	972 MHz
RCS	
Circumference	348.333 m
Injection Energy	400 MeV
Extraction Energy	3 GeV
Repetition Rate	25 Hz
RF Frequency	0.938 MHz → 1.67 MHz
Harmonic Number	2
Number of RF cavities	12
Number of Bending Magnet	24
Main Ring	
Circumference	1567.5 m
Injection Energy	3 GeV
Extraction Energy	30 GeV
Repetition Rate	~0.4 Hz
RF Frequency	1.67 MHz → 1.72 MHz
Harmonic Number	9
Number of RF cavities	10
Number of Bending Magnet	96

Key parameters of Materials and Life Science Experimental Facility

Injection energy	3 GeV
Repetition rate	25 Hz
Neutron Source	
Target material	Mercury
Number of moderators	3
Moderator material	Liquid hydrogen
Moderator temperature/pressure	20 K/1.5 MPa
Number of neutron beam extraction ports	23
Muon production target	
Target material	Graphite
Number of muon beam extraction ports	4
Neutron instruments	
Open for user program (general use)	21
Under commissioning/construction	0
Muon Instruments	
Open for user program (general use)	3
Under commissioning/construction	1/0

Events

Events

J-PARC Hello Science Class at After-School Club

On April 2, at the Okusu Funaba School Children's Club in Tokai Village, a spring holiday handicraft experiment class was held on the theme of tops. In the class, participants used a compass to observe the line of magnetic force of each disc magnet and an electromagnet and tops to carry out a precession experiment.

Students listen to the lecturer carefully.

The experiment with a top is so much fun!

First Media Salon, J-PARC Media Seminar Held: "A full explanation of the latest news on the muon g-2 experiment. Will new physics be discovered beyond the standard model?!"

On April 7, Fermi National Accelerator Laboratory (Fermilab) in the U.S. announced results for the measurement of anomalous magnetic moment (g-2) of muon. The seminar explains an overview of the planned experiment at J-PARC with international collaboration, differences between the Fermilab experiment and the J-PARC experiment, and other related topics. A high level of interest was evident as there were 22 media participants from 9 companies. Prof. Mibe, a staff member of the J-PARC center, and associate professor in KEK*explained the new Muon g-2 experiment to be conducted at J-PARC. Prof. Shimomura, deputy division head of MLF, and professor in KEK explained research aiming to improve the accuracy of g-2 determination by using muonium.

* Professor since June 1, 2021.

Ass.Prof. Mibe

Prof. Shimomura

The room in J-PARC for broadcasting the online seminar

J-PARC Safety Day

At the J-PARC Center, we learned a lesson from the radioactive material leak incident which occurred in May 2013, and we have established a Safety Day in May of each year to give everyone a chance to think about safety.

Safety Day for FY2021 was held in a remote live format on May 28, with 310 participants. After commending examples of good practice in FY2020, Dr. Norio Tani of Accelerator Section II gave a presentation on "Work Management at the RCS Facility."

Next, there was a talk by Mr. Satoru Nabeshima from the Engineering & Maintenance Center of All Nippon Airways Co., Ltd.(ANA) entitled "Assertion Culture Supporting Safety in the Maintenance Departments of the ANA Group."

"Accelerators" Exhibition at National Museum of Nature and Science from July 13 to October 3

In this event, we introduced the history and development of accelerators in Japan, the basis of accelerators and state-of-the-art research on the universe, as well as research results used in familiar places.

On July 24, we held a lecture titled "A tool for chasing dreams: accelerators" by Hitoshi Murayama, the MacAdams Professor of the University of California, Berkeley, and Professor of the Kavli Institute for the Physics and Mathematics of the Universe at the University of Tokyo Institutes for Advanced Study.

Exhibition site

Professor Murayama

Online press conference takes place to start sample analysis of asteroid Ryugu on June 25

The conference was broadcast from the Photon Factory (PF) at KEK Tsukuba Campus and the Muon Experimental Facility at J-PARC's Materials and Life Science Experimental Facility (MLF). Professor Tomoki Nakamura of Tohoku University, the leader of the Stone Material Analysis Team, operated a Gandolphy X-ray camera that analyzes Ryugu samples using the PF's synchrotron radiation BL-3A. Professor Yoshio Takahashi of the University of Tokyo used the PF's BL-19A and Associate Professor Kazuhiko Ninomiya of Osaka University used the MLF's Muon D2 to explain the characteristics of each beam line, experimental methods for samples, or expected analysis results.

From June 28 to July 5, samples of asteroid Ryugu were brought to the Muon Experimental Facility, irradiated with high-intensity negative muons, and analyzed as planned.

Debriefing session on industrial use of J-PARC MLF from July 15 to 16

It has been jointly hosted by four parties, the J-PARC Center, CROSS, Ibaraki Prefecture, and the Industrial Users Society for Neutron Application every year since 2017. The reporting meeting last year was canceled due to COVID-19. However, this year, 352 people participated in the online meeting. There was a strong request from the industry sector to know what neutrons and muons can tell us and how they can be used.

Three J-PARC researchers gave online lectures at Spring X Super School, hosted by KNOWLEDGE CAPITAL on July 3, 10, 17

KNOWLEDGE CAPITAL hosts Spring X Super School as a place to learn "real knowledge" from specialists in various fields such as science, art, culture, and business, to think together, and to hold discussions. This time, three J-PARC researchers gave lectures on YouTube Live under the theme of "Life planning for junior and senior high school students: living as a researcher" for one hour each on Saturday for three weeks.

The first lecture was "Explore the mystery of the universe at J-PARC" by Takashi Kobayashi, Director of the J-PARC Center, the second one was "How to create the strongest beam!" by Yoshinori Kurimoto, Associate Professor at High Energy Accelerator Research Organization, J-PARC Center's Accelerator Division, and the third one was "How I became a corporate researcher working at J-PARC" by Izumi Umegaki, a researcher in Materials Analysis and Evaluation Research Domain at Toyota Central R&D Labs., Inc.

Workshop "Let's Make Top that Spins While Tilted!" at Tokai Village Enjoy Summer School 2021

At the Enjoy Summer School event organized by Tokai Village every year, J-PARC held a workshop on making tops. Participants were 5th and 6th graders in elementary school, and workshops were held at the Shirakata Community Center on August 2, Tokai Village Library on August 6, and online on August 24 due to the declaration of a state of emergency in Ibaraki Prefecture.

Prof. Mibe from J-PARC, giving a lecture on August 2

Participation in Online Craft Workshop "Let's Make Polarized Kaleidoscope" for Kids Kasumigaseki Open Day

The Kids Kasumigaseki Open Day is an activity jointly organized by government offices, ministries, and agencies located in the Kasumigaseki district. This year, the event was mainly held online on August 18 and 19, and elementary school students who gathered at the

booth of the Japan Atomic Energy Agency (JAEA) in the Ministry of Education, Culture, Sports, Science and Technology received an online explanation from the staff at the J-PARC Research Building and learned the principle of polarization by making a polarized kaleidoscope.

JAEA booth at Kasumigaseki

1st J-PARC Lecture Presentation

J-PARC Center has held lecture presentations to help more people understand our latest experiments and research results. The first lecture was held online with the title "A Gift from Space: Uncovering the Origins of Life with Muons" on August 25. It discussed the analysis, conducted with negative muon beams produced at J-PARC from June 28 to July 3, of samples from the asteroid Ryugu brought back by the asteroid explorer Hayabusa 2.

Formation of a Collaborative Alliance of Industrial-Academic Facilities Active at Multiple Quantum Beam Facilities: Aiming to Develop Quantum Beam Users in Industry and Maximize the Results of Industrial Use

Academic researchers primarily from Kyoto University, 16 companies in the polymer, soft matter, and other industries, and three large quantum beam facilities (SPring-8, JRR-3, and J-PARC) joined together on September 30 to form an industry-academia-facility organization called the "Quantum Beam Analysis Alliance" (Representative: Mikihito Takenaka, Professor, Institute for Chemical Research, Kyoto University). In June of this year, joint experiments and technical training on neutron reflectivity measurement were carried out at the MLF, and there were activities aimed at helping participating corporate members master techniques using quantum beams.

5th Symposium Integration of Arts and Sciences, Using Quantum Beams Held on September 9 and 10

To promote research combining humanities and science, the Institute of Materials Structure Science of the High-Energy Accelerator Research Organization (KEK) holds symposiums to bring humanities and science together. This symposium has been held since the fiscal year 2019, and the 5th symposium entitled "Integration of arts and sciences, using Quantum beams", was held online.

At this symposium, participants included researchers specializing in quantum beams, scientific researchers in the areas of archaeology and cultural properties from universities, museums, and other institutions with an interest in the non-destructive analysis, as well as ordinary people. There were 82 registered participants and 14 oral presentations. A variety of analyzed objects were presented including rocks from the asteroid Ryugu, earthenware, stone implements, bronze artifacts, DNA, glue ink, pictures, and Japanese swords.

Participants of the symposium

J-PARC Open House 2021 Held Online on November 13

This year's J-PARC open house was held online, like the last year. There was a live video from the MLF Experimental Hall, nuclear transmutation research facility, MR Accelerator, Hadron Hall, and Neutrino Monitor Building. In addition to talks by researchers, the content included an interior video of accelerators that is not normally shown to the public. Live streaming was achieved through a team effort by about 50 staff members.

Following the keynote address "Exploring the Mysteries of Elementary Particles and the Universe with Neutrinos" by Professor Atsuko Ichikawa of Tohoku University, a representative of the T2K Experiment Group, there was a feature called "Ask Questions of Researchers Active on the World Stage!" Participants were limited to Japanese college of technology and high school

students who applied from all over Japan. They participated online, and the question-and-answer session ran over the scheduled time.

J-PARC staff at the end of the streaming

Exhibition at JASIS 2021 in Makuhari Messe International Exhibition Hall on November 8 – 10

JASIS, organized by the Japan Analytical Instruments Manufacturers' Association and the Japan Scientific Instruments Association, is one of the largest exhibitions in Asia of cutting-edge scientific and analysis systems.

Results using the MLF and JRR-3 were presented, as well as information on the portal site for the usage of the facility.

Over three days, there were about 730 visitors to these JAEA booths, and there was an active exchange of questions.

At JAEA booth

2021 J-PARC Photo Contest

The J-PARC Photo Contest was held this year for the 8th time. We had a total of 21 artworks submitted by 13 people who are involved with the operation of J-PARC and J-PARC users. One grand prize, two outstanding prizes, and six runners-up were selected. Two external judges also helped to select them. The award ceremony was held on November 11, and the J-PARC Center Director Takashi Kobayashi handed each award winner a certificate and a gift. The first prize was awarded to the work "Can You Stand the Heat?" by Harjo Stefanus, Principal Researcher, of the Neutron Use Section.

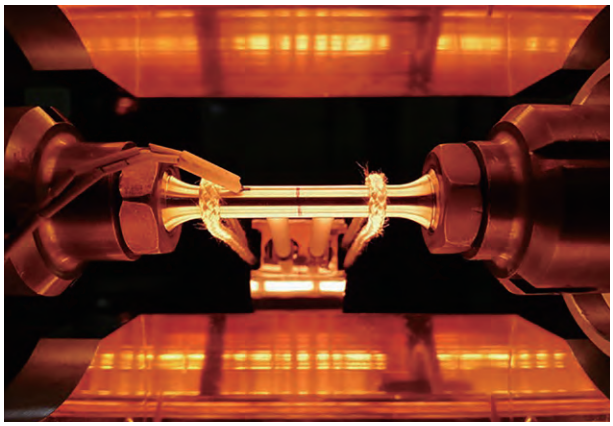

Grand Prize "Can You Stand the Heat?" by Harjo Stefanus

Tour of J-PARC for Ibaraki University, KEK Day on December 27

Twenty students from Ibaraki University's College of Science, College of Engineering, and Graduate School of Science and Engineering visited and toured J-PARC as part of "Ibaraki University, KEK Day", a tour focusing on quantum beam science using state-of-the-art accelerators.

Participants were divided into two groups and toured the Klystron Gallery in the LINAC Building, the MLF, the Hadron Experimental Facility, and the Neutrino Experimental Facility.

Fun Science Class for Parents and Children Held at the Hitachi Civic Center

At the Hitachi Civic Center, a fun science class for parents and children was held on December 12 with the title "What is an Elementary Particle? - A Fascinating Tiny World -" By using tops, elementary school students and their parents learned together about the properties of elementary particles.

Eight groups of parents and children participated in the morning session, and seven groups in the afternoon session.

J-PARC Hello Science "Muon H Line Finally Starts Operation"

Hello Science for December was also held at the Ibaraki Quantum Beam Research Center (IQBRC) as well

as online on December 24. Dr. Takayuki Yamazaki of the Materials and Life Science Division spoke about the Muon H Line.

The H line is a new member of the muon beam line at the MLF of J-PARC that will be added starting this year. The H line will enable high-intensity production of both positive and negative muons, and the beamline will have variable beam energy for outstanding general versatility.

Furthermore, in the future the H line will be extended, one more experimental area will be constructed, and a high-brightness muon beam will be produced. Experiments are being planned, including a muon g-2/EDM experiment and a transmission muon microscope.

16th Tokai Forum: From Tokai Region to the Future – Frontline Research and Decommissioning Technology on February 28

The Tokai Forum is a conference to report on the latest results of research conducted at the Nuclear Fuel Cycle Engineering Laboratories, Nuclear Science Research Institute, and J-PARC Center to facilitate a better understanding of the activities of the Japan Atomic Energy Agency (JAEA). Subsequent to the last year, recorded videos were released this year.

From J-PARC, Director Takashi Kobayashi described the structure and characteristics of three accelerators at J-PARC, and talked about research results of the Materials and Life Science Experimental Facility (MLF), including improved performance of lithium-ion rechargeable batteries, nondestructive analysis of Ogata Koan's sealed medicine and samples of asteroid Ryugu returned by Hayabusa 2, commencement of research for sterile neutrinos, experiment to create a state similar to a neutron star, and advancement of T2K experiment for neutrinos. Then, Assistant Principal Researcher Hiroyuki Kogawa of the Neutron Source Section gave a presentation titled "Development of Damage Suppression Technology on the Mercury Target Vessel at J-PARC," detailing the development process of a mercury target that stably supplies neutrons with the world's highest intensity, where the damage of the vessel that is caused by impact pressure generated in mercury due to incidental proton beams is suppressed by injecting cushioning microbubbles into the mercury.

The International Advisory Committee (IAC), Holds International Advisory Committee Meetings

A series of international advisory committee meetings was held, in which J-PARC received advice on its activities and plans from experts inside and outside Japan. Meetings of the four committees for Transmutation Experimental Facility (TEF) Technical Advisory Committee (T-TAC), Muon Advisory Committee (MAC), Neutron Advisory Committee (NAC), and Accelerator Technical Advisory Committee (A-TAC) were held from February 2 to 21,2022, and the International Advisory Council (IAC) meeting, including reports from these four meetings, was held on March 3 and 4, 2022. At the IAC meeting, J-PARC made a report on its overall response to the advice received at the previous meetings, and the committee members gave high praise and new advice on J-PARC's wide-ranging activities. This year, two committee members in the disciplines of humanities and social sciences joined the IAC meeting, and they recognized that J-PARC's public relations activities and communications were at a very high level and greatly helping in improving people's awareness of its social contributions.

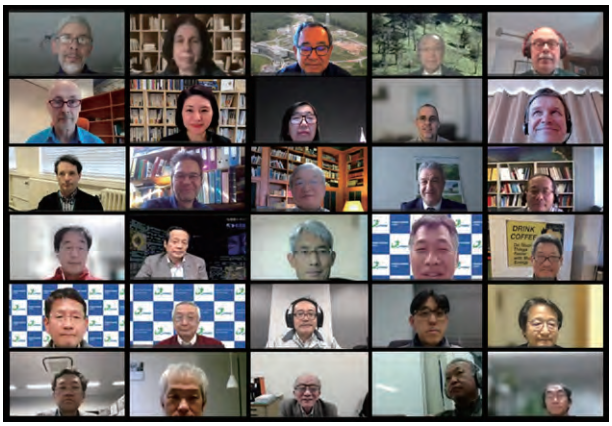

The members of the committee attending IAC online

Held 2nd J-PARC Online Lecture Presentation and J-PARC Hello Science

On March 25, the 2nd Online Lecture Presentation "Diverse Types of Matter in the Universe Created by Elementary Particles called Quarks —J-PARC Tackles the Challenge of Elucidation," and the J-PARC Hello Science Event "Do Hypernuclei Exist in the Universe?" were held, with lectures by Hirokazu Tamura, Professor at Tohoku University. As part of the lecture presentation, there was also a detailed presentation on experiments conducted at J-PARC by Shinya Sawada, Deputy Division Head of the Particle & Nuclear Physics Division.

Atomic nuclei, at the center of the atoms which

comprise matter, are made up of protons and neutrons in all objects on earth, and those protons and neutrons consist of up and down quarks, the two lightest quarks among the six types of quarks. In space, on the other hand, it has been found that the strange quark, the next heaviest quark after the up and down quarks, plays a crucial role. Red supergiant stars are formed at the end stage of stellar evolution. Before long, they cause a supernova explosion, and the star's remains become a black hole or neutron star. A neutron star is the densest object in the universe, with a radius of about 10–15 km, and a mass 1–2 times that of the sun. The part near the surface is made of neutrons, but the core part is thought to be an unknown material containing strange quarks. At the J-PARC Hadron Experimental Facility, research is being done to create a "mini neutron star" on earth and explore its properties in order to elucidate this unknown type of matter.

Visitors

Due to the measure of prevention against COVID-19, we could not have the usual number of visitors.

75 Attendees of "Summer Challenge 2021" from various universities as online visitors (August 18)

Hideo Yura, Director-General of the Reconstruction Agency (October 1)

There were 473 visitors to J-PARC for the period from April 2021 to the end of March 2022.

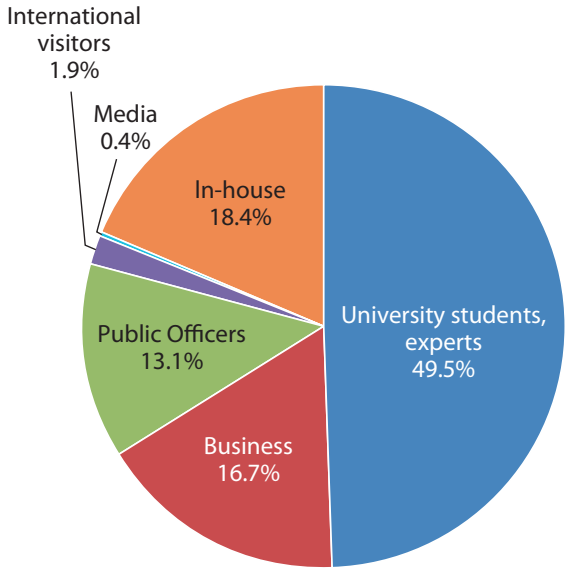

Publications

Publications in Periodical Journals

A-001
H. Hotchi
High-power proton accelerators for pulsed spallation neutron sources
AAPPS Bull. 31, 32 (2021)

A-002
W. Saito, *et al*.
Chemical-Pressure-Induced Point Defects Enable Low Thermal Conductivity for Mg2Sn and Mg2Si Single Crystals
ACS Appl. Energy Mater., 4

A-003
S. Uenuma, *et al*.
Polymer Brush Formation Assisted by Hierarchical Self-Assembly of Topological Supramolecule
ACS Appl. Mater. Interfaces, 13

A-004
M. Harada, *et al*.
Distinguishing adsorbed and deposited ionomers in the catalyst layer of polymer electrolyte fuel cells using contrast variation small-angle neutron scattering
ACS Omega, 6

A-005
K. Chino
Multinetwork Elastomer Using Covalent Bond, Hydrogen Bond, and Clay Plane Bond
ACS Omega, 6

A-006
K. Nakashima, *et al*.
Stabilization of Size-Controlled BaTiO3 Nanocubes via Precise Solvothermal Crystal Growth and Their Anomalous Surface Compositional Reconstruction
ACS Omega, 6

A-007
Q. Li, *et al*.
In-plane low thermal expansion of NiTi via controlled cross rolling
Acta Materialia, 204

A-008
M. M. Nygard, *et al*.
The average and local structure of TiVCrNbDx (x = 0, 2.2, 8) from total scattering and neutron spectroscopy
Acta Materialia, 205

A-009
Q. Li, *et al*.
Tailoring thermal expansion of shape memory alloys through designed reorientation deformation
Acta Materialia, 218

A-010
M. Naeem, *et al*.
Temperature-dependent hardening contributions in CrFeCoNi high-entropy alloy
Acta Materialia, 221

A-011
M. Busi, *et al*.
Nondestructive characterization of laser powder bed fusion parts with neutron Bragg edge imaging
Additive Manufacturing, 39

A-012
A. S. Tremsin, *et al*.
Monitoring residual strain relaxation and preferred grain orientation of additively manufactured Inconel 625 by in-situ neutron imaging
Additive Manufacturing, 46

A-013
C. J. Brett, *et al*.
Humidity-induced Nanoscale Restructuring in PEDOT:PSS and Cellulose reinforced Bio-based Organic Electronics
Adv. Electron. Mater., 7

A-014
M. Kawasaki, *et al*.
In-situ heating neutron- and X-ray diffraction analyses for revealing structural evolution during post-printing treatments of additive-manufactured 316L stainless steel
Adv. Eng. Mater.

A-015
N. Hisano, *et al*.
Elastic properties and structures of pyrope glass under high pressures
American Mineralogist, 106

A-016
R.U. Abbasi, *et al*.
The Cosmic-Ray Composition between 2 PeV and 2 EeV Observed with the TALE Detector in Monocular Mode
ApJ 909, 178 (2021)

A-017
K. Abe, *et al*.
Supernova Model Discrimination with Hyper-Kamiokande
ApJ 916, 15 (2021)

A-018
Y. Oyama
Re-examination of the Time Structure of the SN1987A Neutrino Burst Data in Kamiokande-II
ApJ 922, 223 (2021)

A-019
S. Kumar, *et al*.
Modifications in the nanoparticle-protein interactions for tuning the protein adsorption and controlling the stability of complexes
Appl. Phys. Lett., 118

A-020
P. Wu, *et al*.
Evidence of Spin Reorientation and Anharmonicity in Kagome Ferromagnet Fe3Sn2
Appl. Phys. Lett., 119

A-021
M. Naeem, *et al*.
Martensitic transformation in CrCoNi medium-entropy alloy at cryogenic temperature
Appl. Phys. Lett., 119

A-022
K. Ikeda, *et al*.
Generating Mechanism of Catalytic Effect for Hydrogen Absorption/Desorption Reactions in NaAlH4–TiCl3
Appl. Sci., 11

A-023
R. Aggarwal, *et al*.
An Investigation of Radial Basis Function Method for Strain Reconstruction by Energy-Resolved Neutron Imaging
Appl. Sci., 11(1)

A-024
K. Abe, *et al*.
Supernova Model Discrimination with Hyper-Kamiokande
Astrophys. J., 916, 15-32 (2021)

A-025
A. D. Pant
Muonium behavior in N-acetylglycine-N-methylamide
BIBECHANA, 16

A-026
H. Nakagawa, *et al*.
Conformational dynamics of a multi-domain protein by neutron scattering and computational analysis
Biophys. J., 120

A-027
N. Nishi, *et al*.
Overscreening Induced by Ionic Adsorption at the Ionic Liquid/Electrode Interface Detected Using Neutron Reflectometry with a Rational Material Design
Bull. Chem. Soc. Jpn., 94

A-028
Y. Kameda, *et al*.
Direct Observation of Scattering Angle Dependence of the Inelasticity Effect on the Interference Term Obtained from Time-of-

Flight Neutron Diffraction Experiments
Bull. Chem. Soc. Jpn., 94

A-029
M. Shiozawa, *et al.*
Hyper-Kamiokande Project Has Started
Butsuri, 77, 792 (2021)

A-030
T. Masuda, *et al.*
Hybridized excitation of Higgs-amplitude and phase modes in frustrated quantum magnet
Butsuri, 76

A-031
T. Tanimori, *et al.*
Development of a neutron imaging method based on particle reaction topology
Butsuri, 76

A-032
S. Klotz, *et al.*
Synthesis and characterisation of a new graphitic C-S compound by high pressure decomposition of CS2
Carbon, 185

A-033
S. Yamazoe, *et al.*
Identification of hydrogen species on Pt/Al2O3 by in situ inelastic neutron scattering and their reactivity with ethylene
Catal. Sci. Technol., 11

A-034
S. Behara, *et al.*
Amphoteric behavior of Dy3+ in Na0.5Bi0.5TiO3: neutron diffraction and Raman studies
Ceram. Int., 47

A-035
Y. Yano, *et al.*
Insights into Proton Dynamics in a Photofunctional Salt-Cocrystal Continuum: Single-Crystal X-ray, Neutron Diffraction, and Hirshfeld Atom Refinement
Chem. Eur. J., 27

A-036
K. Fukui, *et al.*
Stabilization Factor of Anion-Excess Fluorite Phase for Fast Anion Conduction
Chem. Mater., 33

A-037
M. Nakamura, *et al.*
Sn-Based Perovskite with a Wide Visible Light Absorption Band Assisted by Hydride Doping
Chem. Mater., 33

A-038
Y. Kitagawa, *et al.*
Site-Selective Eu3+ Luminescence in the Monoclinic Phase of YSiO2N
Chem. Mater., 33

A-039
T.-N. Lam, *et al.*
Tensile Response of As-Cast CoCrFeNi and CoCrFeMnNi High-Entropy Alloys
Crystals, 12

A-040
T. Matsukawa, *et al.*
Detection of hydroxyl and hydride functional groups in a ceria crystal under hydrogen reduction
CrystEngComm, 23

A-041
H. Yukawa, *et al.*
Temperature dependence of hydrogen solubility and diffusivity in hydrogen permeable membrane of pd-cu alloy with b2-type crystal structure
Defect Diffus. Forum, 407

A-042
F. Nemoto, *et al.*
Structural and Dynamical Studies on Liquid Crystalline Ionic Liquids by Thermal Analysis and Neutron Scattering
Ekisho, 25

A-043
K. Yamamoto, *et al.*
Dependence of charge-exchange efficiency on cooling water temperature of a beam transport line
EPJ Techniques and Instrumentation 8 (2021) 9_1

A-044
T. Katabuchi, *et al.*
Discovery of a new low energy neutron resonance of 89Y
Eur. Phys. J. A, 57

A-045
B. Abi, *et al.*
Prospects for beyond the Standard Model physics searches at the Deep Underground Neutrino Experiment
Eur. Phys. J. C 81, 322 (2021)

A-046
B. Abi, *et al.*
Supernova neutrino burst detection with the Deep Underground Neutrino Experiment
Eur. Phys. J. C 81, 423 (2021)

A-047
F. Sakuma, *et al.*
Recent Results and Future Prospects of Kaonic Nuclei at J-PARC
Few-Body Syst. 62, 103 (2021)

A-048
T. Nanamura, *et al.*
The Analysis Status of Σ^+p Scattering Events in the J-PARC E40 Experiment
Few-Body Syst. 62, 110 (2021)

A-049
H. Fujioka, *et al.*
Search for the Lightest Double-Λ Hypernucleus, ${}^{5}_{\Lambda\Lambda}$H, at J-PARC
Few-Body Syst. 62, 47 (2021)

A-050
H. Fujioka, *et al.*
Correction to: Search for the Lightest Double-Λ Hypernucleus, ${}^{5}_{\Lambda\Lambda}$H, at J-PARC [Few-Body Syst (2021) 62:47]
Few-Body Syst. 62, 69 (2021)

A-051
S. Kanda, *et al.*
New precise spectroscopy of the hyperfine structure in muonium with a high-intensity pulsed muon beam
Few-Body Syst., 62, 103 (2021)

A-052
Y. Fujii, *et al.*
Local Dynamics of the Hydration Water and Poly(Methyl Methacrylate) Chains in PMMA Networks
Frontiers in Chemistry, 9

A-053
T. Yamashita, *et al.*
Time evolution calculation of muon catalysed fusion: Emission of recycling muons from a two-layer hydrogen film
Fusion Eng. Des., 169

A-054
K. Okutsu, *et al.*
Design for detecting recycling muon after muon-catalyzed fusion reaction in solid hydrogen isotope target
Fusion Eng. Des., 170

A-055
N. Kawamura, *et al.*
Tritium behavior in isotropic graphite at room temperature
Fusion Eng. Des., 172

A-056
J. Tang, *et al.*
Effect of Nonlinear Elasticity on the Swelling Behaviors of Highly Swollen Polyelectrolyte Gels
Gels, 7

A-057
Y. Tsuji, *et al.*
Neutralization and Salt Effect on the Structure and Mechanical Properties of Polyacrylic Acid Gels under Equivolume Conditions
Gels, 7

A-058
N. Yamada, *et al.*
System Development for Analysis of

Research Achievements and Publication on Web Site at J-PARC MLF
Hamon, Neutron network news, 31

A-059
N. Saito
Preface
Hamon, Neutron network news, 31, 105 (2021)

A-060
A. Sano-Furukawa, *et al*.
High-pressure and high-temperature neutron-diffraction experiments using Kawai-type multi-anvil assemblies
High Press. Res., 41

A-061
S. Yamamoto, *et al*.
Three dimensional (3D) optical imaging system of muon beams using a silver activated zinc sulfide (ZnS(Ag)) sheet combined with a mirror
IEEE Trans Nucl. Sci., 68

A-062
T. Kato, *et al*.
Muon-Induced Single-Event Upsets in 20-nm SRAMs: Comparative Characterization with Neutrons and Alpha Particles
IEEE Trans Nucl. Sci., 68

A-063
T. Okumura, *et al*.
Dynamical Response of Transition-Edge Sensor Microcalorimeters to a Pulsed Charged-Particle Beam
IEEE Trans. Appl. Supercond., 31

A-064
H. Shishido, *et al*.
High Spatial Resolution Neutron Transmission Imaging Using a Superconducting Two-Dimensional Detector
IEEE Trans. Appl. Supercond., 31

A-065
T. Oda, *et al*.
Electric-Field-Dependence Mechanism for Cosmic Ray Failure in Power Semiconductor Devices
IEEE Trans. Electron Devices, 68

A-066
F. Tamura, *et al*.
Development of next-generation timing system for the Japan Proton Accelerator Research Complex
IEEE Trans. Nucl. Sci., 68 (2021) 2043

A-067
S. Dekkers, *et al*.
Radiation Tolerance of Online Trigger System for COMET Phase-I
IEEE Trans. Nucl. Sci., 68, 2020 (2021)

A-068
Y. Iwamiya, *et al*.
Modern alchemy: Making "plastics" from paper
Ind. Eng. Chem. Res., 60

A-069
S. Nakano, *et al*.
Observation of dihydrogen bonds in high-pressure phases of ammonia borane by X-ray and neutron diffraction measurements
Inorg. Chem., 60

A-070
H. Kwon, *et al*.
Programmable Synthesis of Silver Wheels
Inorg. Chem., 60

A-071
Y. Zhang, *et al*.
Investigating the Chemical Ordering in Quaternary Clathrate Ba8AlxGa16–xGe30
Inorg. Chem., 60

A-072
K. Kimura, *et al*.
Coexistence of Magnetoelectric and Antiferroelectric-like Orders in Mn3Ta2O8
Inorganic Chemistry, 60

A-073
S. Tajima, *et al*.
Synthesis and Ion-Transport Properties of EuKGe2O6-, Ca3Fe2Ge3O12-, and BaCu2Ge2O7- Type Oxide-Ion Conductors
Inorganic Chemistry, 60

A-074
D. Urushihara, *et al*.
Structural Transition with a Sharp Change in the Electrical Resistivity and Spin-Orbit Mott Insulating State in a Rhenium Oxide, Sr3Re2O9
Inorganic Chemistry, 60

A-075
S. Harjo
Mechanism of strengthening in cast iron by pulsed neutron beam
Inspection Engineering, 26

A-076
A. Abed Abud, *et al*.
Deep Underground Neutrino Experiment (DUNE) Near Detector Conceptual Design Report
Instruments 2021 5(4), 31 (2021)

A-077
S. Nogami, *et al*.
Structural changes in pH-responsive gelatin/hydroxypropyl methylcellulose phthalate blends aimed at drug-release systems
Int. J. Biol. Macromol., 190

A-078
X.X. Zhang, *et al*.
Multiscale constitutive modeling of additively manufactured Al-Si-Mg alloys based on measured phase stresses and dislocation density
Int. J. Plast., 140

A-079
N. Ishida, *et al*.
Single-phase synthesis, average, electronic, and local structure and cathode properties of pyroxene type LiFeSi2O6
Ionics, 27

A-080
N. Tsuchida, *et al*.
Role of Deformation-Induced Martensite in TRIP Effect of Metastable Austenitic Steels
ISIJ International, 61

A-081
S Harjo, *et al*.
Relation between Intergranular Stress of Austenite and Martensitic Transformation in TRIP Steels Revealed by Neutron Diffraction
ISIJ International, 61

A-082
N. Tsuchida, *et al*.
Effect of Temperature on Stress–Strain Curve in SUS316L Metastable Austenitic Stainless Steel Studied by In Situ Neutron Diffraction Experiments
ISIJ International, 61

A-083
H. SATO, *et al*.
Improvement of Bragg-edge Neutron Transmission Imaging for Evaluating the Crystalline Phase Volume Fraction in Steel Composed of Ferrite and Austenite
ISIJ International, 61

A-084
K. Mishima
中性子寿命の謎，解明に向けた新しい手法 (only Japanese)
Isotope News, 778, (only Japanese)

A-085
K. Maruyama, *et al*.
Magnetic phase diagram of helimagnetic $Ba(Fe_{1-x}Sc_x)_{12}O_{19}$ ($0 \leq x \leq 0.2$) hexagonal ferrite
J. Alloy. Compd., 892

A-086
X.X. Zhang, *et al*.
Strain hardening behavior of additively manufactured and annealed AlSi3.5Mg2.5 alloy
J. Alloys Compd.

A-087
R. Kataoka, *et al*.
Zirconium Hydride-Stabilized Yttrium Hydride (ZSY): Stabiliza- tion of a Face-Centered Cubic YH3 Phase by Zr Substitution
J. Alloys Compd., 851

A-088
KD Liss, *et al*.
Anisotropic thermal lattice expansion and crystallographic structure of strontium aluminide within Al-10Sr alloy as measured by in-situ neutron diffraction
J. Alloys. Compd., 869

A-089
T. Tominaga, *et al*.
Evaluation of sample cell materials for aqueous solutions used in quasi-elastic neutron scattering measurements
J. Appl Cryst., 54

A-090
D. Miura, *et al*.
Development of spin-contrast-variation neutron powder diffractometry for extracting the structure factor of hydrogen atoms
J. Appl. Cryst., 54

A-091
T. Okudaira, *et al*.
Polarization analysis for small-angle neutron scattering with a 3He spin filter at a pulsed neutron source
J. Appl. Cryst., 54

A-092
M. Mizusawa, K. Sakurai
2D real space visualization of d values in polycrystalline bulk materials of different hardness
J. Appl. Crystallogr., 54

A-093
H. Singh, V.K. Aswal
Tuning of micelle adsorption on nanoparticles by combination of surfactants
J. Appl. Phys., 129

A-094
J. G. Nakamura, *et al*.
Hydrogen impurities in p-type semiconductors, GeS and GeTe
J. Appl. Phys., 130

A-095
R. Maruyama, *et al*.
Improved performance of wide bandwidth neutron-spin polarizer due to ferromagnetic interlayer exchange coupling
J. Appl. Phys., 130

A-096
N. Sato, *et al*.
A feasibility study of inverse contrast-matching small-angle neutron scattering method combined with size exclusion chromatography using antibody interactions as model systems
J. Biol. Chem., 169

A-097
E. Y. Kozhunova, *et al*.
Microphase separation of stimuli-responsive interpenetrating network microgels investigated by scattering methods
J. Colloid Interface Sci., 597

A-098
H. Arima-Osonoi, *et al*.
Local structure investigations of Sn and Mn doped in β-Ga2O3 by X-ray absorption spectroscopy
J. Cryst. Growth, 570

A-099
R. Yuge, *et al*.
Charge Compensation Mechanism and Structural Change of Li- Rich Layered Oxide Li1.23Mn0.46Fe0.15Ni0.15O2 Electrode during Charging and Discharging
J. Electrochem. Soc., 168

A-100
K. Hattori, *et al*.
Wigner functions and quantum kinetic theory of polarized photons
J. High Energ. Phys. 2021, 1 (2021)

A-101
S. Choudhury, *et al*.
Test of lepton flavor universality and search for lepton flavor violation in $B \to K\ell\ell$ decays
J. High Energ. Phys. 2021, 105 (2021)

A-102
R. Mizuk, *et al*.
Measurement of the energy dependence of the $e^+e^- \to B\bar{B}$, $B\bar{B}^*$ and $B^*\bar{B}^*$ exclusive cross sections
J. High Energ. Phys. 2021, 137 (2021)

A-103
S. Jia, *et al*.
Measurements of branching fractions and asymmetry parameters of $\Xi_c^0 \to \Lambda\bar{K}^{*0}$, $\Xi_c^0 \to \Sigma^0\bar{K}^{*0}$, and $\Xi_c^0 \to \Sigma^+K^{*-}$ decays at Belle
J. High Energ. Phys. 2021, 160 (2021)

A-104
Y. Hidaka, *et al*.
Global 3-group symmetry and 't Hooft anomalies in axion electrodynamics
J. High Energ. Phys. 2021, 173 (2021)

A-105
K. Uno, *et al*.
Search for lepton-flavor-violating tau-lepton decays to $\ell\gamma$ at Belle
J. High Energ. Phys. 2021, 19 (2021)

A-106
S. H. Park, *et al*.
Search for the dark photon in $B^0 \to A'A'$, $A' \to e^+e^-$, $\mu^+\mu^-$, and $\pi^+\pi^-$ decays at Belle
J. High Energ. Phys. 2021, 191 (2021)

A-107
T. Hayata, *et al*.
Second order chiral kinetic theory under gravity and antiparallel charge-energy flow
J. High Energ. Phys. 2021, 23 (2021)

A-108
K. Hirota, *et al*.
Neutron Imaging Using a Fine-Grained Nuclear Emulsion
J. Imaging, 7

A-109
K. Isegawa, *et al*.
The First Application of a Gd3Al2Ga3O12:Ce Single-Crystal Scintillator to Neutron Radiography
J. Imaging, 7

A-110
N.V. Mdlovu, *et al*.
In vitro intracellular studies of pH and thermo-triggered doxorubicin conjugated magnetic SBA-15 mesoporous nanocarriers for anticancer activity against hepatocellular carcinoma
J. Ind. Eng. Chem., 102

A-111
J. Koga, *et al*.
Measurement of γ rays from 6LiF tile as an inner wall of a neutron-decay detector
J. Instrum., 16

A-112
S. Yamamoto, *et al*.
Optical imaging of decayed positrons and muons with different collimators
J. Instrum., 16

A-113
T. Yajima, *et al*.
Correlated Li-ion migration in the superionic conductor Li 10 GeP 2 S 12
J. Mater. Chem. A, 9

A-114
T. Kato, *et al*.
Origins of peaks of graphitic and pyrrolic nitrogen in N1s X-ray photoelectron spectra of carbon materials: quaternary nitrogen, tertiary amine, or secondary amine?
J. Mater. Sci., 56

A-115
G. Yamamoto, *et al*.
Crystal structure of nesquehonite, MgCO3·3H(D)2O by neutron diffraction and effect of pH on structural formulas of nesquehonite
J. Mineral. Petrol. Sci., 116

A-116
Y. Mori, *et al*.
Neutron diffraction study of hydrogen site occupancy in Fe0.95Si0.05 at 14.7 GPa and 800K.
J. Mineral. Petrol. Sci., 116

A-117
H. Abe, *et al*.
Spontaneous formations of nanoconfined water in ionic liquids by small-angle neutron scattering
J. Mol. Liq.

A-118
H. Abe
Phase variety in ionic liquids: Hydrogen bonding and molecular conformations
J. Mol. Liq., 332

A-119
S. Hashimoto, *et al*.
Experimental analysis on dynamics of liquid molecules adjacent to particles in nanofluids
J. Mol. Liq., 342

A-120
K. Shimada-Takaura, *et al*.
A novel challenge of nondestructive analysis on OGATA Koan's sealed medicine by muonic X-ray analysis
J. Nat. Med., 75

A-121
M. Arai, *et al*.
The performance of neutron diffractometers at long and short pulse spallation sources: Comparison between ESS and J-PARC
J. Neutron Res., 23

A-122
T. Takamuku, *et al*.
Anion effects on the mixing states of 1-methyl-3-octylimidazolium tetrafluoroborate and bis(trifluoromethylsulfonyl)amide with methanol, acetonitrile, and dimethyl sulfoxide on the meso- and microscopic scales
J. Phys. Chem. B, 125

A-123
H. Watanabe, *et al*.
Local Structure of Li+ in Super-concentrated Aqueous LiTFSA Solutions
J. Phys. Chem. B, 125

A-124
Y. Kameda, *et al*.
Experimental Determination of Relationship between Intramolecular O-D Bond Length and Its Stretching Vibrational Frequency of D2O Molecule in the Liquid State
J. Phys. Chem. B, 125

A-125
K. Ito, *et al*.
Dynamics of water in a catalyst layer of a fuel cell by quasielastic neutron scattering
J. Phys. Chem. C, 125

A-126
M. H. Petersen, *et al*.
Assessing diffusion relaxation of interlayer water in clay minerals using a minimalist three-parameter model
J. Phys. Chem. C, 125

A-127
X. Wang, *et al*.
Crystalline Fully Carboxylated Polyacetylene Obtained under High Pressure as a Li-Ion Battery Anode Material
J. Phys. Chem. Lett., 12

A-128
P. Luo, *et al*.
Neutron Spin–Echo Studies of the Structural Relaxation of Network Liquid ZnCl2 at the Structure Factor Primary Peak and Prepeak
J. Phys. Chem. Lett., 12

A-129
N. Yamamoto, *et al*.
Freezable and Unfreezable Hydration Water: Distinct Contributions to Protein Dynamics Revealed by Neutron Scattering
J. Phys. Chem. Lett., 12

A-130
L. J. Bannenberg, *et al*.
Suppression of the Phase Coexistence of the fcc–fct Transition in Hafnium-Hydride Thin Films
J. Phys. Chem. Lett., 12

A-131
M. Tabuchi, Y. Kobayashi
Appearance of pentavalent Fe ion as a result of a charge disproportionation in Fe-substituted Li2MnO3
J. Phys. Chem. Solids, 150

A-132
K. Itoh, R. Yamada, J. Saida, K. Ikeda and T. Otomo
Atomic-level characterization of free volume in the structure of Cu67Zr33 amorphous alloy
J. Phys. Condens. Matter., 33

A-133
S. Hosokawa, *et al*.
Detailed investigations on short- and intermediate-range structures of Ge-Se glasses near the stiffness transition composition
J. Phys. Soc. Jpn., 90

A-134
F. Tamura
Development of the Next-Generation LLRF Control System fo the J-PARC RCS
J. Phys. Soc. Jpn., 18, (2020) 151

A-135
R. Kurasaki, *et al*.
Production Target of Secondary Particles for Slowly-Extracted High-Intensity Proton Beams
J. Phys. Soc. Jpn., 18, 225 (2021)

A-136
T. Nakadaira, T. Matsubara
J-PARC Neutrino Production Target
J. Phys. Soc. Jpn. 18, 225 (2021)

A-137
Y. Kurimoto, *et al*.
Upgrade Plan of J-PARC Main Ring
J. Phys. Soc. Jpn. 18, No. 1, 10 (2021)

A-138
M. Fujita, *et al*.
Reduction Annealing Effects on the Crystal Structure of *T'*-type $La_{1.8}Eu_{0.2}CuO_{4+\alpha-\delta}$
J. Phys. Soc. Jpn., 90

A-139
D. Ueta, *et al*.
Complex Magnetic Phase Diagram in the Non-Centrosymmetric Compound CePtSi3
J. Phys. Soc. Jpn., 90

A-140
D. Ueta, *et al*.
Crystalline electric field level scheme in the non-centrosymmetric CeRhSi3 and CeIrSi3
J. Phys. Soc. Jpn., 90

A-141
K. Iwasa, *et al*.
Magnetic excitations in chiral-structure phase of Ce3Ir4Sn13
J. Phys. Soc. Jpn., 90

A-142
K. Kaneko, *et al*.
Charge-Density-Wave Order and Multiple Magnetic Transitions in Divalent Europium Compound EuAl4
J. Phys. Soc. Jpn., 90

A-143
D. Ueta, *et al*.
Oval-cycloidal Magnetic Structure with Phase-shift in the Non-centrosymmetric Tetragonal Compound CePdSi3
J. Phys. Soc. Jpn., 90

A-144
M. Fujita, *et al*.
Magnetic Excitations of Sr3Ir2O7 Observed by Inelastic Neutron Scattering Technique
J. Phys. Soc. Jpn., 90

A-145
Y. Nambu, S. Shamoto
Neutron Scattering Study on Yttrium Iron Garnet for Spintronics
J. Phys. Soc. Jpn., 90

A-146
K. Nawa, *et al*.
Strongly Electron-Correlated Semimetal RuI3 with a Layered Honeycomb Structure
J. Phys. Soc. Jpn., 90

A-147
K. Kodama, *et al*.
Magnetic structure of short-range ordering in intermetallic antiferromagnet Mn3RhSi
J. Phys. Soc. Jpn., 90

A-148
K. Matsubayashi, *et al*.
Hybridization-Gap Formation and Superconductivity in the Pressure-Induced Semimetallic Phase of the Excitonic Insulator Ta2NiSe5
J. Phys. Soc. Jpn., 90

A-149
S. Shamoto, *et al*.
Spin-flop Phase in a Honeycomb Antiferromagnet Mn0.84Mg0.16TiO3
J. Phys. Soc. Jpn., 90

A-150
I. Hwang, *et al*.
Spin Wave Excitations in Honeycomb Antiferromagnet MnTiO3
J. Phys. Soc. Jpn., 90

A-151
H. K. Yoshida, *et al*.
μSR Study of Kapellasite-type Quantum Kagome Antiferromagnet CaCu3(OH)6Cl2 · 0.6H2O
J. Phys. Soc. Jpn., 91

A-152
Y. Idemoto, *et al*.
Structural and electronic properties of spinel type Mg1+yCo2-x-yMnxO4 for cathode applications in magnesium rechargeable batteries
J. Power Sources, 482

A-153
H. Yamada, *et al*.
Concerted influence of microstructure and adsorbed water on lithium-ion conduction of Li1.3Al0.3Ti1.7(PO4)3
J. Power Sources, 511

A-154
N. Ishida, *et al*.
Average and local structure analysis of Na/Li ion-exchanged Lix(Mn,Ni,Ti)O2 using synchrotron X-ray and neutron sources
J. Solid State Chem., 25

A-155
A. Abed Abud, *et al*.
Searching for solar KDAR with DUNE
JCAP10(2021), 065 (2021)

A-156
B. Aimard, *et al*.
Study of scintillation light collection, production and propagation in a 4 tonne dual-phase LArTPC
JINST 16, P03007, (2021)

A-157
M. Bogomilov, *et al*.
Performance of the MICE diagnostic syste
JINST 16, P08046, (2021)

A-158
B. Aimard, *et al*.
Performance study of a $3 \times 1 \times 1$ m^3 dual phase liquid Argon Time Projection Chamber exposed to cosmic rays
JINST 16, P08063, (2021)

A-159
H. Sasaki, *et al*.
Characterization of Precipitated Phase in Cu-Ni-Si Alloy by Small Angle X-ray Scattering, Small Angle Neutron Scattering and Atom Probe Tomography
Journal of Japan Research Institute for Advanced Copper-base Materials and Technologies, 60

A-160
K. Tashiro, K. Kusaka
New Evolution in Crystal Structure Analysis of Synthetic Polymers on the Basis of Concerted Analysis of X-ray and Neutron Diffraction Data
Journal of the Crystallographic Society of Japan, 63

A-161
N. Yamada
Structure analysis of organic thin film with X-ray and neutron reflectometry : Competitive analysis taking advantage of X-ray or neutrons & comprehensive analysis taking advantages of X-ray and neutrons
Journal of the Japanese Society for Synchrotron Radiation Research, 34, No. 6

A-162
S. Sasada, *et al*.
High-spatial-resolution measurement of magnetization distribution using polarized neutron imaging
Jpn. J. Appl. Phys., 60

A-163
S. Harjo
Observation of metallographic structure by means of pulsed neutron diffraction
Kinzoku, materials science & technology, 91

A-164
S. Harjo
パルス中性子回折による金属組織観察（only Japanese）
Kinzoku, materials science & technology, 91 (only Japanese)

A-165
T. Shinohara, *et al*.
エネルギー分析型中性子イメージング装置 RADEN（螺鈿）の開発 (only Japanese)
Kinzoku, materials science & technology, 91, No. 3(only Japanese)

A-166
H. Iwase, *et al*.
Direct observation of the relationship between thixotropic behavior and shear-induced orientation of clay particles in synesthetic hectorite suspensions
Langmuir, 37

A-167
M. Akamatsu, *et al*.
Contrast variation small-angle neutron scattering study of solubilization of perfumes in cationic surfactant micelles
Langmuir, 37

A-168
M. Harada, *et al*.
Combined small-angle neutron scattering/small-angle X-ray scattering analysis for the characterization of silver nanoparticles prepared via photoreduction in water-in-oil microemulsions
Langmuir, 37

A-169
K. Shimokita, *et al*.
Investigation of Interfacial Water Accumulation between Polypropylene Thin Film and Si Substrate by Neutron Reflectivity
Langmuir, 37

A-170
H. Aoki, *et al*.
Neutron reflectometry tomography for imaging and depth structure analysis of thin films with in-plane inhomogeneity
Langmuir, 37

A-171
Tsukasa Miyazaki, *et al*.
Layered Structure in the Crystalline Adsorption Layer and the Leaching Process of Poly(vinyl alcohol) Revealed by Neutron Reflectivity
Langmuir, 37

A-172
A. Izumi, *et al*.
In Situ Neutron Reflectometry Analysis of Interfacial Structure Formation between Phenolic Resin and Silica during Curing
Langmuir, 37

A-173
H. Taneda, *et al*.
Modification of a Polymer Surface by Partial Swelling Using Non-solvents
Langmuir,37

A-174
H. Ogawa, *et al*.
Molecular Weight Effect on the Transition Processes of a Symmetric PS-b-P2VP during Spin-Coating
Macromolecules

A-175
Y. Kimura, *et al*.
Amphiphilic random cyclocopolymers as versatile scaffolds for ring-functionalized and self-assembled materials
Macromolecules, 54

A-176
H. Saitoh, *et al*.
Hydrogen storage by earth-abundant metals, synthesis and characterization of Al3FeH3.9
Mater. Des.

A-177
X.X.Zhang, *et al*.
Quantifying internal strains, stresses, and dislocation density in additively manufactured AlSi10Mg during loading-unloading-reloading deformation
Mater. Des., 198

A-178
S. Shamoto, *et al*.
Gallium-effect in a lead-free solder for silver-sheathed superconducting tape
Mater. Res. Express., 8

A-179
T. Yamashita, *et al*.
Work hardening behavior of dual phase copper–iron alloy at low temperature
Mater. Sci. Eng. A, 819

A-180
M. Kumagai, *et al*.
In situ diffraction characterization on microstructure evolution in austenitic stainless steel during cyclic plastic deformation and its relation to the mechanical response
Mater. Sci. Eng. A, 820

A-181
Y. S. Kim, *et al*.
Multiple deformation scheme in direct energy deposited CoCrNi medium entropy alloy at 210K
Mater. Sci. Eng. A, 828

A-182
W. Mao, *et al*.
Effect of deformation-induced martensitic transformation on nonuniform deformation of metastable austenitic steel
Mater. Sci. Eng. A, 837

A-183
S. Nishida, *et al*.
Analysis of Residual Stress in Steel Bar Processed by Cold Drawing and Straightening
Mater. Trans., 62

A-184
T. Nakagawa, *et al*.
Structural properties of (Ti, Zr)(Mn,Cr)2M0.1 (M=none, Fe, Co, Ni, and Cu) hydrogen storage alloys: Composition distribution and occupied site of doped element
Mater. Trans., 62

A-185
R. Iizuka, H. Kagi
金属鉄の水素化反応に硫黄が及ぼす影響と地球核の進化過程 (only Japanese)
Materia Japan, 61(only Japanese)

A-186
Y. Iwamoto, *et al*.
Measurements of Displacement Cross Section of Tungsten under 389-MeV Proton Irradiation and Thermal Damage Recovery
Materials Science Forum, Vol 1024, 95-101 (2021)

A-187
Y. S. Kim, *et al*.
Microstructural Evolution and Mechanical Properties of Non-Equiatomic (CoNi)74.66Cr17Fe8C0.34 High-Entropy Alloy
Materials, 15

A-188
J. Kim, *et al*.
Effect of the Difference in Strength of Hard and Soft Components on the Synergetic Strengthening of Layered Materials
Met. Mater. Int., 27

A-189
N. Koga, *et al*.
Effect of Solute Carbon on the Characteristic Hardening of Steel at High Temperature
Metall. Mater. Trans. A, 52

A-190
N. Tsuchida, S. Harjo
Enhancement of Uniform Elongation by Temperature Change during Tensile Deformation in a 0.2C TRIP Steel
Metals, 11

A-191
L. Temleitner, *et al*.
Pressure Dependent Structure of Methanol-Water Mixtures up 1.2 GPa: Neutron Diffraction Experiments and Molecular Dynamics Simulations
Molecules, 26

A-192
H. He, *et al*.
Stacking Fault Driven Phase Transformation in CrCoNi Medium Entropy Alloy
Nano Letters, 21

A-193
R. Yamane, *et al*.
Experimental evidence for the existence of a second partially-ordered phase of ice VI
Nat. Commun., 12

A-194
R. Okuma, M. Kofu, S. Asai, M. Avdeev, A. Koda, H. Okabe, M. Hiraishi, S. Takeshita, K. M. Kojima, R. Kadono, T. Masuda, K. Nakajima, Z. Hiroi
Dimensional reduction by geometrical frustration in a cubic antiferromagnet composed of tetrahedral clusters
Nat. Commun., 12

A-195
P. Park, *et al*.
Spin texture induced by non-magnetic doping and spin dynamics in 2D triangular lattice antiferromagnet h-Y(Mn,Al)O3
Nat. Commun., 12

A-196
S.-Q. Su, *et al*.
Water-oriented magnetic anisotropy transition
Nat. Commun., 12

A-197
S. Gao, *et al*.
Hydride-based antiperovskites with soft anionic sublattices as fast alkali ionic conductors
Nat. Commun., 12

A-198
G. Lin, *et al*.
Field induced quantum spin disordered state in spin-1/2 honeycomb magnet Na2Co2TeO6 with small Kitaev interaction
Nat. Commun., 12

A-199
J. Dove, *et al*.
The asymmetry of antimatter in the proton
Nature 590, 561 (2021)

A-200
P. Hua, *et al*.
Nanocomposite NiTi shape memory alloy with high strength and fatigue resistance
Nature Nanotechnology, 16

A-201
B. Ma, *et al*.
Optimization of a slab geometry type cold neutron moderator for RIKEN accelerator-driven compact neutron source
NIM A, 995

A-202
K. Yamanaka, *et al*.
Surface evolution and corrosion behaviour of Cu-doped carbide-reinforced martensitic steels in a sulfuric acid solution
npj Materials Degradation, 5

A-203
Y. Morita, *et al*.
Development of medium-frequency cavity loaded with multi-ring magnetic alloy cores cooled by chemically inert liquid

Nucl. Instrum. Methods. Phys. Res., A 1010, 165525 (2021)

A-204
S. Ajimura, *et al*.
The JSNS^2 detector
Nucl. Instrum. Methods. Phys. Res., A 1014, 165742 (2021)

A-205
Y. Sugiyama, *et al*.
Pulse shape discrimination of photons and neutrons in the energy range of 0.1 -- 2 GeV with the KOTO un-doped CsI calorimeter
Nucl. Instrum. Methods. Phys. Res., A 987, 164825 (2021)

A-206
M. Kobayashi, *et al*.
Corrigendum to "Cosmic ray tests of a GEM-based TPC prototype operated in Ar-CF_4-isobutane gas mixtures" [Nucl. Instrum. Methods Phys. Res. A 641 (2011) 37-47]
Nucl. Instrum. Methods. Phys. Res., A 988, 164800 (2021)

A-207
F. Tamura, *et al*.
Commissioning of the next-generation LLRF control system for the Rapid Cycling Synchrotron of the Japan Proton Accelerator Research Complex
Nucl. Instrum. Methods. Phys. Res., A 999 (2021) 165211_1

A-208
M. Harada, *et al*.
Experimental characterization of high-energy component in extracted pulsed neutrons at the J-PARC spallation neutron source
Nucl. Instrum. Methods. Phys. Res., A, 1000

A-209
T. D. Vu, *et al*.
Practical tests of neutron transmission imaging with a superconducting kinetic-inductance sensor
Nucl. Instrum. Methods. Phys. Res., A, 1006

A-210
A. S. Tremsin, *et al*.
Calibration and optimization of Bragg edge analysis in energy-resolved neutron imaging experiments
Nucl. Instrum. Methods. Phys. Res., A, 1009

A-211
F. Funama, *et al*.
Double-focusing geometry for phase correction in neutron resonance spin-echo spectroscopy
Nucl. Instrum. Methods. Phys. Res., A, 1010

A-212
A. D. Pant, *et al*.
Muonium response to low oxygen levels in haemoglobin and other biological aqueous solutions and potential application towards monitoring hypoxia
Nucl. Instrum. Methods. Phys. Res., A, 1011

A-213
T. Oda, *et al*.
Phase correction method in a wide detector plane for MIEZE spectroscopy with pulsed neutron beams
Nucl. Instrum. Methods. Phys. Res., A, 1012

A-214
S. Yamamoto, *et al*.
Three-dimensional (3D) optical imaging of muon beam using a plastic scintillator plate in water
Nucl. Instrum. Methods. Phys. Res., A, 1015

A-215
Y. Tsuchikawa, *et al*.
Measurement of Doppler broadening of prompt gamma-rays from various zirconium- and ferro-borons
Nucl. Instrum. Methods. Phys. Res., A, 991

A-216
N. Teshima, *et al*.
Development of a multiwire proportional chamber with good tolerance to burst hits
Nucl. Instrum. Methods. Phys. Res., A, 999

A-217
H. Takeshita, *et al*.
Measurement of nuclide production cross sections for proton-induced reactions on Mn and Co at 1.3, 2.2, and 3.0 GeV
Nucl. Instrum. Methods. Phys. Res., B 511, pp. 30–41 (2021)

A-218
A. Volkov, *et al*.
Properties of straw tubes for the tracking detector of the COMET experiment
Nucl. Instrum. Methods. Phys., A 1004, 165242 (2021)

A-219
A. D. Pant, *et al*.
Study of muonium behavior in n-type silicon for generation of ultra cold muonium in vacuum
Phys. B, 613

A-220
L. A. Ma, *et al*.
Na-ion mobility in P2-type Na0.5 Mg x Ni0.17–x Mn 0.83O2 ($0 \leq x \leq 0.07$) from electrochemical and muon spin relaxation studies
Phys. Chem. Chem. Phys., 23

A-221
D. Gao, *et al*.
Phase transition and chemical reactivity of 1H-tetrazole under high pressure up to 100 GPa
Phys. Chem. Chem. Phys., 23

A-222
M. Kawano, *et al*.
Assessment of the UCST-type liquid-liquid phase separation mechanism of imidazolium-based ionic liquid, [C8mim][TFSI], and 1,4-dioxane by SANS, NMR, IR, and MD simulations
Phys. Chem. Chem. Phys., 23

A-223
Y. Zhai, *et al*.
Relevance of hydrogen bonded associates to the transport properties and nanoscale dynamics of liquid and supercooled 2-propanol
Phys. Chem. Chem. Phys., 23

A-224
S. Kanda, *et al*.
New precise spectroscopy of the hyperfine structure in muonium with a high-intensity pulsed muon beam
Phys. Lett. B 815, 136154 (2021)

A-225
Y. Fujimoto, K. Fukushima, Y. Hidaka
Deconfining phase boundary of rapidly rotating hot and dense matter and analysis of moment of inertia
Phys. Lett. B 816, 136184 (2021)

A-226
S. Nishimura, *et al*.
Rabi-oscillation spectroscopy of the hyperfine structure of muonium atoms
Phys. Rev. A, Vol 104, L020801 (2021)

A-227
H. Hotchi
Effects of the Montague resonance on the formation of the beam distribution during multiturn injection painting in a high-intensity proton ring
Phys. Rev. Accel. Beams (Internet), 23(5), p.050401_1 - 050401_13, 2020/05

A-228
P. K. Saha, *et al*.
First measurement and online monitoring of the stripper foil thinning and pinhole formation to achieve a longer foil lifetime in high-intensity accelerators
Phys. Rev. Accel. Beams (Internet), 23(8), p.082801_1 - 082801_13, 2020/08

A-229
Y. Shobuda, *et al*.
Titanium nitride-coated ceramic break for wall current monitors with an improved broadband frequency response
Phys. Rev. Accel. Beams (Internet), 23(9), p.092801_1 - 092801_18, 2020/09

A-230
R. Kitamura, *et al*.

Development of negative muonium ion source for muon acceleration
Phys. Rev. Accel. Beams 24, 033403(2021)

A-231
B. Yee-Rendon, *et al*.
Design and beam dynamic studies of a 30-MW superconducting linac for an accelerator-driven subcritical system
Phys. Rev. Accel. Beams 24, 120101 (2021)

A-232
I. Yamada, *et al*.
High-intensity beam profile measurement using a gas sheet monitor by beam induced fluorescence detection
Phys. Rev. Accel. Beams, 24 (2021) 042801_1

A-233
J. Kamiya, *et al*.
Improved vacuum system for high-power proton beam operation of the rapid cycling synchrotron
Phys. Rev. Accel.Beams, 24 (2021) 083201_1

A-234
Z. H. Zhu, *et al*.
Muon spin relaxation and fluctuating magnetism in the pseudogap phase of YBa2Cu3Oy
Phys. Rev. B, 103

A-235
M. Hiraishi, *et al*.
Anomalous diamagnetism of electride electrons in transition metal silicides
Phys. Rev. B, 103

A-236
H. Okabe, *et al*.
Local electronic structure of dilute hydrogen in β–MnO2
Phys. Rev. B, 103

A-237
P. Miao, *et al*.
Origin of magnetvolume effect in a cobaltite
Phys. Rev. B, 103

A-238
T. Omi, *et al*.
Antiferromagnetic-to-ferrimagnetic phase transition with large electric-polarization change in a frustrated polar magnet CaBaCo4O7
Phys. Rev. B, 103

A-239
P. Wu, *et al*.
Strong anharmonicity in tin monosulfide evidenced by local distortion, high-energy optical phonons, and anharmonic potential
Phys. Rev. B, 103

A-240
W. Chen, *et al*.
Spin-orbit phase behavior of Na2Co2TeO6 at low temperatures
Phys. Rev. B, 103

A-241
J. Sugiyama, *et al*.
Pressure dependence of ferromagnetic phase boundary in BaVSe3 studied with high-pressure μ+SR
Phys. Rev. B, 103

A-242
M. Miyajima, *et al*.
Spin-gap formation due to spin-Peierls instability in π-orbital-ordered NaO2
Phys. Rev. B, 104

A-243
N. Higa, *et al*.
Critical slowing-down and field-dependent paramagnetic fluctuations in the skyrmion host EuPtSi: μSR and NMR studies
Phys. Rev. B, 104

A-244
M. Matsuura, *et al*.
Microscopic dynamics of lithium diffusion in single crystal of the solid-state electrolyte La2/3–xLi3xTiO3 (x = 0.13) studied by quasielastic neutron scattering
Phys. Rev. B, 104

A-245
Yanyan Shangguan, *et al*.
Evidence for strong correlations at finite temperatures in the dimerized magnet Na2Cu2TeO6
Phys. Rev. B, 104

A-246
K. Miwa, *et al*.
Measurement of the differential cross sections of the $\Sigma^- p$ elastic scattering in momentum range 470 to 850 MeV/*c*
Phys. Rev. C 104, 45204 (2021)

A-247
T. Ishikawa, *et al*.
Resonance-like structure near the ηd threshold in the $\gamma d \to \pi^0 \eta d$ reaction
Phys. Rev. C 104, L052201 (2021)

A-248
C. Beleno, *et al*.
Measurement of the branching fraction of the decay $B^+ \to \pi^+\pi^-\ell^+\nu_\ell$ in fully reconstructed events at Belle
Phys. Rev. D 103, 112001 (2021)

A-249
J. T. McNeil, *et al*.
Measurement of the resonant and nonresonant branching ratios in $\Xi_c^0 \to \Xi^0 K^+ K^-$
Phys. Rev. D 103, 112002 (2021)

A-250
K. Abe, *et al*.
First T2K measurement of transverse kinematic imbalance in the muon-neutrino charged-current single-π^+ production channel containing at least one proton
Phys. Rev. D 103, 112003 (2021)

A-251
Y. Guan, *et al*.
Measurement of branching fractions and *CP* asymmetries for $D_s^+ \to K^+(\eta, \pi^0)$ and $D_s^+ \to \pi^+(\eta, \pi^0)$ decays at Belle
Phys. Rev. D 103, 112005 (2021)

A-252
K. Abe, *et al*.
Improved constraints on neutrino mixing from the T2K experiment with 3.13 × 1021 protons on target
Phys. Rev. D 103, 112008 (2021)

A-253
S. Cao, *et al*.
Physics potential of the combined sensitivity of T2K-II, NOνA extension, and JUNO
Phys. Rev. D 103, 112010 (2021)

A-254
K. Abe, *et al*.
Neutron-antineutron oscillation search using a 0.37 megaton-years exposure of Super-Kamiokande
Phys. Rev. D 103, 12008 (2021)

A-255
S. Kumano, Q. Song
Transverse-momentum-dependent parton distribution functions up to twist 4 for spin-1 hadrons
Phys. Rev. D 103, 14025 (2021)

A-256
U. A. Acharya, *et al*.
Transverse momentum dependent forward neutron single spin asymmetries in transversely polarized $p+p$ collisions at $\sqrt{s}$ = 200 GeV
Phys. Rev. D 103, 32007 (2021)

A-257
A. Aguilar-Arevalo, *et al*.
Search for three body pion decays $\pi^+ \to l^+\nu X$
Phys. Rev. D 103, 52006 (2021)

A-258
U. A. Acharya, *et al*.
Transverse single-spin asymmetries of midrapidity π^0 and η mesons in polarized $p+p$ collisions at $\sqrt{s}$ = 200 GeV
Phys. Rev. D 103, 52009 (2021)

A-259
S. X. Li, *et al*.
Measurements of the branching fractions of $\Lambda_c^+ \to p\eta$ and $\Lambda_c^+ \to p\pi^0$ decays at Belle
Phys. Rev. D 103, 72004 (2021)

A-260
E. Waheed, *et al*.

Measurement of the CKM matrix element $|V_{cb}|$ from $B^0 \to D^{*-}\ell^+\nu_\ell$ at Belle [Phys. Rev. D 100, 052007 (2019)]
Phys. Rev. D 103, 79901 (2021)

A-261
T. Hayata, Y. Hidaka
Thermalization of Yang-Mills theory in a (3 + 1)-dimensional small lattice system
Phys. Rev. D 103, 84502 (2021)

A-262
K. Abe, *et al.*
T2K measurements of muon neutrino and antineutrino disappearance using 3.13×10^{21} protons on targe
Phys. Rev. D 103, L011101 (2021)

A-263
T. J. Moon, *et al.*
First determination of the spin and parity of the charmed-strange baryon $\Xi_c(2970)^+$
Phys. Rev. D 103, L111101 (2021)

A-264
S. Dubey, *et al.*
Search for $B_s^0 \to \eta' X_{s\bar{s}}$ at Belle using a semi-inclusive method
Phys. Rev. D 104, 12007 (2021)

A-265
L. Cao, *et al.*
Measurements of partial branching fractions of inclusive $B \to X_u\ell^+\nu_\ell$ decays with hadronic tagging
Phys. Rev. D 104, 12008 (2021)

A-266
S. Jia, *et al.*
Search for the $\eta_{c2}(1D)$ in $e^+e^- \to \gamma\eta_{c2}(1D)$ at $\sqrt{s}$ near 10.6 GeV at Belle
Phys. Rev. D 104, 12012 (2021)

A-267
K. Abe, *et al.*
Diffuse supernova neutrino background search at Super-Kamiokande
Phys. Rev. D 104, 122002 (2021)

A-268
J. Yelton, *et al.*
Measurement of the masses and widths of the $\Sigma_c(2455)^+$ and $\Sigma_c(2520)^+$ baryons
Phys. Rev. D 104, 52003 (2021)

A-269
Y. Li, *et al.*
Evidence for the decay $\Omega_c^0 \to \pi^+\Omega(2012)^- \to \pi^+ (\bar{K}\Xi)^-$
Phys. Rev. D 104, 52005 (2021)

A-270
S. X. Li, *et al.*
Measurement of the branching fraction of $\Lambda_c^+ \to p\omega$ decay at Belle
Phys. Rev. D 104, 72008 (2021)

A-271
Y. Hidaka, R. D. Pisarski
Effective models of a semi-quark-gluon plasma
Phys. Rev. D 104, 74036 (2021)

A-272
T. Hayata, *et al.*
Diagnosis of information scrambling from Hamiltonian evolution under decoherence
Phys. Rev. D 104, 74518 (2021)

A-273
N. K. Nisar, *et al.*
Search for the decay $B_s^0 \to \eta'\eta$
Phys. Rev. D 104, L031101 (2021)

A-274
H. Atmacan, *et al.*
Search for $B^0 \to \tau^\pm\ell^\mp$ ($\ell = e, \mu$) with a hadronic tagging method at Belle
Phys. Rev. D 104, L091105 (2021)

A-275
J. K. Ahn, *et al.*
Study of the $K_L \to \pi^0\nu\bar{\nu}$ Decay at the J-PARC KOTO Experiment
Phys. Rev. Lett. 126, 121801 (2021)

A-276
S. Wehle, *et al.*
Test of Lepton-Flavor Universality in $B^+ \to K^*\ell^+\ell^-$ Decays at Belle
Phys. Rev. Lett. 126, 161801 (2021)

A-277
S. H. Hayakawa, *et al.*
Observation of Coulomb-Assisted Nuclear Bound State of Ξ^- –^{14}N System
Phys. Rev. Lett. 126, 62501 (2021)

A-278
Y. B. Li, *et al.*
Measurements of the Branching Fractions of the Semileptonic Decays $\Xi_c^0 \to \Xi^-\ell^+\nu_\ell$ and the Asymmetry Parameter of $\Xi_c^0 \to \Xi^-\pi^+$
Phys. Rev. Lett. 127, 121803 (2021)

A-279
U. A. Acharya, *et al.*
Probing Gluon Spin-Momentum Correlations in Transversely Polarized Protons through Midrapidity Isolated Direct Photons in $p^\uparrow + p$ Collisions at $\sqrt{s} = 200$ GeV
Phys. Rev. Lett. 127, 162001 (2021)

A-280
F. Abudinen, *et al.*
Search for $B^+ \to K^+\nu\bar{\nu}$ Decays Using an Inclusive Tagging Method at Belle II
Phys. Rev. Lett. 127, 181802 (2021)

A-281
F. Abudinen, *et al.*
Precise Measurement of the D^0 and D^+ Lifetimes at Belle II
Phys. Rev. Lett. 127, 211801 (2021)

A-282
L. Cao, *et al.*
Measurement of Differential Branching Fractions of Inclusive $B \to X_u\ell^+\nu_\ell$ Decays
Phys. Rev. Lett. 127, 261801 (2021)

A-283
W. Hong, *et al.*
Extreme Suppression of Antiferromagnetic Order and Critical Scaling in a Two-Dimensional Random Quantum Magnet
Phys. Rev. Lett., 126

A-284
T. Okumura, *et al.*
Deexcitation Dynamics of Muonic Atoms Revealed by High-Precision Spectroscopy of Electronic K X rays
Phys. Rev. Lett., 127

A-285
M. Nagao, *et al.*
Relationship between viscosity and acyl tail dynamics in lipid bilayers
Phys. Rev. Lett., 127

A-286
T. Hayashida, *et al.*
Phase transition and domain formation in ferroaxial crystals
Phys. Rev. Mater., 5

A-287
S. Shamoto, *et al.*
Broken C4 symmetry in the tetragonal state of uniaxial strained BaCo0.9Ni0.1S1.9
Phys. Rev. Res., 3

A-288
S. Hasegawa, *et al.*
Nontrivial temperature dependence of magnetic anisotropy in multiferroics Ba2MnGe2O7
Phys. Rev. Res., 3

A-289
K. Hagiwara, *et al.*
Superconducting gap and pseudogap in the surface states of the iron-based superconductor PrFeAsO1–y studied by angle-resolved photoemission spectroscopy
Phys. Rev. Research, 3

A-290
Y. Hirano, *et al.*
Position distribution calculation of annihilation radiations and bremsstrahlung x rays in water during irradiation of positive muons: a Monte Carlo simulation study
Phys. Scr., 96

A-291
O. K. Forslund, *et al.*
Co-existence of short- and long-range magnetic order in LaCo2P2
Phys. Scr., 96

A-292
J.-H. Hong, *et al*.
Poly[oligo(2-ethyl-2-oxazoline) methacrylate] as a surface modifier for bioinertness
Polym. J., 53

A-293
S. Hiroshige, *et al*.
Temperature-dependent relationship between the structure and mechanical strength of volatile organic compound-free latex films prepared from poly(butyl acrylate-co-methyl methacrylate) microspheres
Polym. J., 53

A-294
T. Maeda, M. Kitagawa, A. Hotta
Degradation of thermoresponsive laponite/PEG-b-PLGA nanocomposite hydrogels controlled by blending PEG-b-PLGA diblock copolymers with different PLGA molecular weights
Polymer Degradation and Stability, 187

A-295
S. Ishida, *et al*.
Superconductivity-driven ferromagnetism and spin manipulation using vortices in the magnetic superconductor EuRbFe4As4
Proc. Nat. Acad. Sci. U.S.A., 118

A-296
A. Arbuzov, *et al*.
On the physics potential to study the gluon content of proton and deuteron at NICA SPD
Prog. Part. Nucl. Phys. 119, 103858 (2021)

A-297
S. Igarashi, *et al*.
Accelerator design for 1.3-MW beam power operation of the J-PARC Main Ring
Prog. Theor. Exp. Phys. 2021, 033G01 (2021)

A-298
K. Abe, *et al*.
Measurements of $\overline{\nu}_\mu$ and $\overline{\nu}_\mu + \nu_\mu$ charged-current cross-sections without detected pions or protons on water and hydrocarbon at a mean anti-neutrino energy of 0.86 GeV
Prog. Theor. Exp. Phys. 2021, 043C01 (2021)

A-299
J. Park, *et al*.
Slow control and monitoring system at the JSNS^2
Prog. Theor. Exp. Phys. 2021, 063C01 (2021)

A-300
M. Yoshimoto, *et al*.
First observation of a nuclear *s*-state of a Ξ hypernucleus, $^{15}_{\Xi}$C
Prog. Theor. Exp. Phys. 2021, 073D02 (2021)

A-301
A. Orii, *et al*.
Search for tens of MeV neutrinos associated with gamma-ray bursts in Super-Kamiokande
Prog. Theor. Exp. Phys. 2021, 103F01 (2021)

A-302
K. S. Tanaka, *et al*.
Development of microwave cavities for measurement of muonium hyperfine structure at J-PARC
Prog. Theor. Exp. Phys., 2021

A-303
Y. Onuki, S. Sato
In Situ Observation for Deformation-Induced Martensite Transformation during Tensile Deformation of SUS 304 Stainless Steel by Using Neutron Diffraction PART II: Transformation and Texture Formation Mechanisms
Quantum Beam Sci., 5

A-304
F. Grazzi, *et al*.
A multi-technique tomography-based approach for non-invasive characterization of additive manufacturing components in view of vacuum/UHV applications: preliminary results
Rendiconti Lincei. Scienze Fisiche e Naturali

A-305
Y. Nishizawa, *et al*.
Nanostructure and thermoresponsiveness of poly(N-isopropyl methacrylamide)-based hydrogel microspheres prepared via aqueous free radical precipitation polymerization
RSC Advances, 11

A-306
M. Uchida, *et al*.
Above-ordering-temperature large anomalous Hall effect in a triangular-lattice magnetic semiconductor
Sci. Adv., 7

A-307
Y. Hao, *et al*.
Field-tuned magnetic structure and phase diagram of the honeycomb magnet YbCl3
Sci. China: Phys., Mech. Astron., 64

A-308
M. Kofu, *et al*.
Spin glass behavior and magnetic boson peak in a structural glass of a magnetic ionic liquid
Sci. Rep., 11

A-309
R. Iizuka-Oku, *et al*.
Behavior of light elements in iron-silicate-water-sulfur system during early Earth's evolution
Sci. Rep., 11

A-310
M. Akamatsu, *et al*.
Rapid controlled release by photo-irradiation using morphological changes in micelles formed by amphiphilic lophine dimers
Sci. Rep., 11

A-311
Y. Ohtsuka, *et al*.
Emergence of spin-orbit coupled ferromagnetic surface state derived from Zak phase in a nonmagnetic insulator FeSi
Science Advances, 7

A-312
H. Aoki, *et al*.
Deep learning approach for an interface structure analysis with a large statistical noise in neutron reflectometry
Scientific Reports, 11

A-313
Y. Su, *et al*.
Neutron Bragg-edge transmission imaging for microstructure and residual strain in induction hardened gears
Scientific Reports, 11

A-314
M. Busi, *et al*.
A parametric neutron Bragg edge imaging study of additively manufactured samples treated by laser shock peening
scientific reports, 11

A-315
M.S. Lee, *et al*.
In-situ neutron diffraction study of lattice deformation behaviour of commercially pure titanium at cryogenic temperature
Scientific reports, 12

A-316
H. Nakao, *et al*.
Development of membrane-insertable lipid scrambling peptides: A time-resolved smallangle neutron scattering study
Struct. Dyn., 8

A-317
T. D. Vu, *et al*.
Homogeneity of neutron transmission imaging over a large sensitive area with a four-channel superconducting detector
Supercond. Sci. Technol., 34

A-318
S. Harjo, *et al*.
Relation between intergranular stress in austenite and martensitic transformation in TRIP steels revealed by neutron diffraction
TETSU-TO-HAGANE, 107

A-319
J. Hendriks, *et al*.
Bayesian non-parametric Bragg-edge fitting for neutron transmission strain imaging

The J. Strain Anal. Eng. Des., 56

A-320
H. Yoshida, *et al*.
Observation of Adsorbed Hydrogen Species on Supported Metal Catalysts by Inelastic Neutron Scattering
Topics in Catalysis, 64

A-321
T. Suzuki, *et al*.
Residual stress evaluation by pulsed neutron stress measurement for cruciform welded joints treated with ultrasonic impact method
Trans. Jpn. Soc. Mech. Eng., 87

A-322
N. Yamashita, *et al*.
Highly Swollen Adsorption Layer Formed by Polymeric Friction Modifier Providing Low Friction at Higher Temperature
Tribol. Lett., 69

A-323
K. Sakai, *et al*.
Observation of Grease Fluidity in a Ball Bearing Using Neutron Imaging Technology
Tribology Online, 16

A-324
A. Yoshiasa, *et al*.
High-temperature diffraction experiments and phase diagram of ZrO2 and ZrSiO4
Zeitschrift für Naturforschung B

A-325
J. Sugiyama, *et al*.
How Li diffusion in spinel Li[Ni1/2Mn3/2]O4 is seen with μ±SR
Zeitschrift für Physikalische Chemie

Conference Reports and Books

B-001
Y. Kondo, *et al*.
Reference design of the RFQ for the JAEA ADS linac
JPS Conf. Proc. 33, 011015 (2021)

B-002
S. Saito, *et al*.
Status of LBE studies and experimental plan at JAEA
JPS Conf. Proc. 33, 011041 (2021)

B-003
F. Maekawa, *et al*.
A Plan of Materials Irradiation Facility at J-PARC for Development of ADS and High-power Accelerator Facilities
JPS Conf. Proc. 33, 011042 (2021)

B-004
B. Yee-Rendon, *et al*.
Present Status of the R&D of the Superconducting Linac for the JAEA-ADS
JPS Conf. Proc. 33, 011043 (2021)

B-005
G. Ariyoshi, *et al*.
Measurement of liquid metal flows with electro-magnetic probe
JPS Conf. Proc. 33, 011044 (2021)

B-006
H. Takeshita, *et al*.
Nuclide production cross sections of Ni and Zr irradiated with 0.4-, 1.3-, 2.2-, and 3.0-GeV protons
JPS Conf. Proc. 33, 011045 (2021)

B-007
H. Iwamoto, *et al*.
Estimation of uncertainty in proton-induced spallation neutron multiplicities for Pb, W, Fe, and C targets
JPS Conf. Proc. 33, 011046 (2021)

B-008
H. Matsuda, *et al*.
Measurement of Nuclide Production Cross-Sections of natFe for 0.4–3.0 GeV Protons in J-PARC
JPS Conf. Proc. 33, 011047 (2021)

B-009
H. Obayashi, *et al*.
Remote Handling Technology for Lead-Bismuth Spallation Target System
JPS Conf. Proc. 33, 011048 (2021)

B-010
J. Tamura, *et al*.
RF design of the prototype spoke cavity for the JAEA-ADS linac
JPS Conf. Proc. 33, 011049 (2021)

B-011
S. Meigo, *et al*.
Measurement of displacement cross section for proton in the kinetic energy range from 0.4 GeV to 3 GeV
JPS Conf. Proc. 33, 011050 (2021)

B-012
T. Sasa, *et al*.
250kW LBE Spallation Target for ADS Development in J-PARC
JPS Conf. Proc. 33, 011051 (2021)

B-013
Y. Sumi, *et al*.
Basic design of L-band disk-loaded structure for muon LINAC
Proc. Ann. Mtg. PASJ(Internet), 133-137(2021)

B-014
K. Nii, *et al*.
Reports of electropolishing implementation for quarter-wave resonators
Proc. Ann. Mtg. PASJ(Internet), 334-337(2021)

B-015
Y. Takeuchi, *et al*.
Detailed design of the Disk-and-Washer Cavity for Muon Linear Accelerator
Proc. Ann. Mtg. PASJ(Internet), 343-347(2021)

B-016
T. Takayanagi, *et al*.
LTD SEMICONDUCTOR SWITCH POWER SUPPLY FOR J-PARC KICKER
Proc. Ann. Mtg. PASJ(Internet), 53-57(2021)

B-017
M. Sugita, *et al*.
Experimental verification of magnetic field measurement probe for RCS bump magnet
Proc. Ann. Mtg. PASJ(Internet), 641-644(2021)

B-018
M. Mizusawa, K. Sakurai
PROJECTION-TYPE X-RAY DIFFRACTION IMAGING FOR POLYCRYSTALLINE MATERIALS: APPLICATION TO VICKERS HARDNESS TEST BLOCKS
Advances in X-ray Analysis, 64

B-019
S. Mihara
Investigation of the Last Flavor Violation in Particle Physics
AIP Conf. Proc. 2319, 20001 (2021)

B-020
K. Tanaka
Major Accelerator Facilities for Nuclear Physics in Asia Pacific
AIP Conf. Proc. 2319, 80008 (2021)

B-021
T. Ishikawa, *et al*.
ωN scattering length from ω photoproduction on the proton near the threshold
AIP Conf. Proc. 2319, 80017 (2021)

B-022
A. Ueno, *et al*.
110 mA operation of J-PARC cesiated RF-driven H^- ion source
AIP Conf. Proc. 2373, 040002_1 (2021)

B-023
T. Shibata, *et al*.
High-speed Emittance Measurements for Beams Extracted from J-PARC RF Ion Source

AIP Conf. Proc. 2373, 050002 (2021)

B-024
Y. Takayama, *et al*.
Texture evolutions in aluminum and Al-3%Mg alloy subjected to shear deformation and subsequent annealing
IOP Conf. Ser.: Mater. Sci. Eng., 1121

B-025
M. Yotsuzuka, *et al*.
Simulation of the Beam Commissioning Method for a Muon APF IH-DTL in the J-PARC Muon *g* - 2/EDM Experiment
JPS Conf. Proc. 33, 11040 (2021)

B-026
T. Yoshioka, *et al*.
Positron Tracking Detector for Muon *g* - 2/EDM Experiment at J-PARC
JPS Conf. Proc. 33, 11108 (2021)

B-027
N. Kawamura, *et al*.
A new approach for Mu – $\overline{\mathrm{Mu}}$ Conversion Search
JPS Conf. Proc. 33, 11120 (2021)

B-028
C. Zhang, *et al*.
Simulation Study of Laser Ionization of Muonium by 1S-2S Excitation for the Muon *g* - 2/EDM Experiment at J-PARC
JPS Conf. Proc. 33, 11125 (2021)

B-029
H. Yasuda, *et al*.
Development of Spin Flip Analysis for the J-PARC Muon *g* - 2/EDM Experiment
JPS Conf. Proc. 33, 11126 (2021)

B-030
Y. Nakazaw, *et al*.
Multipacting simulations of coaxial coupler for IH-DTL prototype in muon accelerator
JPS Conf. Proc. 33, 11128 (2021)

B-031
Y. Takeuchi, *et al*.
Error Studies for Muon Linac in the Muon g -- 2/EDM Experiment at J-PARC
JPS Conf. Proc. 33, 11129 (2021)

B-032
T. Matsubara
T2K future prospects with J-PARC neutrino beam and near detector upgrades
JPS Conf. Proc. 33, 11141 (2021)

B-033
H. Harada, *et al*.
Simulation study of heavy ion acceleration in J-PARC
JPS Conf. Proc. 33 (2021) 011028_1

B-034
Y. Kurimoto, *et al*.
J-PARC Main Ring Upgrade toward High Repetition Rate Operation
JPS Conf. Proc. 33, 011001 (2021)

B-035
C. Ohmori, *et al*.
J-PARC Contributions to the LHC Injector Upgrade (LIU) Project
JPS Conf. Proc. 33, 011006 (2021)

B-036
H. Oguri, *et al*.
Status of the J-PARC RF-Driven H- Ion Source
JPS Conf. Proc. 33, 011008 (2021)

B-037
T. Shibata, *et al*.
Phase Space Formation of High Intensity 60 and 80 mA H- Beam with Orifice in J-PARC Front-End
JPS Conf. Proc. 33, 011010 (2021)

B-038
K. Okabe, *et al*.
High Intensity Beam Studies for the New MEBT1 Design
JPS Conf. Proc. 33, 011011 (2021)

B-039
R. Kitamura, *et al*.
Bunch-Size Measurement of the High-Intensity H- Beam with 3 MeV by the Bunch-Shape Monitor
JPS Conf. Proc. 33, 011012 (2021)

B-040
R. Kitamura, *et al*.
Bunch-Size Measurement of the High-Intensity H^- Beam with 3 MeV by the Bunch-Shape Monitor
JPS Conf. Proc. 33, 011012 (2021)

B-041
T. Morishita
Precise Survey and Alignment Results of the J-PARC Linac
JPS Conf. Proc. 33, 011013 (2021)

B-042
H. Takahashi, *et al*.
Monitoring System of Number of Particles in J-PARC Linac and RCS
JPS Conf. Proc. 33, 011014 (2021)

B-043
Y. Kondo, *et al*.
Reference Design of the RFQ for JAEA ADS Linac
JPS Conf. Proc. 33, 011015 (2021)

B-044
K. Yamamoto, *et al*.
Reliability of J-PARC Accelerator System Over the Past Decade
JPS Conf. Proc. 33, 011016 (2021)

B-045
N. Hayashi, *et al*.
High Intensity Measurement Issues at the J-PARC RCS
JPS Conf. Proc. 33, 011017 (2021)

B-046
H. Hotchi, *et al*.
1.2-MW-Equivalent High-Intensity Beam Tests in J-PARC RCS
JPS Conf. Proc. 33, 011018 (2021)

B-047
M. Yoshimoto, *et al*.
Analysis of J-HBC Stripper Foil for the J-PARC RCS
JPS Conf. Proc. 33, 011019 (2021)

B-048
T. Takayanagi, *et al*.
Kicker Power Supply for J-PARC 3-GeV RCS with SiC-MOSFET
JPS Conf. Proc. 33, 011020 (2021)

B-049
F. Tamura, *et al*.
Flexible Chopper Gate Pulse Generation for the J-PARC RCS
JPS Conf. Proc. 33, 011021 (2021)

B-050
M. Yamamoto, *et al*.
Operation Experience of Tetrode Vacuum Tubes in J-PARC Ring RF System
JPS Conf. Proc. 33, 011022 (2021)

B-051
J. Kamiya, *et al*.
Recent Status & Improvements of the RCS Vacuum System
JPS Conf. Proc. 33, 011023 (2021)

B-052
I. Yamane
Application of Doppler-free Two-Photons Excitation to Laser Stripping of J-PARC 400 MeV H- Beam
JPS Conf. Proc. 33, 011024 (2021)

B-053
P. K. Saha, *et al*.
Studies of Laser Power Reduction for the Laser Stripping of 400 MeV H- Beam at J-PARC RCS
JPS Conf. Proc. 33, 011025 (2021)

B-054
H. Harada, *et al*.
Development of Laser System for Laser Stripping Injection
JPS Conf. Proc. 33, 011026 (2021)

B-055
H. Harada, *et al*.
New Method for High Resolution Analysis of Betatron Tune in a Rapid Cycling Synchrotron or a Booster Ring

JPS Conf. Proc. 33, 011027 (2021)

B-056
H. Harada, *et al*.
Simulation Study of Heavy Ion Acceleration in J-PARC
JPS Conf. Proc. 33, 011028 (2021)

B-057
S. Igarashi, *et al*.
Study on the Beam Intensity Upgrade of J-PARC Main Ring
JPS Conf. Proc. 33, 011029 (2021)

B-058
T. Yasui, *et al*.
Injection Optics Matching of the High Intensity Beam at J-PARC MR
JPS Conf. Proc. 33, 011030 (2021)

B-059
Y. Sugiyama, *et al*.
Simulation of Phase-space Offset Injection with Second Harmonic RF for Longitudinal Emittance Blow-up in J-PARC MR
JPS Conf. Proc. 33, 011031 (2021)

B-060
Y. Morita, *et al*.
Design of VHF System in J-PARC Main Ring
JPS Conf. Proc. 33, 011032 (2021)

B-061
T. Shibata, *et al*.
The Eddy Current Type New Septum Magnet for Upgrading of Fast Extraction in MR of J-PARC
JPS Conf. Proc. 33, 011033 (2021)

B-062
T. Shibata, *et al*.
The New High Field Septum Magnets for Upgrading of Fast Extraction in MR of J-PARC
JPS Conf. Proc. 33, 011034 (2021)

B-063
M. Tomizawa, *et al*.
Initial Tests for Electrostatic Septum Using Carbon Nanotube Wires
JPS Conf. Proc. 33, 011035 (2021)

B-064
T. Shimogawa, *et al*.
Proposal of Non-destructive Device for Slow Extraction
JPS Conf. Proc. 33, 011036 (2021)

B-065
J. Takano
Layer Short Circuits of Bending Magnets in the J-PARC Main Ring and 3-50BT
JPS Conf. Proc. 33, 011037 (2021)

B-066
K. Kadowaki, *et al*.
Evaluation of Soundness of Magnets in 3-50BT Line
JPS Conf. Proc. 33, 011038 (2021)

B-067
M. J. Shirakata
Neutron and Gamma Impact on Devices with Iron Shields
JPS Conf. Proc. 33, 011039 (2021)

B-068
M. Yotsuzuka, *et al*.
Simulation of the Beam Commissioning Method for a Muon APF IH-DTL in the J-PARC Muon g - 2/EDM Experiment
JPS Conf. Proc. 33, 011040 (2021)

B-069
J. Tamura, *et al*.
RF Design of the Prototype Spoke Cavity for the JAEA-ADS Linac
JPS Conf. Proc. 33, 011049 (2021)

B-070
Y. Nakazawa, *et al*.
Multipacting simulations of coaxial coupler for IH-DTL prototype in muon accelerator
JPS Conf. Proc. 33, 011128 (2021)

B-071
Y. Takeuchi, *et al*.
Error Studies for Muon Linac in the Muon g -- 2/EDM Experiment at J-PARC
JPS Conf. Proc. 33, 011129 (2021)

B-072
M. Ohta, *et al*.
Magnetic Field Dependence on Crystallization Process of FINEMET® Nano-crystalline Alloy Detected by μSR Method
JPS Conf. Proc. 33

B-073
N. Kawamura, *et al*.
A New Approach for Mu – Mu Conversion Search
JPS Conf. Proc. 33

B-074
M. Yotsuzuka, *et al*.
Simulation of the Beam Commissioning Method for a Muon APF IH-DTL in the J-PARC Muon g – 2=EDM Experiment
JPS Conf. Proc. 33

B-075
N. Kawamura on behalf of muon science section MLF J-PARC
Current Status of Muon Science Facility
JPS Conf. Proc. 33

B-076
K. Ninomiya, *et al*.
Muonic X-ray Identification of Nuclear Materials Sealed in a Box
JPS Conf. Proc. 33

B-077
T. Yoshioka, *et al*.
Positron Tracking Detector for Muon g – 2 = EDM Experiment at J-PARC
JPS Conf. Proc. 33

B-078
C. Zhang, *et al*.
Simulation Study of Laser Ionization of Muonium by 1S-2S Excitation for the Muon g – 2 = EDM Experiment at J-PARC
JPS Conf. Proc. 33

B-079
H. Yasuda, *et al*.
Development of Spin Flip Analysis for the J-PARC Muon g – 2 = EDM Experiment
JPS Conf. Proc. 33

B-080
Y. Nakazawa, *et al*.
Multipacting Simulations of Coaxial Coupler for IH-DTL Prototype in Muon Accelerator
JPS Conf. Proc. 33

B-081
Y. Takeuchi, *et al*.
Error Studies for Muon Linac in the Muon g – 2 = EDM Experiment at J-PARC
JPS Conf. Proc. 33

B-082
N. Kawamura, *et al*.
Safety Measure Against Tritium in the MLF Muon Target
JPS Conf. Proc. 33

B-083
M. Matsuura, *et al*.
Position Dependency of the Scattered Intensity in the Time-of-flight Backscattering Spectrometer DNA
JPS Conf. Proc. 33

B-084
T. Tominaga, *et al*.
Corrosion of Aluminum-based Containers for Neutron Studies with Aqueous Samples under Low Temperatures
JPS Conf. Proc. 33

B-085
T. Tominaga, *et al*.
Water dynamics of double-network polymers in a primally hierarchical structure
JPS Conf. Proc. 33

B-086
T. Tominaga, *et al*.
Position-Encoded Automatic Cell Elevator for BL02, J-PARC MLF
JPS Conf. Proc. 33

B-087
T. Tominaga, *et al*.
Quartz Cell for a Backscattering Spectrometer
JPS Conf. Proc. 33

B-088
T. Yamada, *et al*.
Commissioning for QENS Experiments at Pressures Up to 200 MPa at MLF, J-PARC
JPS Conf. Proc. 33

B-089
T. Yamada, T. Tominaga
In Situ Quasi-Elastic Neutron Scattering of Nafion Membrane with Water–Vapor Pressure Control System
JPS Conf. Proc. 33

B-090
M. Nakada, *et al*.
Static and Dynamic Structure Analysis of Intermediate Water on Polyvinyl Pyrrolidone Using Neutron Scattering
JPS Conf. Proc. 33

B-091
Y. Tsuchikawa, *et al*.
Feasibility study of PGAA for boride identification in simulated melted core materials
JPS Conf. Proc. 33

B-092
K. Sakai, *et al*.
Study of neutron–nuclear spin correlation term with a polarized Xe target
JPS Conf. Proc. 33

B-093
T. Okudaira, *et al*.
A Neutron Depolarization Measurement of Single Crystal Fe by Using a 3He Neutron Spin Filter and Magnetic Super-mirrors
JPS Conf. Proc. 33

B-094
S. Itoh, *et al*.
Dynamical studies in condensed matter on High Resolution Chopper Spectrometer (HRC) – 2nd phase of HRC project –
JPS Conf. Proc. 33

B-095
Y. Kawakita, *et al*.
Mode distribution analysis for superionic melt of CuI by coherent quasielastic neutron scattering
JPS Conf. Proc. 33

B-096
K. Nakajima, *et al*.
Recent update of AMATERAS: a cold-neutron disk-chopper spectrometer
JPS Conf. Proc. 33

B-097
Y. Shoda, *et al*.
Structural analysis of polybutadienes with urethane linkages by small-angle neutron scattering
JPS Conf. Proc. 33

B-098
K. Ohishi, *et al*.
Small angle neutron scattering study near the critical field at low temperature in MnSi
JPS Conf. Proc. 33

B-099
F. Kaneko, *et al*.
Application of simultaneous measurement system combining wide q-range small-angle neutron scattering and polarized Fourier transform infrared spectroscopy: Cocrystal of syndiotactic polystyrene with methyl benzoate
JPS Conf. Proc. 33

B-100
H. Iwase, *et al*.
Rheo-SANS study on shear thinning behavior of cationic gemini surfactant (12–2–12) in salt-free solution
JPS Conf. Proc. 33

B-101
J. Kobayashi, *et al*.
Structural analysis of microemulsion formed from polymer surfactant polyglycerol esters in the manufacturing process
JPS Conf. Proc. 33

B-102
T. Honda, *et al*.
Adsorbed polymer effects on particle dispersion in polymeric matrix examined by SANS
JPS Conf. Proc. 33

B-103
Y. Sakaguchi, *et al*.
Recent development of the sample environment for light irradiation experiments at the Materials and Life Science Experimental Facility
JPS Conf. Proc. 33

B-104
M. Iguchi, *et al*.
Thermal Stability and Interfacial Segregation for Polymer Thin Films Blended with a Homologue Having Different Tacticity
JPS Conf. Proc. 33

B-105
F. Nemoto, *et al*.
Installation of a Rheometer on Neutron Reflectometer SOFIA at J-PARC toward Rheo-NR and Observation for Crystallization Behavior of Cocoa Butter in Chocolate
JPS Conf. Proc. 33

B-106
R. Maruyama, *et al*.
Improvement in sputtering rate uniformity over large deposition area of large-scale ion beam sputtering system
JPS Conf. Proc. 33

B-107
K. Maruyama, *et al*.
Helimagnetism of Ba(Fe1–xScx)12O19 Studied by Magnetization Measurement and Neutron Diffraction
JPS Conf. Proc. 33

B-108
A. Nakao, *et al*.
Determination of Crystallographic Planes for a Polyhedral Single Crystal
JPS Conf. Proc. 33

B-109
Y. Ishikawa, *et al*.
Electrostatic Potential Mapping by Maximum Entropy Method based on Mott-Bethe relations
JPS Conf. Proc. 33

B-110
K. Kodama, *et al*.
Magnetic Pair Distribution Function of Spin-glass System Mn0.5Fe0.5TiO3
JPS Conf. Proc. 33

B-111
S. Hosokawa, *et al*.
Local- and Intermediate-Range Atomic Order in Ga2Ge3Se9 Glass: Complementary Use of X-Rays and Neutrons
JPS Conf. Proc. 33

B-112
S. Hosokawa, *et al*.
Local- and Intermediate-Range Order in Room Temperature Superionic Conducting Ag-GeSe3 Glasses
JPS Conf. Proc. 33

B-113
D. Setoyama, *et al*.
Non-Destructive 3D Neutron Imaging for Power Electronic Module
JPS Conf. Proc. 33

B-114
Y. Miyazaki, *et al*.
Observation of Eu Adsorption Band in the CMPO/SiO2–P Column by Neutron Resonance Absorption Imaging
JPS Conf. Proc. 33

B-115
Y. Abe, *et al*.
Visualization of the Boron Distribution in Core Material Melting and Relocation Specimen by Neutron Energy Resolving Method
JPS Conf. Proc. 33

B-116
K. Sakai, *et al*.
Upgrade History and Present Status of the General Control System for the Materials and Life Science Experimental Facility at J-PARC
JPS Conf. Proc. 33

B-117
H. Nakagawa, *et al*.
Sequence-dependent hydration water dynamics of dodecameric DNA
JPS Conf. Proc. 33

B-118
M. Takahashi, *et al*.
Phase Transitions and Atomic Ordering in Cu–Pd–Fe Ternary Alloys
JPS Conf. Proc. 33

B-119
K. Oikawa, *et al*.
Microstructure Distribution of Japanese Sword Cross Sections Analyzed by the Diffractometer TAKUMI at J-PARC
JPS Conf. Proc. 33

B-120
T. Yamashita, *et al*.
Neutron Diffraction Mapping Measurement for Japanese Nails in the Ancient and Present Days
JPS Conf. Proc. 33

B-121
T. Yamashita, *et al*.
Stress Partitioning Behavior of Duplex Alloys Consisting of BCC and FCC Phases at Low Temperature
JPS Conf. Proc. 33

B-122
T. Nakamura, *et al*.
A Two-Dimensional Scintillation Neutron Detector for TAKUMI Diffractometer in J-PARC MLF
JPS Conf. Proc. 33

B-123
K. Okabe, *et al*.
High intensity beam studies for the new MEBT1 design
JPS Conf. Proc. 33 (2021), 011011_1

B-124
K. Yamamoto, *et al*.
Reliability of J-PARC accelerator system over the past decade
JPS Conf. Proc. 33 (2021), 011016_1

B-125
N. Hayashi, *et al*.
High intensity measurement issues at the J-PARC RCS
JPS Conf. Proc. 33 (2021), 011017_1

B-126
H. Hotchi, *et al*.
1.2-MW-equivalent high-intensity beam tests in J-PARC RCS
JPS Conf. Proc. 33 (2021), 011018_1

B-127
Y. Yoshimoto, *et al*.
Analysis of J-HBC stripper foil for the J-PARC RCS
JPS Conf. Proc. 33 (2021), 011019_1

B-128
T. Takayanagi, *et al*.
Kicker power supply for J-PARC 3-GeV RCS with SiC-MOSFET
JPS Conf. Proc. 33 (2021), 011020_1

B-129
F. Tamura, *et al*.
Flexible chopper gate pulse generation for the J-PARC RCS
JPS Conf. Proc. 33 (2021), 011021_1

B-130
M. Yamamoto, *et al*.
Operation experience of Tetrode vacuum tubes in J-PARC Ring RF system
JPS Conf. Proc. 33 (2021), 011022_1

B-131
J. Kamiya, *et al*.
Recent status & improvements of the RCS vacuum system
JPS Conf. Proc. 33 (2021), 011023_1

B-132
P. K. Saha, *et al*.
Studies of laser power reduction for the laser stripping of 400 MeV H^- beam at J-PARC RCS
JPS Conf. Proc. 33 (2021), 011025_1

B-133
H. Harada, *et al*.
Development of laser system for laser stripping injection
JPS Conf. Proc. 33 (2021), 011026_1

B-134
H. Harada, *et al*.
New method for high resolution analysis of betatron tune in a rapid cycling synchrotron or a booster ring
JPS Conf. Proc. 33 (2021), 011027_1

B-135
Y. Kasugai, *et al*.
Behavior of Tritium Release from a Stainless Vessel of the Mercury Target as a Spallation Neutron Source
JPS Conf. Proc. 33 (2021), 011144

B-136
K. Yano, *et al*.
Precise Neutron Lifetime Measurement An integration test with a Gaseous and a Solenoidal Magnet
JPS Conf. Proc. 33(2021), 11117

B-137
K Aizawa, *et al*.
Kink Deformation Dynamics of LPSO Alloy from the Experimental Viewpoint of Multilayer Structure Deformation
Magnesium 2021

B-138
Y. Onuki, *et al*.
In Situ Neutron Diffraction Measurement during Bainite Transformation and Accompanying Carbon Enrichment in Austenite at iMATERIA, J-PARC MLF
Materials Science Forum, 1016

B-139
T. Wakui, *et al*.
New Design of High Power Mercury Target Vessel of J-PARC
Materials Science Forum, 1024

B-140
T. Naoe, *et al*.
Effect of Gas Microbubble Injection and Narrow Channel Structure on Cavitation Damage in Mercury Target Vessel
Materials Science Forum, 1024

B-141
S. Kumano, R. Petti
Possible studies on generalized parton distributions and gravitational form factors in neutrino reactions
PoS(NuFact2021) 402, 092 (2022)

B-142
K. Noguchi, *et al*.
Extinction Measurement at J-PARC MR with Slow-Extracted Pulsed Proton Beam for COMET Experiment
PoS(NuFact2021) 402, 104 (2022)

B-143
T. Maruyama on behalf of JSNS2 and JSNS2 -II collaborations
The status of JSNS2 and JSNS2-II
PoS(NuFact2021) 402, 159 (2022)

B-144
K. Oishi, *et al*.
Detector Systems Development for Inter-Bunch Extinction Measurements at the 8 GeV Slow Extracted Pulsed Proton Beam for the COMET Experiment at J-PARC
PoS(NuFact2021) 402, 216 (2022)

B-145
T. O. Yamamoto, *et al*.
X-ray spectroscopy experiments on exotic Xi atoms at J-PARC
PoS(PANIC2021) 380, 211((2022)

B-146
T. Akaishi, *et al*.
Experimental status toward the direct lifetime measurement of Hypertriton using the (K-, pi0) reaction at J-PARC
PoS(PANIC2021) 380, 214 (2022)

B-147
M. Yotsuzuka, *et al*.
DEVELOPMENT OF BUNCH WIDTH MONITOR WITH HIGH TIME RESOLUTION FOR LOW EMITTANCE MUON BEAM IN THE J-PARC

MUON g-2/EDM EXPERIMENT
Proc. 12th Int. Particle Acc. Conf.(Internet), 1004-1007(2021)

B-148
Y. Sumi, *et al*.
BASIC DESIGN STUDY FOR DISK-LOADED STRUCTURE IN MUON LINAC
Proc. 12th Int. Particle Acc. Conf.(Internet), 1801-1804(2021)

B-149
Y. Nakazawa, *et al*.
DEVELOPMENT OF AN APF IH-DTL IN THE J-PARC MUON g-2/EDM EXPERIMENT
Proc. 12th Int. Particle Acc. Conf.(Internet), 2544-2547(2021)

B-150
Y. Takeuchi, *et al*.
DEVELOPMENT OF A DISK-AND-WASHER CAVITY FOR THE J-PARC MUON g-2/EDM Experiment
Proc. 12th Int. Particle Acc. Conf.(Internet), 658-661(2021)

B-151
B. Yee-Rendon, *et al*.
Design of the MEBT for the JAEA-ADS Project
Proc. 12th International Particle Accelerator Conference (IPAC 21), pp. 790-792 (2021)

B-152
B. Yee-Rendon, *et al*.
Multipacting Studies for the JAEA-ADS Five-cell Elliptical Superconducting RF Cavities
Proc. 12th International Particle Accelerator Conference (IPAC 21), pp. 793-795, (2021)

B-153
J. Tamura, *et al*.
Present Status of the Spoke Cavity Prototyping for the JAEA-ADS Linac
Proc. 20th Int. Conf. on RF Superconductivity (SRF2021)

B-154
Y. Kondo, *et al*.
DEVELOPMENT OF QWRS FOR THE FUTURE UPGRADE OF JAEA TANDEM SUPERCONDUCTING BOOSTER
Proc. 20th Int. Conf. on RF Superconductivity(internet), 299-301(2021)

B-155
S. Meigo, *et al*.
Durabilityo of Secondary Electron Emission for High-intensity Beam on SiC Wire
Proc. Ann. Mtg. Part. Accel. Soc. Jpn. (Internet), pp. 296-301 (2021)

B-156
B. Yee-Rendon, *et al*.
Fast Fault Recovery Scenario for the JAEA-ADS Linac
Proc. Ann. Mtg. Part. Accel. Soc. Jpn. (Internet), pp. 61-65 (2021)

B-157
F. Tamura, *et al*.
Performance of the next-generation LLRF control system for the J-PARC RCS
Proc. Ann. Mtg. Part. Accel. Soc. Jpn. (2021), 170

B-158
T. Nakanoya, *et al*.
Radiation shielding installation for beam injection section of 3GeV synchrotron
Proc. Ann. Mtg. Part. Accel. Soc. Jpn. (2021), 238

B-159
K. Yamamoto, *et al*.
Neutron measurement in the accelerator tunnel of J-PARC Rapid Cycling Synchrotron
Proc. Ann. Mtg. Part. Accel. Soc. Jpn. (2021), 494

B-160
T. Takayanagi, *et al*.
LTD semiconductor switch power supply for J-PARC kicker
Proc. Ann. Mtg. Part. Accel. Soc. Jpn. (2021), 53

B-161
M. Sugita, *et al*.
Experimental verification of magnetic field measurement probe for RCS bump magnet
Proc. Ann. Mtg. Part. Accel. Soc. Jpn. (2021), 641

B-162
M. Nomura, *et al*.
Evaluations with autoencoder whether the image used for image recognition is appropriate
Proc. Ann. Mtg. Part. Accel. Soc. Jpn. (2021), 80

B-163
A. Ono, *et al*.
Development of semiconductor clover switch for short-circuit protection of Klystron for J-PARC accelerator
Proc. Ann. Mtg. Part. Accel. Soc. Jpn. (2021), 831

B-164
H. Okita, *et al*.
Evaluation of the frequency response of the RF gap voltage monitor of the J-PARC RCS
Proc. Ann. Mtg. Part. Accel. Soc. Jpn. (2021), 840

B-165
M. Yoshimoto
Initiatives to address the lifetime improvement of HBC stripper foil for 3GeV synchrotron of J-PARC
Proc. Ann. Mtg. Part. Accel. Soc. Jpn. (2021), 850

B-166
M. Otani, *et al*.
MUON ACCELERATOR EXPLORES UNKNOWN ELEMENTARY PARTICLE PHYSICS
Proc. Ann. Mtg. Part. Accel. Soc. Jpn. 2021, 1 (2021)

B-167
K. Sumi, *et al*.
BASIC DESIGN OF L-BAND DISK-LOADED STRUCTURE FOR MUON LINAC
Proc. Ann. Mtg. Part. Accel. Soc. Jpn. 2021, 133 (2021)

B-168
R. Kurasaki, *et al*.
DEVELOPMENT OF A LARGE-DIAMETER PILLOW-SEAL USING WELDED STAINLESS-STEEL PLATES
Proc. Ann. Mtg. Part. Accel. Soc. Jpn. 2021, 243 (2021)

B-169
H. Iinuma, *et al*.
UPDATE AND DETAIL DESIGN OF BEAM TRANSPORT LINE FOR MUON G-2/EDM EXPERIMENT AT J-PARC
Proc. Ann. Mtg. Part. Accel. Soc. Jpn. 2021, 267 (2021)

B-170
Y. Takeuchi, *et al*.
DETAILED DESIGN OF THE DISK-AND-WASHER CAVITY FOR MUON LINEAR ACCELERATOR
Proc. Ann. Mtg. Part. Accel. Soc. Jpn. 2021, 343 (2021)

B-171
K. Aoki, *et al*.
DESIGN AND FABRICATION OF MAGNETIC MEASUREMENT SYSTEM WITH HALL ELEMENTS FOR MUON TRANSPORT SOLENOID OF COMET EXPERIMENT
Proc. Ann. Mtg. Part. Accel. Soc. Jpn. 2021, 458(2021)

B-172
R. Muto, *et al*.
DIFFUSERS FOR LOSS REDUCTION IN SLOW EXTRACTION AT J-PARC MAIN RING
Proc. Ann. Mtg. Part. Accel. Soc. Jpn. 2021, 470 (2021)

B-173
K. Agari, *et al*.
ELECTRIC FIELD SIMULATION OF HIGH SENSITIVITY RESIDUAL GAS IONIZATION PROFILE MONITOR FOR J-PARC HADRON HIGH-P BEAMLINE
Proc. Ann. Mtg. Part. Accel. Soc. Jpn. 2021, 675 (2021)

B-174
Y. Sato, *et al*.
NEW CONTROL SYSTEM FOR THE MAGNET POWER SUPPLIES IN HADRON EXPERIMENTAL FACILITY AT J-PARC
Proc. Ann. Mtg. Part. Accel. Soc. Jpn. 2021, 714 (2021)

B-175
H. Watanabe, *et al*.
DESIGN OF A BEAM WINDOW FOR THE B-BEAMLINE AT J-PARC HADRON FACILITY
Proc. Ann. Mtg. Part. Accel. Soc. Jpn. 2021, 810 (2021)

B-176
M. Abe, *et al*.
UPDATED MAGNETIC DESIGN OF MUON STORAGE MAGNET FOR G-2/EDM PRECISION MEASUREMENTS
Proc. Ann. Mtg. Part. Accel. Soc. Jpn. 2021, 835 (2021)

B-177
A. Toyoda, *et al*.
DEVELOPMENT OF HIGH SENSITIVITY RESIDUAL GAS IONIZATION PROFILE MONITOR FOR J-PARC HADRON HIGH-P BEAMLINE (2)
Proc. Ann. Mtg. Part. Accel. Soc. Jpn. 2021, 866 (2021)

B-178
M. Otani, *et al*.
MUON ACCELERATOR EXPLORES UNKNOWN ELEMENTARY PARTICLE PHYSICS
Proc. Ann. Mtg. Part. Accel. Soc. Jpn., 1 (2021)

B-179
F. Tamura, *et al*.
PERFORMANCE OF THE NEXT-GENERATION LLRF CONTROL SYSTEM FOR THE J-PARC RCS
Proc. Ann. Mtg. Part. Accel. Soc. Jpn., 170 (2021)

B-180
Y. Kawabata, *et al*.
PROGRESS OF J-PARC MR DISASTER PREVENTION SYSTEM
Proc. Ann. Mtg. Part. Accel. Soc. Jpn., 18 (2021)

B-181
T. Yasui, *et al*.
COMPENSATION OF THIRD-ORDER STRUCTURE RESONANCES IN J-PARC MR
Proc. Ann. Mtg. Part. Accel. Soc. Jpn., 198 (2021)

B-182
K. Akutsu, *et al*.
Development of new waterproof thin−layers for the magnetic alloy core: structural studies using neutron reflectometry
Proc. Ann. Mtg. Part. Accel. Soc. Jpn., 2021

B-183
Y. Kurimoto
Modeling of Image Current for 2.5 Dimensional PIC Simulations
Proc. Ann. Mtg. Part. Accel. Soc. Jpn., 203 (2021)

B-184
K. Shinto, *et al*.
Effect of an 2-MHz RF source on the H- beam extracted from an rf-driven high-intensity H- ion source
Proc. Ann. Mtg. Part. Accel. Soc. Jpn., 230 (2021)

B-185
T. Nakanoya, *et al*.
Radiation shielding installation work for 3GeV synchrotron injection section
Proc. Ann. Mtg. Part. Accel. Soc. Jpn., 238 (2021)

B-186
T. Shibata, *et al*.
THE NEW LOW-FIELD SEPTUM MAGNET FOR UPGRADING OF FAST EXTRACTION IN MR J-PARC(7)
Proc. Ann. Mtg. Part. Accel. Soc. Jpn., 262 (2021)

B-187
M. Furusawa, *et al*.
REPAIRMENT OF A TRANSFORMER-RECTIFIER UNIT AND INSTALLATION INTO THE NEW RF SYSTEM IN J-PARC MR-RF
Proc. Ann. Mtg. Part. Accel. Soc. Jpn., 283 (2021)

B-188
A. Kobayashi, *et al*.
EVALUATION AND COUNTERMEASURES FOR IMPEDANCE OF FAST EXTRACTION SEPTA AND FAST EXTRACTION KICKERS AT THE J-PARC MAIN RING
Proc. Ann. Mtg. Part. Accel. Soc. Jpn., 287 (2021)

B-189
A. Kobayashi, *et al*.
Evaluation and countermeasures for impedance of fast extraction septa and fast extraction kickers at the J-PARC main ring
Proc. Ann. Mtg. Part. Accel. Soc. Jpn., 287-291 (2021).

B-190
S. Meigo, *et al*.
Durability of secondary electron emission for high-intensity beam on SiC wire
Proc. Ann. Mtg. Part. Accel. Soc. Jpn., 296 (2021)

B-191
Yusuke Takeuchi, *et al*.
DETAILED DESIGN OF THE DISK-AND-WASHER CAVITY FOR MUON LINEAR ACCELERATOR
Proc. Ann. Mtg. Part. Accel. Soc. Jpn., 343 (2021)

B-192
K. Futatsukawa, *et al*.
Development of DFB・DFF system for J-PARC Linac LLRF
Proc. Ann. Mtg. Part. Accel. Soc. Jpn., 371 (2021)

B-193
Takanori SHIBATA, *et al*.
SYNCHRONIZATION SYSTEM OF ION SOURCE RF AND CAVITY RF IN J-PARC LINAC
Proc. Ann. Mtg. Part. Accel. Soc. Jpn., 417 (2021)

B-194
Y. Morita, *et al*.
DESIGN OF OUTPUT FILTER RESISTORS BASED ON PULSE LOAD CAPABILITY FOR J-PARC MR MAIN MAGNET POWER SUPPLY
Proc. Ann. Mtg. Part. Accel. Soc. Jpn., 439 (2021)

B-195
T. Asami, *et al*.
EVALUATION OF THE EFFECTS OF EDDY CURRENTS ON VACUUM DUCTS IN J-PARC MR
Proc. Ann. Mtg. Part. Accel. Soc. Jpn., 454 (2021)

B-196
S. IWATA, *et al*.
RESEARCH ON THE PLACEMENT OF EDDY SEPTUM MAGNETS AND FAILURE IN J-PARC MR FAST EXTRACTION
Proc. Ann. Mtg. Part. Accel. Soc. Jpn., 461 (2021)

B-197
Ryotaro MUTO, *et al*.
DIFFUSERS FOR LOSS REDUCTION IN SLOW EXTRACTION AT J-PARC MAIN RING
Proc. Ann. Mtg. Part. Accel. Soc. Jpn., 470 (2021)

B-198
Y. Hashimoto, *et al*.
DEVELOPMENT OF A WIDE DYNAMIC-RANGE BEAM PROFILE MONITOR USING OTR AND FLUORESCENCE FOR INJECTED BEAMS IN J-PARC MAIN RING (2)
Proc. Ann. Mtg. Part. Accel. Soc. Jpn., 481 (2021)

B-199
K. Yamamoto, *et al*.
Neutron measurement in the accelerator tunnel of J-PARC Rapid Cyclyng Synchrotron
Proc. Ann. Mtg. Part. Accel. Soc. Jpn., 494 (2021)

B-200
T. Takayanagi, *et al*.
LTD semiconductor switch power supply for J-PARC kicker
Proc. Ann. Mtg. Part. Accel. Soc. Jpn., 53 (2021)

B-201
M. Sugita, *et al*.
Experimental verification of magnetic field measurement probe for RCS bump magnet
Proc. Ann. Mtg. Part. Accel. Soc. Jpn., 641 (2021)

B-202
P. K. Saha, *et al*.
RECENT PROGRESS OF LASER STRIPPING POP DEMONSTRATION STUDY AT J-PARC RCS
Proc. Ann. Mtg. Part. Accel. Soc. Jpn., 656 (2021)

B-203
P. K. Saha, *et al*.
RECENT PROGRESS OF LASER STRIPPING POP DEMONSTRATION STUDY AT J-PARC RCS
Proc. Ann. Mtg. Part. Accel. Soc. Jpn., 656-660 (2021).

B-204
Y. Sugiyama, *et al*.
BUNCH MANIPULATION BEFORE THE EXTRACTION BY A SECOND HARMONICS SUPERPOSITION AT THE J-PARC MR
Proc. Ann. Mtg. Part. Accel. Soc. Jpn., 66 (2021)

B-205
M. Tomizawa, *et al*.
ELECTROSTATIC SEPTUM ACCIDENT AND RECOVERY BY A QUADRUPOLE POWER SUPPLY TRIP IN THE STRAIGHT SECTIONS
Proc. Ann. Mtg. Part. Accel. Soc. Jpn., 661 (2021)

B-206
T. Toyama, *et al*.
Evaluation by causality for measurement data of longitudinal coupling impedances with stretched-wire method
Proc. Ann. Mtg. Part. Accel. Soc. Jpn., 666-669 (2021).

B-207
N. Hayashi, *et al*.
Analysis of Machine Protection System events in the J-PARC Linac/RCS
Proc. Ann. Mtg. Part. Accel. Soc. Jpn., 679 (2021)

B-208
N. Hayashi, *et al*.
ANALYSIS OF MACHINE PROTECTION SYSTEM EVENTS IN THE J-PARC LINAC/RCS
Proc. Ann. Mtg. Part. Accel. Soc. Jpn., 679-682 (2021).

B-209
S. Mizobata, *et al*.
OVERVIEW OF CAPACITOR BANK MONITORING SYSTEM FOR HIGH VOLTAGE SUPPLY FOR J-PARC KLYSTRON
Proc. Ann. Mtg. Part. Accel. Soc. Jpn., 742 (2021)

B-210
Y. Shobuda, *et al*.
Titanium nitride-coated ceramic break for wall current monitors with an improved broadband frequency response
Proc. Ann. Mtg. Part. Accel. Soc. Jpn., 75-79 (2021)

B-211
T. Shibata, *et al*.
THE NEW HIGH-FIELD SEPTUM MAGNET FOR UPGRADING OF FAST EXTRACTION IN MR J-PARC(3)
Proc. Ann. Mtg. Part. Accel. Soc. Jpn., 826 (2021)

B-212
Y. Lee, *et al*.
DEVELOPMENT OF AN OPTIMIZATION ALGORITHM FOR BEAM PROFILE MEASUREMENT USING MULTIPLE 16-ELECTRODE BPMS
Proc. Ann. Mtg. Part. Accel. Soc. Jpn., 83 (2021)

B-213
A. Ono, *et al*.
Development of semiconductor clover switch for short-circuit protection of klystron for J-PARC accelerator
Proc. Ann. Mtg. Part. Accel. Soc. Jpn., 831 (2021)

B-214
H. Okita, *et al*.
EVALUATION OF THE FREQUENCY RESPONSE OF THE RF GAP VOLTAGE MONITOR OF THE J-PARC RCS
Proc. Ann. Mtg. Part. Accel. Soc. Jpn., 840 (2021)

B-215
M. Yoshimoto, *et al*.
Initiatives to address the lifetime improvement of HBC stripper foil for 3GeV synchrotron of J-PARC
Proc. Ann. Mtg. Part. Accel. Soc. Jpn., 850 (2021)

B-216
H. Takahashi, *et al*.
Update of MPS modules for J-PARC Linac and RCS (2)
Proc. Ann. Mtg. Part. Accel. Soc. Jpn., 914 (2021)

B-217
H. Takahashi, *et al*.
Update of MPS modules for J-PARC linac and RCS, 2
Proc. Ann. Mtg. Part. Accel. Soc. Jpn., 914-917 (2021).

B-218
K. Futatsukawa, *et al*.
PRESENT STATUS OF J-PARC LINAC LLRF SYSTEM
Proc. Ann. Mtg. Part. Accel. Soc. Jpn., 937 (2021)

B-219
Y. Kurimoto
STUDY ON USAGE OF ELECTRON LENS FOR HIGH INTENSITY PROTON RINGS
Proc. Ann. Mtg. Part. Accel. Soc. Jpn., 995 (2021)

B-220
K. Shinto, *et al*.
Effect of a 2-MHz RF source on the H- beam extracted from an rf-driven high-intensity H- ion source
Proc. Ann. Mtg. PASJ (Internet), 230-233 (2021)

B-221
K. Hirano, *et al*.
RF dielectric properties of alumina ceramics for L-band RF window
Proc. Ann. Mtg. PASJ (Internet), 276-278 (2021)

B-222
Y. Sato, *et al*.
Analysis of the J-PARC linear accelerator RF down phenomena 2
Proc. Ann. Mtg. PASJ (Internet), 924-928 (2021)

B-223
Y. Yamaguchi, *et al*.
Beam loss monitor using nuclear reaction with high threshold-energy in the vicinity of J-PARC muon target
Proc. Ann. Mtg. PASJ(Internet), 486-490(2021)

B-224
M. Tomizawa, *et al*.
Slow Extraction Operation at J-PARC Main Ring
Proc. HB'21, Batavia, IL, USA, Oct. 2021, pp. 219-224

B-225
I. Yamada, *et al*.
MEASUREMENT AND RECONSTRUCTION OF A BEAM PROFILE USING A GAS SHEET MONITOR BY BEAM-INDUCED FLUORESCENCE DETECTION IN J-PARC
Proc. IBIC2021, 168 (2021)

B-226
Y.i Hashimoto, *et al*.
DEVELOPMENT OF A PROFILE MONITOR USING OTR AND FLUORESCENCE FOR INJECTED BEAMS IN J-PARC MAIN RING
Proc. IBIC2021, 263 (2021)

B-227
M. Yang, *et al*.
DEVELOPMENT OF TIMING READ-BACK SYSTEM FOR STABLE OPERATION OF J-PARC
Proc. ICALEPCS2021, 927 (2021)

B-228
K. Nakayoshi, *et al*.
Development of a Voltage Interlock System for Normal-Conducting Magnets in the Neutrino Experimental Facility at J-PARC
Proc. ICALEPCS'21, Shanghai, China, Oct. 2021, pp. 738-741

B-229
R. Matsushita, *et al*.
DEVELOPMENT OF PULSED BEAM SYSTEM FOR THE THREE DIMENSIONAL SPIRAL INJECTION SCHEME IN THE J-PARC MUON g-2/EDM EXPERIMENT
Proc. IPAC, Vol 2021, 809(2021)

B-230
M. Yotsuzuka, *et al*.
DEVELOPMENT OF BUNCH WIDTH MONITOR WITH HIGH TIME RESOLUTION FOR LOW EMITTANCE MUON BEAM IN THE J-PARC MUON g-2/EDM EXPERIMENT
Proc. IPAC2021, 1004 (2021)

B-231
K. Sumi, *et al*.
BASIC DESIGN STUDY FOR DISK-LOADED STRUCTURE IN MUON LINAC
Proc. IPAC2021, 1801 (2021)

B-232
M. Yamamoto, *et al*.
VACUUM TUBE OPERATION TUNING FOR A HIGH INTENSITY BEAM ACCELERATION IN J-PARC RCS
Proc. IPAC2021, 1884 (2021)

B-233
K. Ishii, *et al*.
DEVELOPMENT OF DISASTER PREVENTION SYSTEM FOR ACCELERATOR TUNNEL
Proc. IPAC2021, 2228 (2021)

B-234
Y. Nakazawa, *et al*.
DEVELOPMENT OF AN APF IH-DTL IN THE J-PARC MUON g - 2/EDM EXPERIMENT
Proc. IPAC2021, 2544 (2021)

B-235
H. Okita, *et al*.
CONSIDERATION OF TRIPLE-HARMONIC OPERATION FOR THE J-PARC RCS
Proc. IPAC2021, 3020 (2021)

B-236
F. Tamura, *et al*.
NON-ADIABATIC LONGITUDINAL BUNCH MANIPULATION AT FLATTOP OF THE J-PARC MR
Proc. IPAC2021, 3023 (2021)

B-237
K. Yamamoto
RECENT STATUS OF J-PARC RAPID CYCLING SYNCHROTRON
Proc. IPAC2021, 3027 (2021)

B-238
R. Muto, *et al*.
SIMULATION STUDY ON DOUBLE DIFFUSER FOR LOSS REDUCTION IN SLOW EXTRACTION AT J-PARC MAIN RING
Proc. IPAC2021, 3069 (2021)

B-239
S. Iwata, *et al*.
LAYOUT OF THE NEW SEPTUM MAGNETS FOR FAST EXTRACTION IN J-PARC MAIN RING
Proc. IPAC2021, 3103 (2021)

B-240
Y. Shobuda, *et al*.
A POSSIBLE MODIFICATION OF CERAMIC CHAMBERS IN THE INJECTION AREA AT THE RCS IN J-PARC
Proc. IPAC2021, 3205 (2021)

B-241
E. Cicek, *et al*.
A RECENT UPGRADE ON PHASE DRIFT COMPENSATION SYSTEM FOR A STABLE BEAM INJECTION AT J-PARC LINAC
Proc. IPAC2021, 3357 (2021)

B-242
M. Otani, *et al*.
SIMULATION OF IMAGING USING ACCELERATED MUON BEAMS
Proc. IPAC2021, 3740 (2021)

B-243
T. Asami, *et al*.
A SIMULATION STUDY OF BEAM PIPE EDDY CURRENT EFFECTS ON BEAM OPTICS
Proc. IPAC2021, 4288 (2021)

B-244
T. Yasui, *et al*.
COMPENSATIONS OF THIRD-ORDER RESONANCES IN J-PARC MR
Proc. IPAC2021, 744 (2021)

B-245
Y. Sato
Upgrading J-PARC Accelerator for Hyper-Kamiokande Project
Proc. IPAC2021, wexb02 (2021)

B-246
M. Yotsuzuka, *et al*.
Development of Bunch Width Monitor with High Time Resolution for Low Emittance Muon Beam in the J-PARC Muon g-2 / EDM Experiment
Proc. IPAC'21, Campinas, SP, Brazil, May 2021, pp. 1004-1007

B-247
Y. Fukao, *et al*.
Construction Status of the COMET Experimental Facility
Proc. IPAC'21, Campinas, SP, Brazil, May 2021, pp. 1907-1909

B-248
M. A. Rehman, *et al*.
The First Trial of XY-Coupled Beam Phase Space Matching for Three-Dimensional Spiral Injection
Proc. IPAC'21, Campinas, SP, Brazil, May 2021, pp. 553-556

B-249
Y. Takeuchi, *et al*.
Development of a Disk-and-Washer Cavity for the J-PARC Muon g-2/EDM Experiment
Proc. IPAC'21, Campinas, SP, Brazil, May 2021, pp. 658-661

B-250
K. Oda, *et al*.
Developments of a Pulse Kicker System for the Three-Dimensional Spiral Beam Injection of the J-PARC Muon g-2/EDM Experiment
Proc. IPAC'21, Campinas, SP, Brazil, May 2021, pp. 726-729

B-251
T. Kume, *et al*.
Evaluation of the Free Spectral Range of an Etalon by Referring an Optical Frequency Comb
Proc. LEM

B-252
J. Kamiya, *et al*.
Some methods of making titanium vacuum chamber act as getter pump for UHV/XHV
Proc. of 12th International Particle Accelerator Conference (2021) 3471

B-253
Y. Shobuda, *et al*.
A Possible modification of ceramic chambers in the injection area at the RCS in J-PARC
Proc. of 12th International Particle Accelerator Conference, 3205-3208 (2021)

B-254
P. K. Saha, *et al*.
Foil Hits Reduction by Minimizing Injection Beam Size at the Foil in J-PARC RCS
Proc. of 12th International Particle Accelerator Conference, 590-593 (2021)

B-255
G. Ichikawa, *et al*.
Neutron lifetime experiment with pulsed cold neutrons at J-PARC
Proc. of Science, Vol PANIC2021, 457(2021)

B-256
T. Mogi, *et al*.
Improvement of systematic uncertainties for the neutron lifetime experiment at J-PARC
Proc. of Science, Vol PANIC2021, 458(2021)

B-257
K. Yano, *et al*.
Precise Neutron Lifetime Measurement: An Integration Test with a Gaseous and a Solenoidal Magnet
Proc. of the 3rd J-PARC Symposium (J-PARC2019), JPS Conf. Proc., 33

B-258
S. Imajo, *et al*.
Ultracold Neutron Time Focusing Experiment and Performance Evaluation of an Improved UCN Rebuncher at J-PARC/MLF
Proc. of the 3rd J-PARC Symposium (J-PARC2019), JPS Conf. Proc., 33

B-259
N. Sumi, *et al*.
Precise Neutron Lifetime Measurement Using Pulsed Neutron Beams at J-PARC
Proc. of the 3rd J-PARC Symposium (J-PARC2019), JPS Conf. Proc., 33

B-260
N. Yamamoto, *et al*.
Development of Pulsed Neutron Interferometer
Proc. of the 3rd J-PARC Symposium (J-PARC2019), JPS Conf. Proc., 33

B-261
M. Hiromoto, *et al*.
Proof-of-principle Experiment for the Study of a New Intermediate-range Interaction Using Coherent Neutron Scattering
Proc. of the 3rd J-PARC Symposium (J-PARC2019), JPS Conf. Proc., 33

B-262
K. Haga, *et al*.
DEVELOPMENT OF THE HIGH-POWER SPALLATION NEUTRON TARGET OF J-PARC
Proc. The 19th International Topical Meeting on Nuclear Reactor Thermal Hydraulics (NURETH-19), Log nr.: 3392

B-263
F. Funama, *et al*.
A study of Focusing TOF-MIEZE Spectrometer with Small-angle Neutron Scattering
Proc. The Physical Society of Japan Conference

Proceeding, 33

B-264
S. Kumano, Q.-T. Song
Possible studies of gluon transversity in the spin-1 deuteron at hadron-accelerator facilities
SckiPost Phys. Proc. 8, 100 (2022)

B-265
S. Kumano, Q.-T. Song
Transverse-momentum-dependent parton distribution functions for spin-1 hadrons
SckiPost Phys. Proc. 8, 174 (2022)

KEK Reports

C-001
Safety Division, J-PARC Center
Annual Report on the Activities of Safety in J-PARC, FY2020
KEK Internal 2021-005

C-002
M. A. Rehman, *et al*.
THE FIRST TRIAL OF XY-COUPLED BEAM PHASE SPACE MATCHING FOR THREE-DIMENSIONAL SPIRAL INJECTION
KEK Preprint 2021-17

C-003
S. Igarashi, *et al*.
Accelerator technical design report for 1.3 MW operation at J-PARC Main Ring
KEK Report 2021-2

JAEA Reports

D-001
Safety Division, J-PARC Center
Annual Report on the Activities of Safety in J-PARC, FY2020
JAEA-Review 2021-057(2021)

D-002
A. Ono, *et al*.
Construction of a design model for an electromagnet power supply with safety and reliability in the accelerator
JAEA-Technology 2020-023(2021)

D-003
A. Ono, *et al*.
Proposal of safe and secure maintenance method to realize long-term stable operation of electromagnet power supply
JAEA-Technology 2021-005(2021)

D-004
K. Takano, *et al*.
Noise countermeasures for inverter-controlled multi-stage roots vacuum pumps in J-PARC LINAC L3BT
JAEA-Technology 2021-017(2021)

D-005
T. Nakanoya, *et al*.
Report of the design examination and the installation work for the radiation shield at the beam injection area in the 3 GeV synchrotron
JAEA-Technology 2021-019(2021)

D-006
K. Yamaki, *et al*.
Development of Logging Data Processing Tool for Lead-bismuth Experimental Devices
JAEA-Technology 2020-021 (2021)

Others

E-001
JVSS (N. Yamada)
中性子反射率法 (only Japanese)
図説 表面分析ハンドブック (only Japanese)

J-PARC Annual Report 2021
Vol.1: Highlight

December 2022

J-PARC

JAPAN PROTON ACCELERATOR RESEARCH COMPLEX

High Energy Accelerator Research Organization (KEK)
Japan Atomic Energy Agency (JAEA)

2-4 Shirakata, Tokai-mura, Naka-gun, Ibaraki 319-1195, Japan

http://j-parc.jp/